THE EARTH-RESISTIVITY METHOD OF GEOPHYSICAL SURVEYING

by

W.R. BURNETT, B.Sc.

Thesis submitted for the Degree of Ph.D. of the University of Edinburgh.

PREFACE

This thesis is a record of work carried out at the Mining Department of the University of Edinburgh under the direction of Professor R. McAdam, Hood Professor of Mining. The main part of the thesis relates to the traverse method of electrical resistivity surveying. This is treated theoretically at first, and examples from field and laboratory work are cited to show the application and use of such theory. In addition, some attention is paid to electrical depth determinations and the effect of lateral resistivity variations on these measurements.

The thanks of the author are due to the National Coal Board, to the then Directorate of Open-Cast Coal Production and to the Fife County Council, who all suggested field problems which could be solved by earth-resistivity methods, and willingly provided surveyors and assistants to help in the field work.

Edinburgh, May 1953.

C O N T E N T S

INTRODUCTION

INTRODUCTION

The greatest variable among the electrical characteristics of the earth is its resistivity, the resistivity or specific resistance of a material being defined as the resistance in ohms across the opposite faces of a unit cube of the material. The common unit is the ohm-centimetre. The permeability of the ground may be regarded as uniform, while the dielectric constant varies within rather wide limits, from 1 to 80. Resistivity, however, may vary from 10^2 to 10^7 ohm-cm.

That a difference existed in the resistivities of rocks has been realised since as early as 1850, and attempts were probably made to use this variation as a means of prospecting. One of the earliest references in coal-mining is by Wood (1)* who made laboratory tests of coal, limestone, slag, etc. He was interested in the comparison of different materials for the purpose of using them as ballast for electrical railway tracks. It is interesting to note his results.

Coal	-	4×10^{10} ohm-cm.
Limestone	-	2×10^{6} ohm-cm.
Slag	-	4×10^{5} ohm-cm.

That coal should have as great a resistance as this would be very valuable in geophysical prospecting, but unfortunately such a resistivity is not found in nature. There have been several reports of more or less successful electrical surveys for the

* Figures in brackets ( ) refer to bibliography at the end.

purpose of finding coal seams, (2), (3), (4), (5) and (6).

The electrical method of surveying has been developed in the present century, although the first investigations were made by R.W. Fox in 1830 in the Cornish mines (7). His method depended on the spontaneous polarization produced in some ores which when undergoing oxidation became sources of electric current.

The resistivity method did not achieve practical utility until Wenner (8) suggested a method employing four electrodes, current being allowed to pass through the earth via two electrodes and the potential difference between the other two measured at the same time. His original idea was that the four electrodes should be co-linear and at equal distances apart, the outer two carrying current with potential measured across the inner two. Since then many other electrode configurations have been applied, all, however, employing four electrodes as above (9). The most popular of these methods, other than Wenner's, is the single electrode probe method, where the other current electrode is placed so far from the single electrode as to be considered at an infinite distance from it. The potential gradient is then measured around the single electrode. The Wenner and single electrode probe methods will be considered later.

The bulk of work on resistivity problems has been confined to depth probing, while little has been done on the measurement or effect of longitudinal variations in resistivity. Most of this work is therefore devoted to such longitudinal variations, and theoretical analyses applied to different

geological structures will be presented. Practical studies, following on the theoretical results, are based on laboratory experiments and field surveys. Afterwards, criticisms of methods used for the interpretation of depth probings are given, the field results being obtained in the course of the traverse surveys previously mentioned.

CHAPTER II.

INSTRUMENTS

INSTRUMENTS

The simplest form of instrument for earth-resistivity surveying would be one whereby current was passed into the earth from d.c. batteries and potential measured by a potentiometer. Due to polarization at the electrodes, these would require to be of the non-polarizing type. Electrolysis at ordinary metal electrodes would cause the current to decline rapidly. Such a non-polarizing electrode consists of a porous cup which contains a rod of metal and a saturated solution of a salt of the metal. The metal ordinarily used is copper in a solution of copper sulphate. Saturation is ensured by providing an excess of crystals of the salt. When a current is passed through, the copper will go into solution or be precipitated depending on the direction of current, the process being reversible. Contact potential cannot be entirely eliminated since there is always contact between the electrolyte and the earth through the porous cup; it is, however, so reduced as to be negligible. Also, if current is allowed to flow through the potential electrodes, then there must be a potential drop whose value will depend on the contact resistance. This is overcome by balancing the potential difference caused by the current flowing in the earth with that produced by the standard cell of a potentiometer. A galvanometer in the circuit allows the point of balance to be indicated when the reading on it is zero. Since no current now passes through the potential electrodes there can be no potential drop due to

contact resistance, but contact resistance at the current electrodes is not so important since any variation will not affect the ratio of current and potential. The resistance must not be too high because this would decrease the sensitivity of the instruments.

To overcome the difficulties attendant on the use of porous pot non-polarizing electrodes, Gish and Rooney designed a system comprising double commutators, (10), (11) and (12). The simplified circuit diagram is shown in Fig. 1.

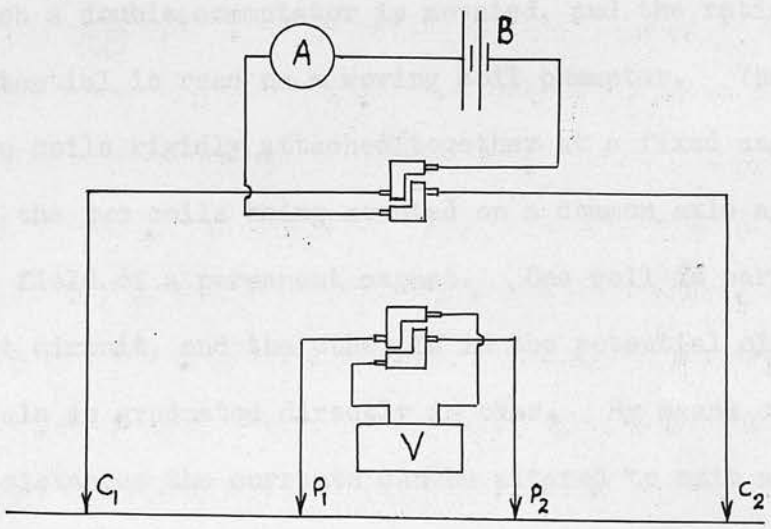

Fig.1. Gish-Rooney Circuit

Power is again derived from batteries B, current is measured by a d.c. milliammeter A, and potential by the potentiometer V. The polarity of the current is reversed at 20 or 30 times per second by manual rotation of the commutator. Another commutator on the same shaft reverses the potential at

the same frequency, an alternating current being therefore applied to the earth through the current electrodes. The alternating potential thus produced is rectified so that it can be measured by the potentiometer.

Evershed and Vignoles, Ltd. have marketed a Megger Earth Tester originally intended for the measurement of the resistances of earth plates, etc. for electrical engineering purposes. Fundamentally, the circuit of the Megger is similar to that required for the Gish-Rooney Circuit, (13) and (14). Here, power is supplied by a hand-driven d.c. generator, on the shaft of which a double commutator is mounted, and the ratio of current and potential is read on a moving coil ohmmeter. The ohmmeter has two coils rigidly attached together at a fixed angle to each other, the two coils being mounted on a common axle and moving in the field of a permanent magnet. One coil is part of the current circuit, and the other is in the potential circuit. The scale is graduated directly in ohms. By means of shunts and resistances the currents can be altered to suit a wide range of conditions, and the ohmmeter has four ranges, viz. 0 - 3, 30, 300 and 3,000 ohms, respectively. These ranges are not entirely suitable for geophysical surveying as the upper ranges are rarely required and the lower scale readings are not sufficiently sensitive for large electrode spacings. Also, before calculating apparent resistivity, certain corrections must be applied to the reading in ohms since a small but appreciable current flows in the potential circuit. The corrections are obtained by calibration.

On account of these limitations, Messrs. Evershed and Vignoles have developed a Megger Earth Tester to meet the special requirements of geophysical surveying. Figs. 2 and 3 show the complete equipment and a simplified wiring diagram is given in Fig. 4. The instrument consists of a hand-driven generator with two windings. The main winding supplies the testing current, and the auxiliary winding develops a lower electromotive force which is applied to the resistor AB. The testing current passes through the shunted control coil of the ohmmeter and through the reversing contactor T_2 so that the current through the soil, between the electrodes C_1 and C_2, is alternating. A condenser is inserted between one of the potential electrodes and the reversing contactor T_1. The readings are, therefore, unaffected by any electrolytic or back e.m.f. or stray currents in the ground. An alternating potential difference exists between the two electrodes P_1 and P_2, and this, after being rectified by the reversing contactor T_1, is balanced by the adjustable potential divider BC which is supplied from the auxiliary winding of the generator. Thus, the sliding contact C is adjusted until a null reading is obtained on the galvanometer. The deflection on the ohmmeter is again proportional to the ratio of potential to current. The ranges available are 0 - 0.3, 1, 3, 10 and 30 ohms, each scale division on the lower scale representing 0.01 ohms. In practice, it was found that the instrument read all readings perfectly to 300 feet (the maximum electrode spacing used),

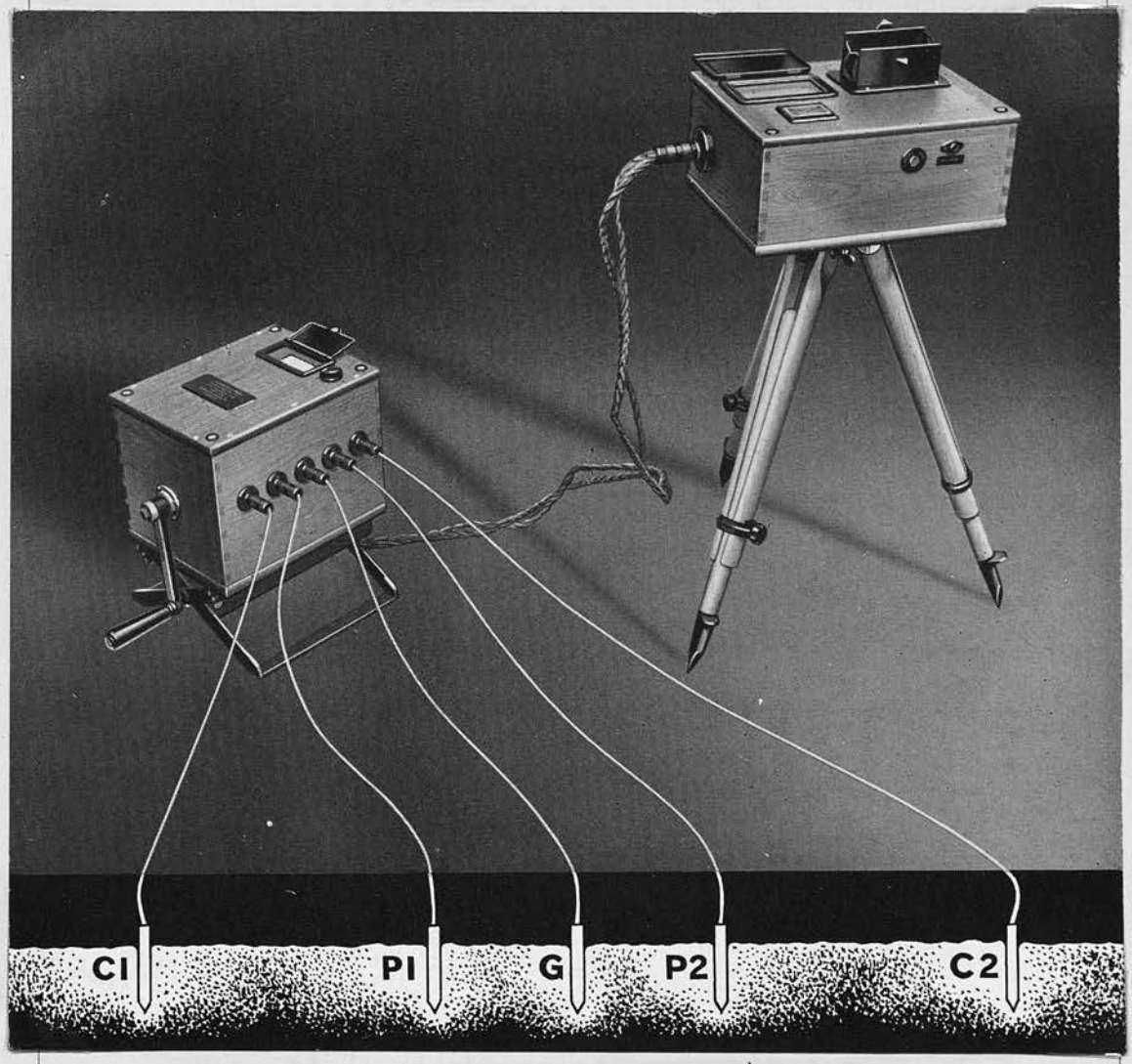

Fig. 2, The Geophysical Megger Earth Tester

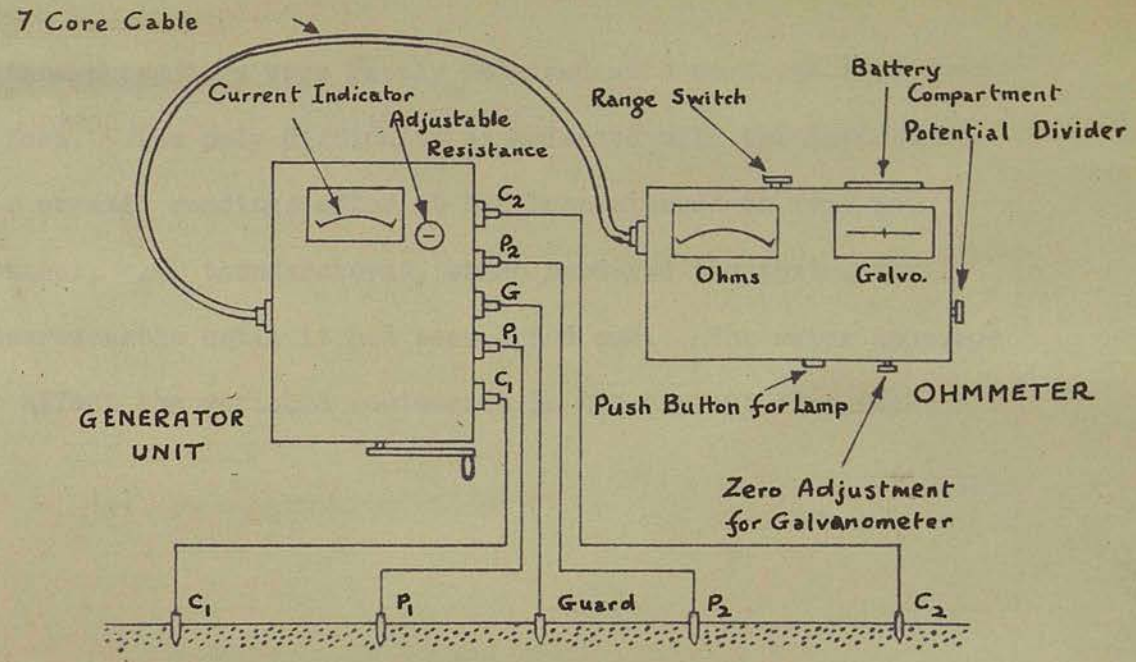

Fig. 3 Connections when using a Geophysical Megger Earth Tester

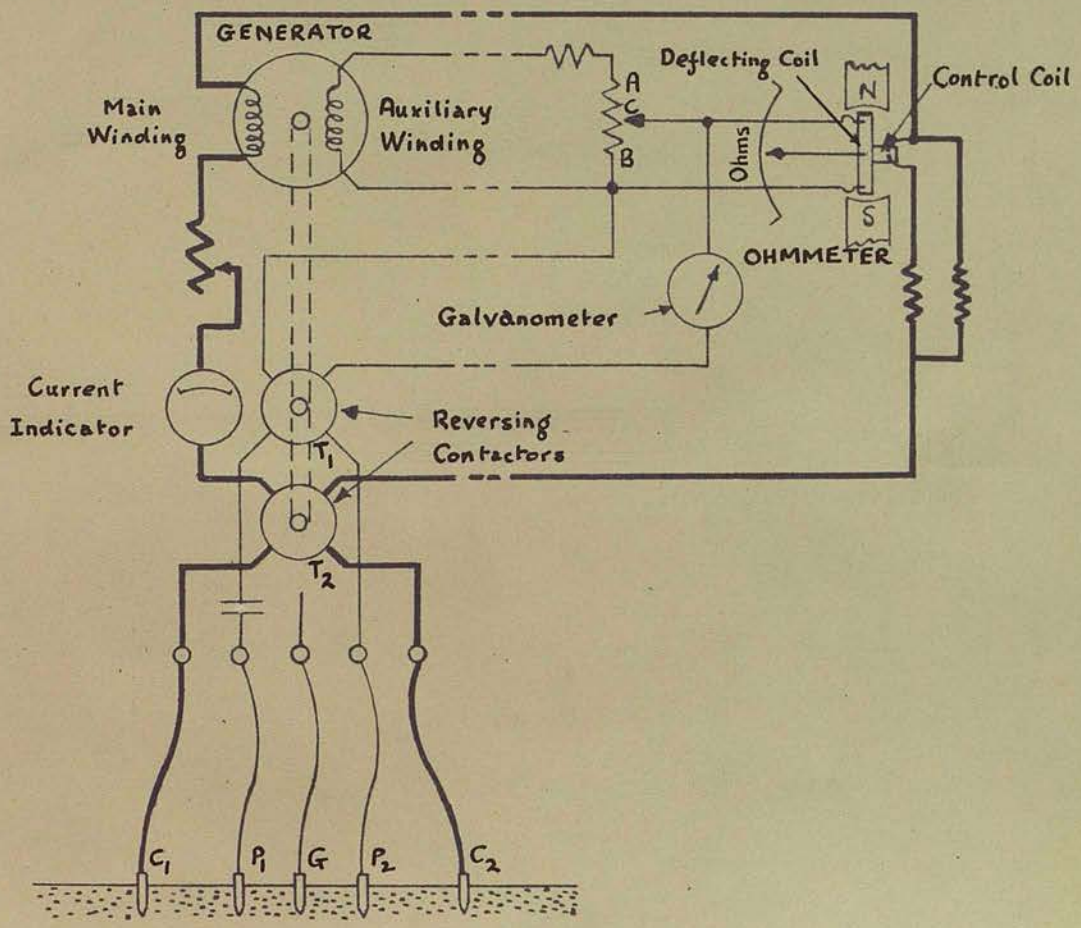

Fig. 4 Principle of the Geophysical Megger Earth Tester

although readings were rarely obtained with spacings less than 5 feet. The only difficulty experienced with the instrument was erratic readings after it had been exposed to very wet weather, e.g. thunderstorms, which rendered the instrument unserviceable until it had been dried out. The water appeared to affect the variable resistance in the current circuit.

CHAPTER III.

THEORY OF RESISTIVITY MEASUREMENTS

THEORY OF RESISTIVITY MEASUREMENTS

In the theory here presented the earth is considered as a semi-infinite, isotropic medium. Isotropy in this case implies that the resistivity in all directions in the medium is the same. This is nearly true for unconsolidated deposits, but for sedimentary formations and even more so with those rocks which have been subjected to intense compaction and dynamo-metamorphism, the apparent resistivity parallel to the bedding may be several times the apparent normal resistivity. Some authors have taken this difference into account, (15) and (16), but in the main it is usually neglected.

Potential due to a Point Source in an Infinite Homogeneous Medium.

If we consider a source of current of strength I to be surrounded by an infinite isotropic homogeneous conductor of resistivity, ρ , we can find the potential at any point. The point will be surrounded by a closed spherical surface with a total current of I flowing across the surface. If r is the radius of the sphere, the current density, i, on this surface will be given by:-

$$i = \frac{I}{4 \pi r^2}$$

If the potential difference over a length dl of a conductor is dV, then Ohm's Law may be stated in its differential form, thus:-

$$i = -\frac{1}{\rho} \cdot \frac{dV}{dl}$$

Since we are considering a spherical surface, the direction

normal to the surface will be along the radius and

$$\frac{dV}{dl} = \frac{dV}{dr} .$$

Combining these three equations,

$$\frac{dV}{dr} = -\frac{I\rho}{4\pi r^2}$$

$$\therefore V = -\int \frac{I\rho}{4\pi r^2} \cdot dr$$

$$= \frac{I\rho}{4\pi r} + C .$$

Since at infinity the potential must be zero, the constant C is zero, and:-

$$V = \frac{I\rho}{4\pi r} .$$

In a semi-infinite homogeneous medium bounded by a medium of infinite resistivity with the point source situated at the interface between these two media, the expression for potential becomes

$$V = \frac{I\rho}{2\pi r} ,$$

since the current can only flow across a hemi-spherical surface of surface area, $2\pi r^2$.

Configuration of Electrodes.

In the measurement of the resistivity of the earth, particularly in geophysical surveying, the four electrode system is commonly used, current being introduced from a battery or generator at A and led out at B as in Fig. 5. The potential difference across the other two electrodes, C and D, is also

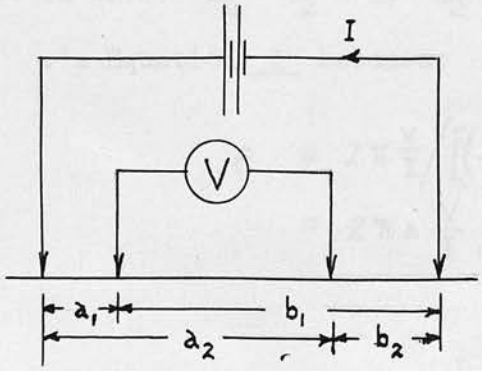

Fig. 5

measured. Let the electrode intervals be denoted by a_1, a_2, b_1 and b_2, as shown.

We may calculate the potentials at points C and D due to a source of current I amperes at A and an equal sink at B.

Potential at C due to A $= \frac{I\rho}{2\pi a_1}$

Potential at C due to B $= -\frac{I\rho}{2\pi b_1}$

Similarly,

Potential at D due to A $= \frac{I\rho}{2\pi a_2}$

Potential at D due to B $= -\frac{I\rho}{2\pi b_2}$

The total potential at C is then the sum of the effects of A and B, and similarly with D.

$$\therefore V_C = \frac{I\rho}{2\pi}\left(\frac{1}{a_1} - \frac{1}{b_1}\right)$$

$$\text{and } V_D = \frac{I\rho}{2\pi}\left(\frac{1}{a_2} - \frac{1}{b_2}\right)$$

The potential drop, V, measured across C and D is therefore:-

$$V = \frac{I\rho}{2\pi}\left[\left(\frac{1}{a_2} - \frac{1}{b_1}\right) - \left(\frac{1}{a_2} - \frac{1}{b_2}\right)\right]$$

$$\therefore \rho = 2\pi \frac{V}{I} \Big/ \left[\left(\frac{1}{a_1} - \frac{1}{b_1}\right) - \left(\frac{1}{a_2} - \frac{1}{b_2}\right)\right] \qquad 1$$

(a) Wenner Configuration.

In this method, (8), the four electrodes are co-linear and the electrode intervals are kept equal to a constant a, and so we have:- $a_1 = b_2 = a$; $a_2 = b_1 = 2a$.

$\therefore$ Equation 1 becomes;

$$\rho = 2\pi \frac{V}{I} \Big/ \left[\left(\frac{1}{a} - \frac{1}{2a}\right) - \left(\frac{1}{2a} - \frac{1}{a}\right)\right]$$

$$= 2\pi a \frac{V}{I} \qquad 2$$

In practice, of course, the ground is never made up of one homogeneous material extending to infinity. However, it is an advantage to measure the quantities a, V and I at the surface, and to calculate ρ_a , known as the apparent resistivity. It is worth remembering that this formula still holds when the current and potential leads are transposed. This was often found useful in the field when leakage of current was suspected.

(b) Single Electrode Probe.

In this method the current electrode B is placed at an infinite distance from A. The lines of current flow will therefore extend radially from A, and equipotential surfaces will be in the form of hemispherical bowls, since equipotentials must always be orthogonal to the current lines. The potential drop, V, is measured between two electrodes C and D. It is usually stated that B is sufficiently far from A if it is at least five times more distant than the maximum distance of D from A. This is investigated below.

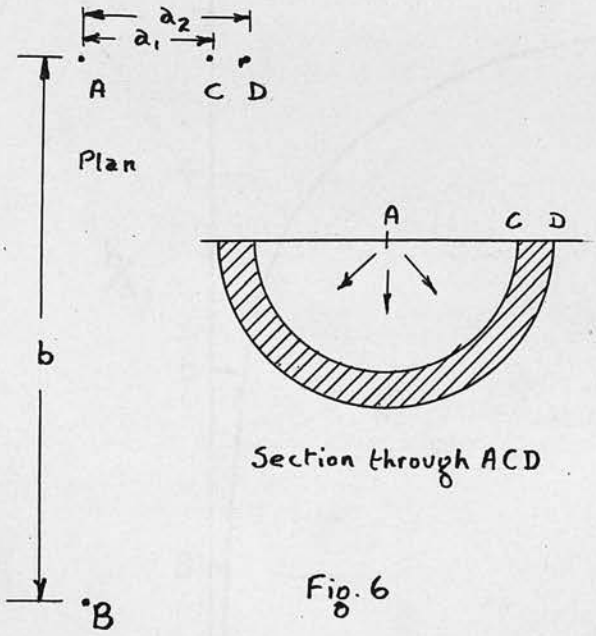

Fig. 6

Let AC = a_1, AD = a_2, AB = b,

then BC = $\sqrt{a_1^2 + b^2}$ and BD = $\sqrt{a_2^2 + b^2}$

From Equation 1

$$\rho = 2\pi \frac{V}{I} \Big/ \left[\left(\frac{1}{a_1} - \frac{1}{a_2} \right) - \left(\frac{1}{\sqrt{a_1^2 + b^2}} - \frac{1}{\sqrt{a_2^2 + b^2}} \right) \right]$$

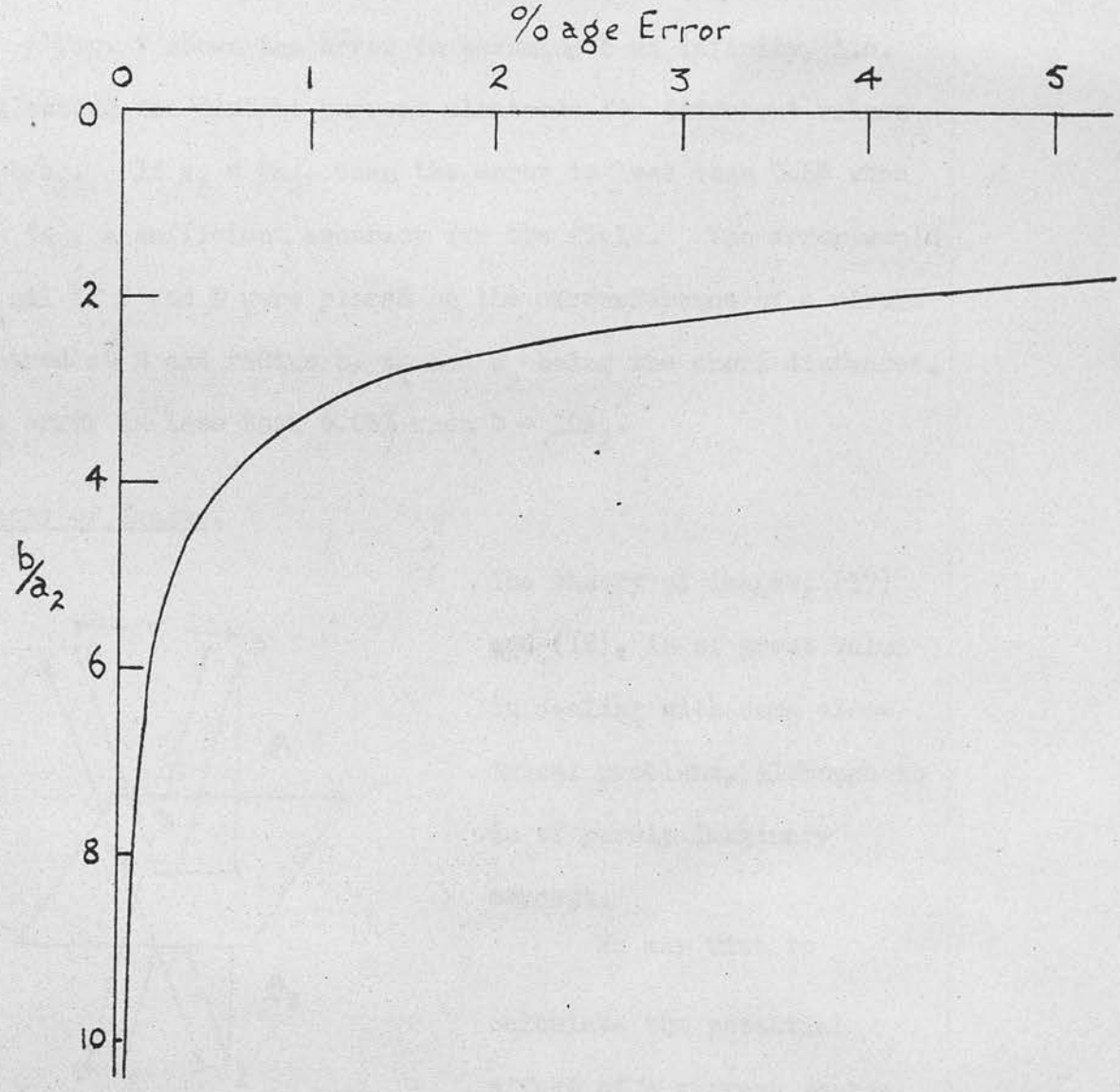

Fig.7, Percentage Error in Assuming Distant Current Electrode at Infinity.

The term $\left(\frac{1}{\sqrt{a_1^2+b^2}} - \frac{1}{\sqrt{a_2^2+b^2}}\right)$ tends to zero as b is increased.

Then $\rho = 2\pi \frac{V}{I} \Big/ \left(\frac{1}{a_1} - \frac{1}{a_2}\right) = 2\pi \frac{V}{I} \cdot \frac{a_2 - a_1}{a_1 a_2}$.

This is the formula used for the single electrode probe method.

Fig. 7 shows the error in assuming b at infinity, i.e. neglecting the distant current electrode for different values of b/a_2. If $a_1 = \frac{1}{2}a_2$, then the error is less than 0.6% when $b = 5a_2$, a sufficient accuracy for the field. The error would be nil if C and D were placed on the circumference of a circle centred at B and radius b, a_1 and a_2 being the chord distances. The error is less than 0.08% when $b = 10a_2$.

Theory of Images.

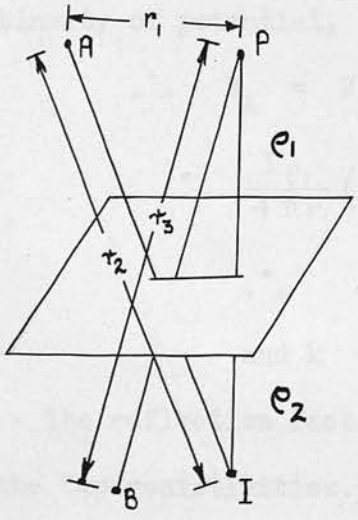

Fig. 8

The theory of images, (17) and (18), is of great value in dealing with some electrical problems, although it is of purely imaginary concept.

We may wish to calculate the potential effect of a current source at a point in one medium of resistivity ρ_1 when there is present a second medium of different resistivity ρ_2. The effect of such a difference in resistivity may be represented by replacing one medium with a plate having definite transmission and reflection properties. Referring to Fig. 8 we

may determine the potential at A by finding the intensity due directly to a current source at P and indirectly to the image of P at I. The apparent source at I will be diminished by a factor k. The effect of a source is inversely proportional to distance from the source, and therefore

$$V_A = \frac{I\rho_1}{4\pi}\left(\frac{1}{r_1} + \frac{k}{r_2}\right)$$

The potential at B will be due to the source P only, the strength being reduced by transmission through the plate, the amount lost being k times the original intensity.

Therefore, the potential at B is

$$V_B = \frac{I\rho_2}{4\pi}\left(\frac{1}{r_3} - \frac{k}{r_3}\right)$$

The image I has no effect at B since it is a virtual image on the same side of the plate.

At the boundary plane between the media there must be continuity of potential,

$$\therefore \quad V_A = V_B, \text{ and } r_1 = r_2 = r_3$$

$$\therefore \quad \frac{I\rho_1}{4\pi r}(1+k) = \frac{I\rho_2}{4\pi r}(1-k)$$

$$\therefore \quad \frac{\rho_1}{\rho_2} = \frac{1-k}{1+k}$$

$$\text{and } k = \frac{\rho_2-\rho_1}{\rho_2+\rho_1} = \frac{1-\frac{\rho_1}{\rho_2}}{1+\frac{\rho_1}{\rho_2}}$$

The reflection factor is thus a function of the ratio of the two resistivities. If the second medium is a perfect insulator ($\rho_2 = \infty$) then k = 1, and if a conductor ($\rho_2 = 0$), k = -1.

CHAPTER IV.

RESISTIVITY TRAVERSES

RESISTIVITY TRAVERSES

In addition to depth probing, traversing is a popular and often rewarding method of electrical surveying. The aim is to determine longitudinal variations in resistivity. The usual configuration employed is the Wenner with a constant electrode interval, i.e. the four electrodes are placed in a straight line at equal intervals apart, and the entire system is moved bodily.

The following techniques have been defined by M. King Hubbert (19) -

1. A traverse profile is a series of observations taken along a line of traverse while both electrode interval and the bearing are kept constant.
2. A longitudinal traverse profile is a traverse profile wherein the line of electrodes is parallel to the line of traverses.
3. A transverse traverse profile is a traverse profile taken with the line of electrodes at right angles to the line of traverses.

He went on to describe a longitudinal traverse over a known fault, in which he found that when the fault plane was located between one of the potential electrodes and one of the current electrodes the apparent resistivity was lower than the surrounding values, but when the fault was between the potential electrodes the resistivity was relatively high. This produced a W-shaped anomaly with a very high middle. Laboratory experiments with a thin sheet of metal simulating a conductive

fault plane gave exactly similar results. H.N. Johnson in the discussion of Hubbert's paper showed that a vertical insulator gave exactly the same effect. L.G. Howell, later on in the same discussion, treated the subject theoretically and practically, examining the potential distribution at the surface of a medium of uniform resistivity in which was placed a very thin vertical sheet of infinite extent, the sheet being treated both as a perfect insulator and a perfect conductor. The theoretical curve for an insulator was similar to Hubbert's profile over a fault, thus showing that the fault profile was due to the fault plane having a greater resistivity than the country rock. Similar results in the laboratory with metal sheets have been due to a film of dirt or oxide on the surfaces, so that the metal sheet tended to act as an insulator. When the sheet is thoroughly cleaned, it gives the profile characteristic of a conductor.

Howell evolved formulae and calculated curves for longitudinal traverses over an insulator and a conductor. It is suggested that it may be of interest to investigate traverses at varying angles to the strike of the sheet, since the strike of the anomaly may not be known beforehand, and, of course, in the general case it is not known.

Longitudinal Traverses.

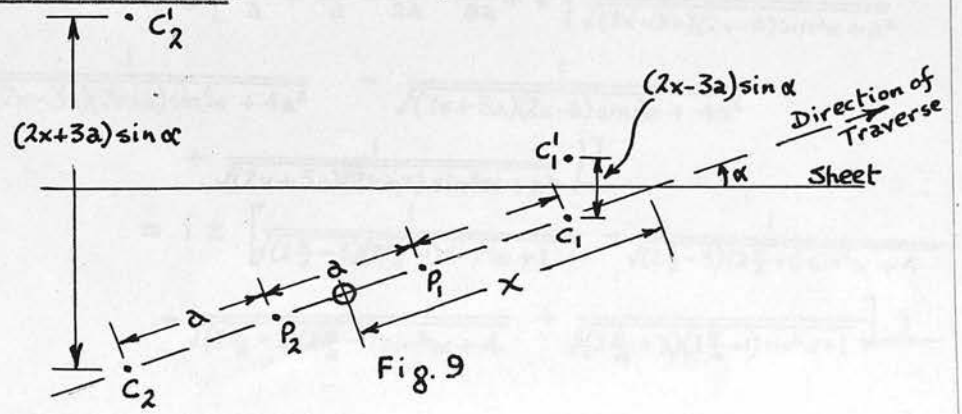

Fig. 9

Let the sheet be a perfect insulator or a perfect conductor with a reflection coefficient of $k = \pm 1$. The distance of the centre of the electrode system from the sheet, measured along the direction of traverse, is x; the angle between the direction of traverse and the sheet is α ; the sheet is surrounded by a medium of resistivity, ρ_1 .

Sheet to the right of C_1 (Fig. 9.)

The potentials at P_1 and P_2 are due to the current sources C_1 and C_2 plus the image effects of C_1' and C_2''. The image effects are multiplied by the factor $k = \pm 1$.

The various distances concerned are:-

$C_1P_1 = a$ $\qquad C_1P_2 = 2a$

$C_1'P_1 = \sqrt{(2x-3a)(2x-a)\sin^2\alpha + a^2}$ $\qquad C_1'P_2 = \sqrt{(2x-3a)(2x+a)\sin^2\alpha + 4a^2}$

$C_2P_1 = 2a$ $\qquad C_2P_2 = a$

$C_2'P_1 = \sqrt{(2x+3a)(2x-a)\sin^2\alpha + 4a^2}$ $\qquad C_2'P_2 = \sqrt{(2x+3a)(2x+a)\sin^2\alpha + a^2}$

$$\therefore \text{Potential at } P_1 = V_1 = \frac{I\rho_1}{2\pi}\left[\frac{1}{C_1P_1} + \frac{1}{C_1'P_1} - \frac{1}{C_2P_1} - \frac{1}{C_2'P_1}\right]$$

$$\text{and} \quad " \quad " \quad P_2 = V_2 = \frac{I\rho_1}{2\pi}\left[\frac{1}{C_1P_2} + \frac{1}{C_1'P_2} - \frac{1}{C_2P_2} - \frac{1}{C_2'P_2}\right]$$

$$\therefore V = V_1 - V_2 = \frac{I\rho_1}{2\pi}\left[\frac{1}{C_1P_1} + \frac{1}{C_2P_2} - \frac{1}{C_2P_1} - \frac{1}{C_1P_2} + \frac{1}{C_1'P_1} - \frac{1}{C_1'P_2} - \frac{1}{C_2'P_1} + \frac{1}{C_2'P_2}\right]$$

But the apparent resistivity is defined by

$$\rho_a = 2\pi a \frac{V}{I} \qquad (2)$$

$$\therefore V = \frac{I\rho_a}{2\pi a}$$

$$\text{and} \quad \frac{\rho_a}{\rho_1} = a\left[\frac{1}{C_1P_1} + \frac{1}{C_2P_2} - \cdots\cdots\right]$$

$$= a\left[\frac{1}{a} + \frac{1}{a} - \frac{1}{2a} - \frac{1}{2a} + k\left\{\frac{1}{\sqrt{(2x-3a)(2x-a)\sin^2\alpha + a^2}}\right.\right.$$

$$\left. - \frac{1}{\sqrt{(2x-3a)(2x+a)\sin^2\alpha + 4a^2}} - \frac{1}{\sqrt{(2x+3a)(2x-a)\sin^2\alpha + 4a^2}}\right.$$

$$\left.\left. + \frac{1}{\sqrt{(2x+3a)(2x+a)\sin^2\alpha + a^2}}\right\}\right]$$

$$= 1 \pm \left[\frac{1}{\sqrt{(2\frac{x}{a}-3)(2\frac{x}{a}-1)\sin^2\alpha + 1}} - \frac{1}{\sqrt{(2\frac{x}{a}-3)(2\frac{x}{a}+1)\sin^2\alpha + 4}}\right.$$

$$\left. - \frac{1}{\sqrt{(2\frac{x}{a}+3)(2\frac{x}{a}-1)\sin^2\alpha + 4}} + \frac{1}{\sqrt{(2\frac{x}{a}+3)(2\frac{x}{a}+1)\sin^2\alpha + 1}}\right] \qquad (3)$$

Sheet between C_1 and P_1 (Fig. 10).

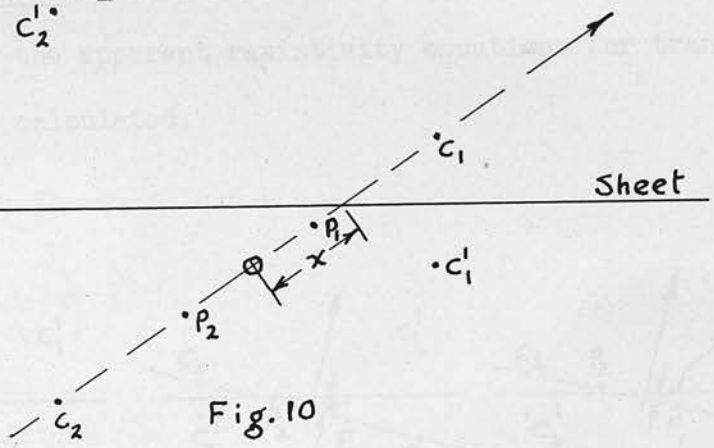

Fig. 10

C_1 has now no effect on the potential electrodes, P_1 and P_2, as it is cut off by the interposition of the vertical sheet.

The relevant distances are now:-

$C_2P_1 = 2a$ $\qquad C_2P_2 = a$

$C_2'P_1 = \sqrt{(2x+3a)(2x-a)\sin^2\alpha + 4a^2}$ $\qquad C_2'P_2 = \sqrt{(2x+3a)(2x+a)\sin^2\alpha + a^2}$

and we have

$$\frac{\rho_a}{\rho_1} = \frac{1}{2} \pm \left[\frac{1}{\sqrt{(2\frac{x}{a}+3)(2\frac{x}{a}+1)\sin^2\alpha + 1}} - \frac{1}{\sqrt{(2\frac{x}{a}+3)(2\frac{x}{a}-1)\sin^2\alpha + 4}} \right] \quad 4$$

Sheet between P_1 and P_2.

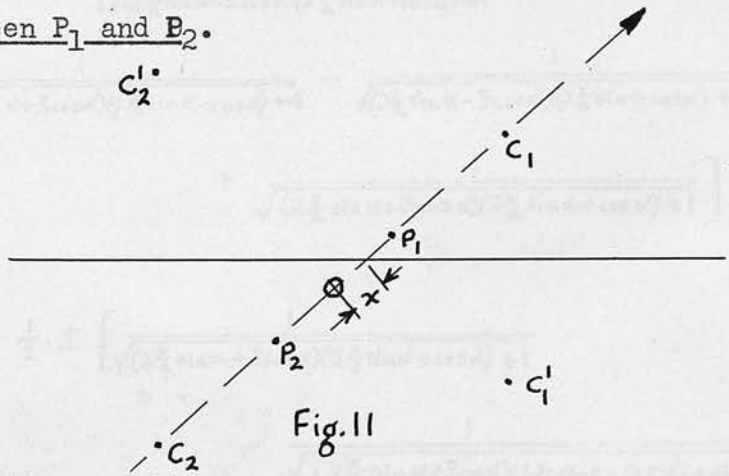

Fig. 11

In this case the image of C_1 will affect P_1 but not P_2, and vice versa with C_2.

The result is

$$\frac{\rho_a}{\rho_1} = 2 \pm \left[\frac{1}{\sqrt{(3-2\frac{x}{a})(1-2\frac{x}{a})\sin^2\alpha + 1}} + \frac{1}{\sqrt{(3+2\frac{x}{a})(1+2\frac{x}{a})\sin^2\alpha + 1}} \right] \quad 5$$

Transverse Traverses.

Similarly the apparent resistivity equations for transverse traverses may be calculated.

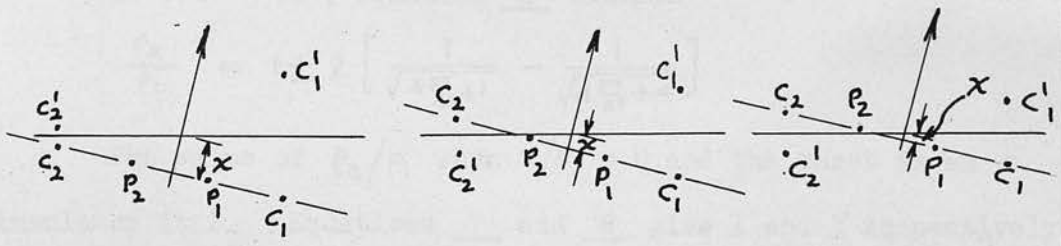

Case I Case II Case III

Fig. 12

The three necessary equations are:-

Case I

$$\frac{\rho_a}{\rho_1} = 1 \pm \left[\frac{1}{\sqrt{(2\frac{x}{a}\sin\alpha - 3\cos\alpha)(2\frac{x}{a}\sin\alpha - \cos\alpha) + 1}} - \frac{1}{\sqrt{(2\frac{x}{a}\sin\alpha + 3\cos\alpha)(2\frac{x}{a}\sin\alpha - \cos\alpha) + 4}} - \frac{1}{\sqrt{(2\frac{x}{a}\sin\alpha - 3\cos\alpha)(2\frac{x}{a}\sin + \cos\alpha) + 4}} + \frac{1}{\sqrt{(2\frac{x}{a}\sin\alpha + 3\cos\alpha)(2\frac{x}{a}\sin\alpha + \cos\alpha) + 1}} \right] \quad 6$$

Case II

$$\frac{\rho_a}{\rho_1} = \frac{1}{2} \pm \left[\frac{1}{\sqrt{(2\frac{x}{a}\sin\alpha + 3\cos\alpha)(2\frac{x}{a}\sin\alpha + \cos\alpha) + 1}} - \frac{1}{\sqrt{(2\frac{x}{a}\sin\alpha + 3\cos\alpha)(2\frac{x}{a}\sin\alpha - \cos\alpha) + 4}} \right] \quad 7$$

Case III

$$\frac{\rho_a}{\rho_1} = 2 \pm \left[\frac{1}{\sqrt{(3\cos\alpha - 2\frac{x}{a}\sin\alpha)(\cos\alpha - 2\frac{x}{a}\sin\alpha) + 1}} + \frac{1}{\sqrt{(3\cos\alpha + 2\frac{x}{a}\sin\alpha)(\cos\alpha + 2\frac{x}{a}\sin\alpha) + 1}} \right] \quad 8$$

In the case of a transverse traverse with the line of electrodes at right angles to the direction of advance, and parallel to the strike of the sheet, we must use equation 6 to give the whole shape of the apparent resistivity curve.

If $\alpha = 90^\circ$, equation 6 becomes

$$\frac{\rho_a}{\rho_1} = 1 \pm 2\left[\frac{1}{\sqrt{4\frac{x^2}{a^2}+1}} - \frac{1}{\sqrt{4\frac{x^2}{a^2}+4}}\right]$$

The value of ρ_a/ρ_1 when $x/a = 0$ and the sheet is an insulator is 2. Equations 7 and 8 give 1 and 3 respectively. This simply means that the value of apparent resistivity when the electrodes lie along the sheet is indeterminate since no current can flow or potential be measured. The curve on either side will, however, be correct, and this tends to the value 2.

From these equations, curves (Figs. 13 to 16) have been drawn showing how the apparent resistivity varies in traverses across vertical sheets. The angles α are given values from 0° to 90°, at intervals of 15°. These curves indicate the following points:-

1. Longitudinal Traverses over Vertical Insulators (Fig. 13).

All the curves show an increase in apparent resistivity as the electrode system approaches the sheet, reaching a value slightly less than 1.5 times the normal resistivity as the first current electrode reaches the sheet. When the sheet is between a current and potential electrode the resistivity is below normal, while between the potential electrodes there is an increase in resistivity. The reason for this paradox is that, with the sheet situated between a current and potential electrode, there

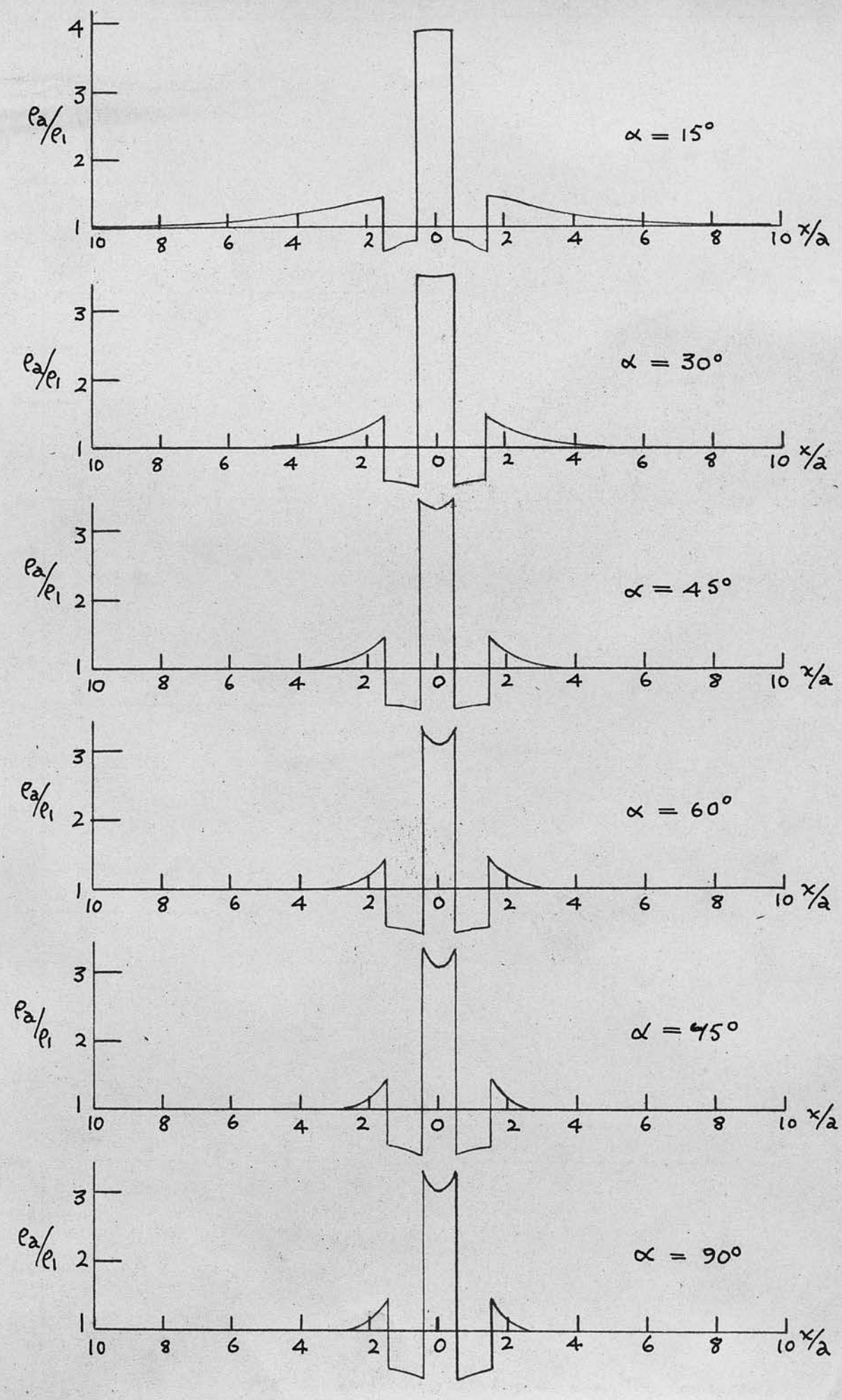

Fig. 13 Longitudinal Traverses over Thin Insulators

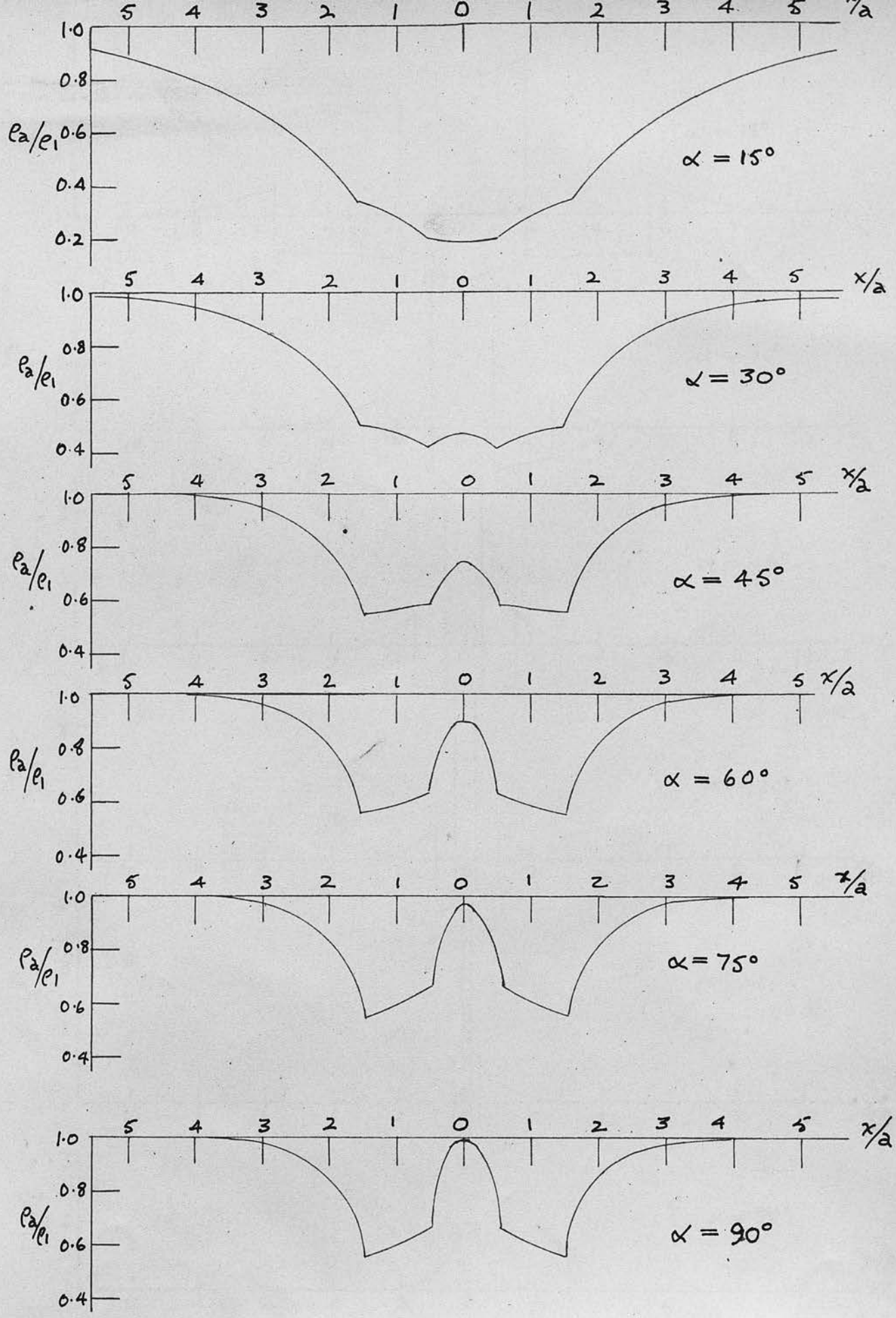

Fig. 14 Longitudinal Traverses over Thin Conductors

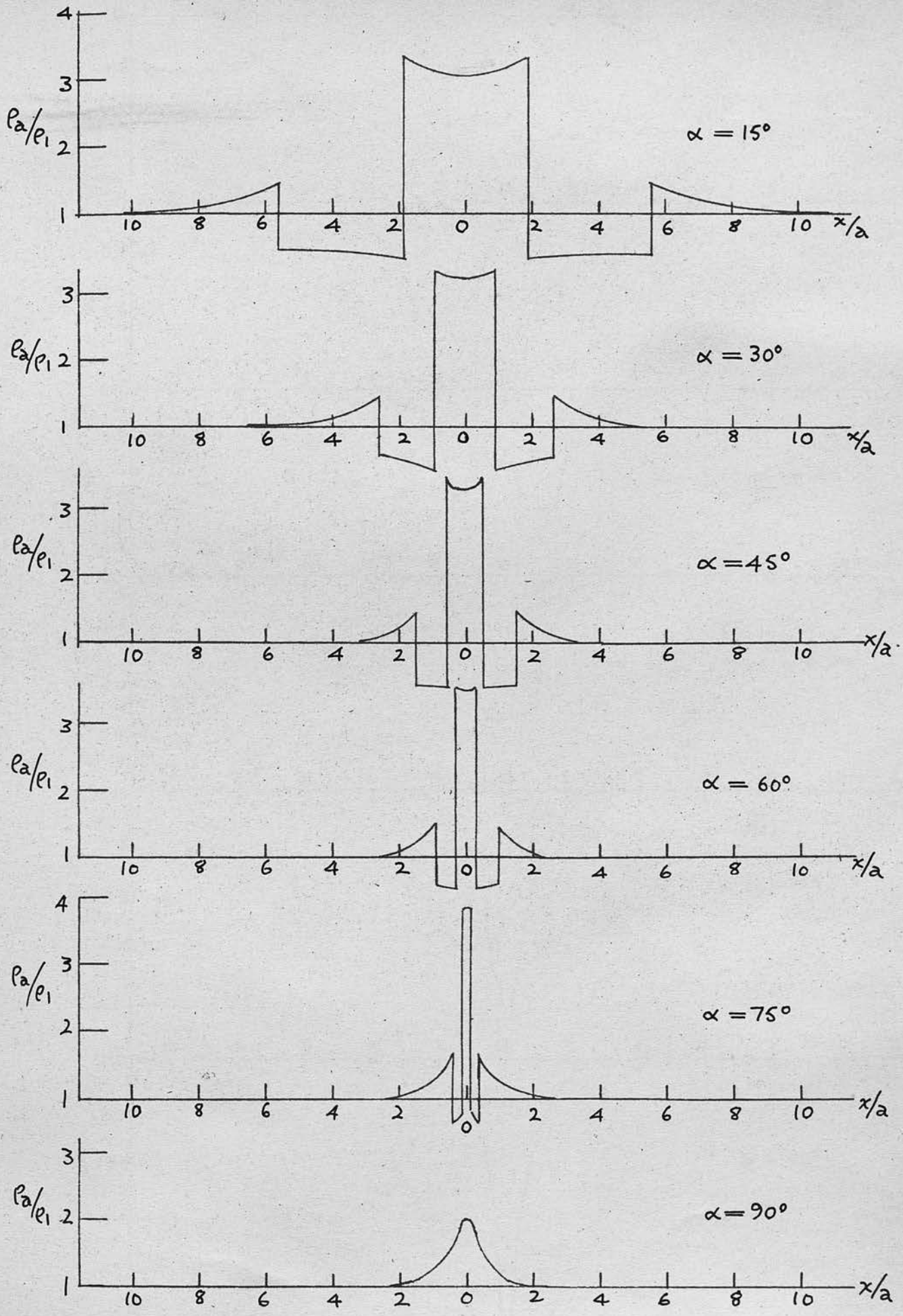

Fig. 15 Transverse Traverses over Thin Insulators

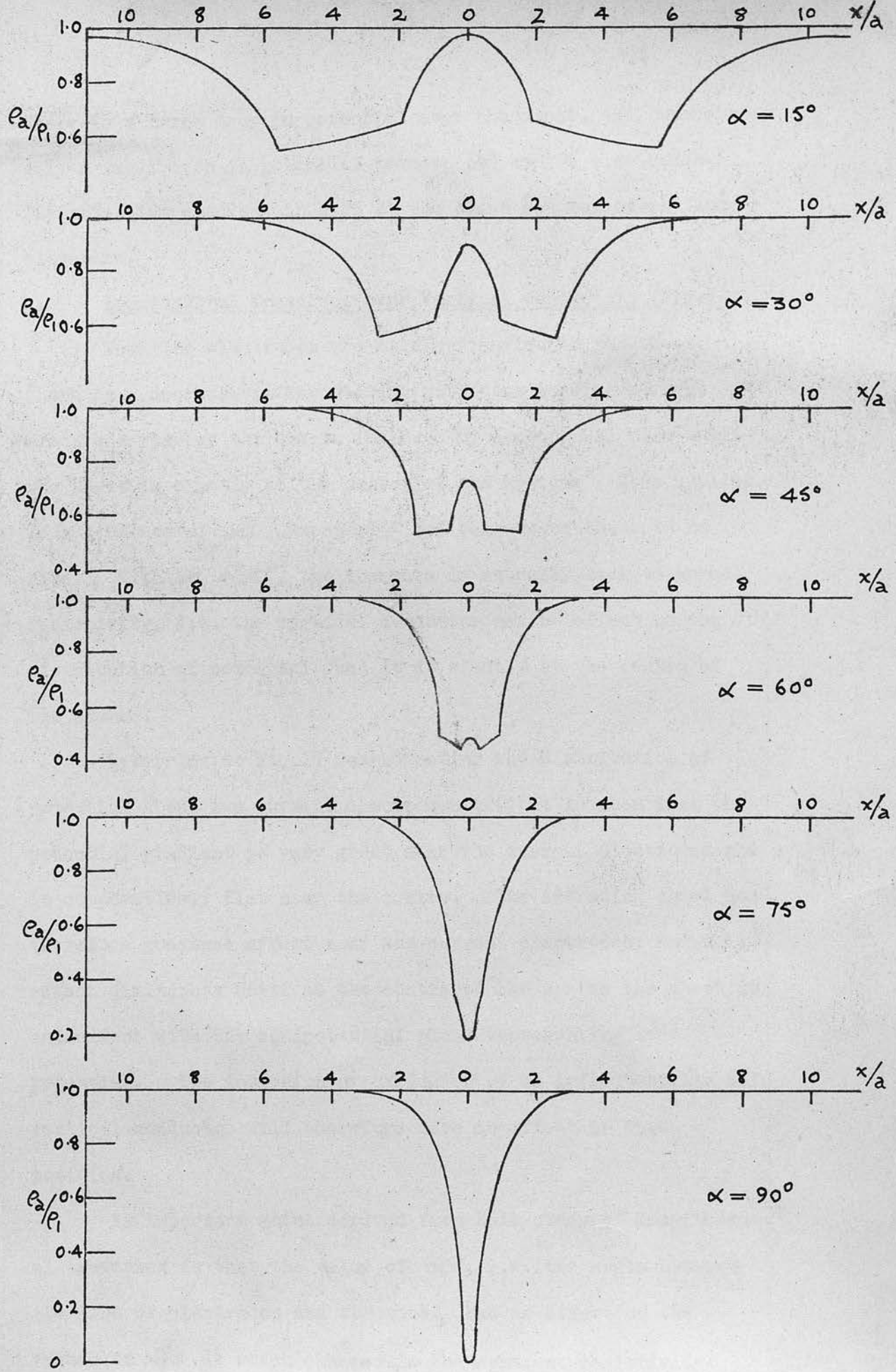

Fig. 16 Transverse Traverses over Thin Conductors

there is a large drop in potential over the sheet, and, therefore, only a small drop in potential between the centre electrodes. The potential gradient is high at the sheet and relatively low elsewhere.

2. Longitudinal Traverses over Vertical Conductors (Fig.14).

When the electrodes are at right angles to the sheet, there is a decrease in resistivity until the leading current electrode reaches the sheet, followed by a continual rise until the sheet is exactly at the centre of the system. This applies to all values of α , except 15° and below when there is no rise. With $\alpha = 90^{\circ}$, the increase is actually back to normal resistivity, i.e. the vertical conductor has no effect on the distribution of potential when it is exactly at the centre of the system.

Referring to Fig.17 demonstrating the distribution of potential about two current electrodes (20) it is seen that the potential gradient is very great near the current electrodes and is comparatively flat near the centre. The intruding sheet has therefore greatest effect near the current electrodes, and this effect diminishes until at the centre of the system the sheet is coincident with the equipotential plane representing zero potential. The inclusion or exclusion of an infinitesmally thin vertical conductor will therefore have no effect in that position.

An important point derived from this study of longitudinal traverses is that the value of α , i.e. the angle between the line of electrodes and the sheet, has no effect on the values of x/a at which changes in the apparent resistivity

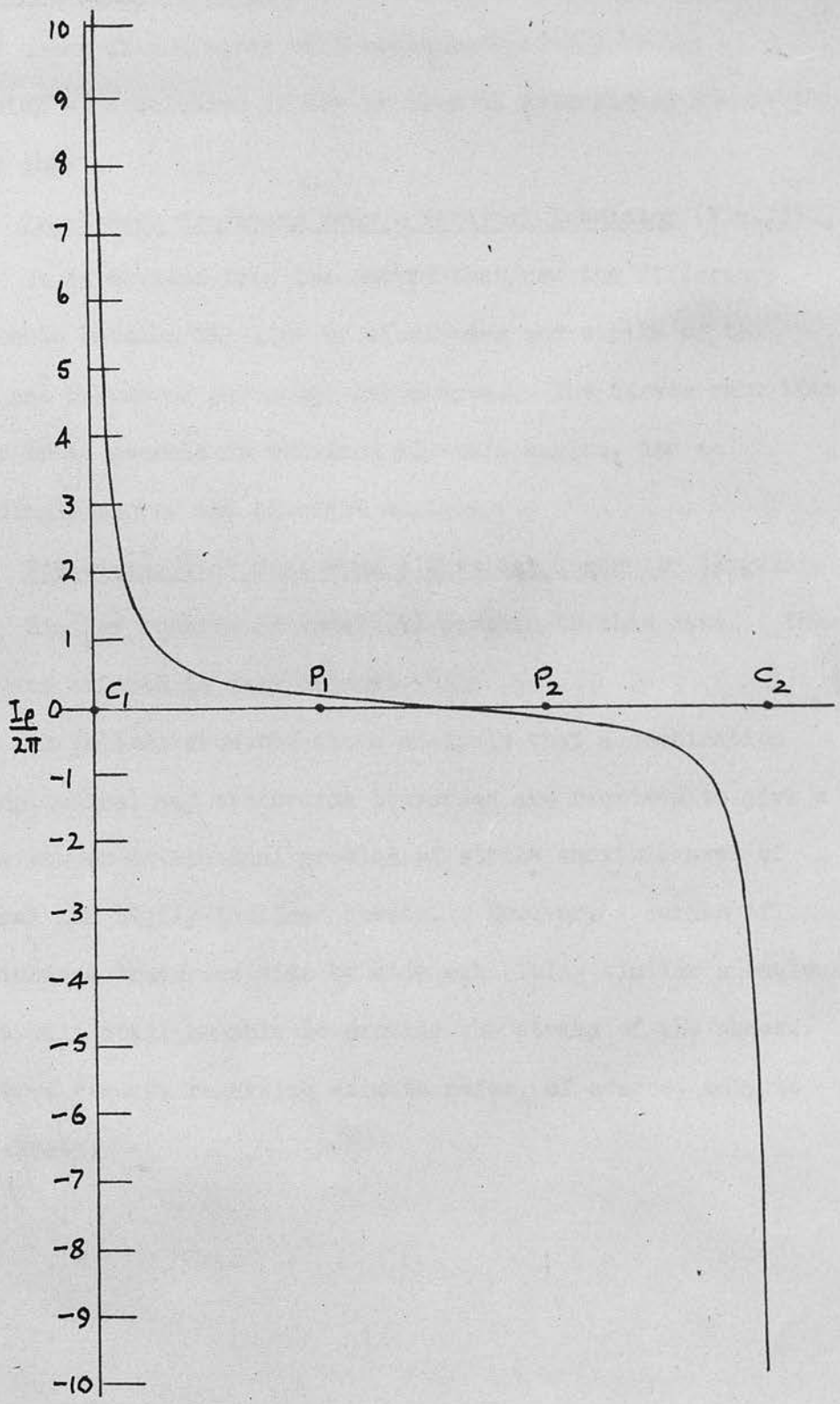

Fig. 17, Distribution of Potential between Two Current Electrodes, 10 cm. apart

curve occur. Indeed, in the case of an insulator a thin sheet buried under slight cover will contribute little to the provision of a solution to the problem of determining the strike of the sheet.

3. Transverse Traverses over a Vertical Insulator (Fig.15).

It is obvious from the curves that now the difference of azimuth between the line of electrodes and strike of the sheet has become of paramount importance. The curves show that a very broad anomaly is obtained at small angles, and an exceedingly narrow one at right angles.

4. Transverse Traverses over a Vertical Conductor (Fig.16).

Similar remarks as under (3) pertain to this case. The effect of azimuth is very evident.

It follows from the above analysis that a combination of longitudinal and transverse traverses are required to give a unique answer to the dual problem of strike and thickness of vertical and highly inclined sheets. However, a series of longitudinal traverses side by side exhibiting similar anomalous curves will still be able to provide the strike of the sheet. The above remarks regarding azimuth refer, of course, only to thin sheets.

CHAPTER V.

GENERAL PROBLEM OF TRAVERSES OVER VERTICAL SHEETS OF DIFFERENT THICKNESSES AND RESISTIVITIES

GENERAL PROBLEM OF TRAVERSES OVER VERTICAL SHEETS OF DIFFERENT THICKNESSES AND RESISTIVITIES

The problem of traversing over infinitesmally thin insulating and conducting sheets has been investigated in Chapter IV. We come now to the examination of the case more probable in nature, viz. that of traverses over vertical sheets such as dykes and fault planes. The faults will normally provide very thin anomalies, and their resistivities will also vary greatly. A fault full of broken, shattered rock will tend to have a high resistivity. If it contains water and this water is able to flow freely (probably the commonest case), then the water will be relatively pure and the resistivity again high. If the fault plane is a mineralised zone it is possible that the fault may be conductive compared with the adjacent strata. Thicker sheets may be represented by dykes or vertical strata of different resistivities.

Statement of Problem.

The solution desired is that of the potential at any point due to a current source, the two media of resistivity ρ_1 being separated by a parallel-sided sheet of resistivity ρ_2 and thickness d, as in Fig. 18.

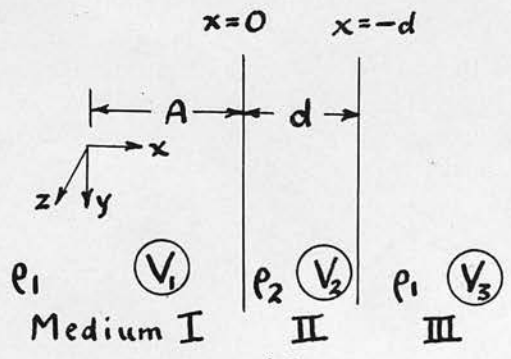

Fig. 18

The method used is similar to that used in "Exploration Geophysics" by J.J. Jakosky, pp. 483-9, for the

derivation of the two-layer formula for horizontal strata.

Solution of Problem.

Let the plane yz (x = 0) separate two media I and II with resistivities ρ_1 and ρ_2, and another yz plane (x = -d) separate two media of resistivities ρ_2 and ρ_1.

So we have:-

in medium I, $x \geqslant 0$;

in medium II, $0 \geqslant x \geqslant -d$;

in medium III, $x \leqslant -d$.

Consider a small source of current S situated at a distance A from the yz plane (x = 0) in the positive direction. To arrive at the potential distribution we have to find the potentials due to the source and its various images in the three media, the potentials having to be expressed in terms of the current source. The potential values in the respective media are V_1, V_2 and V_3. The images are shown in Fig. 19.

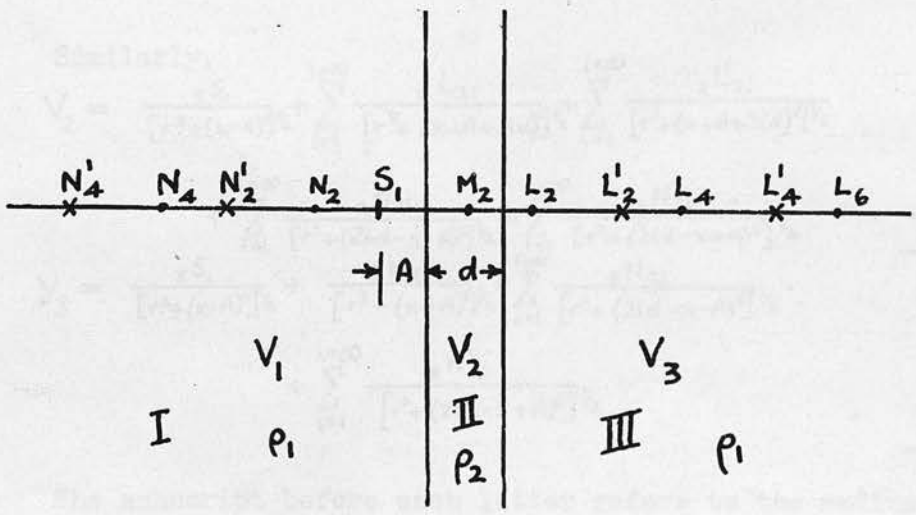

Fig. 19 Images due to a Point Source in Medium I

Referring to Fig.19 the current source S_1 has an image M_2 in medium II due to reflection in the plane yz (x = 0). By successive reflections in the two planes we obtain the images L_2, N_2, L_4, N_4 ..... L_{2i}, N_{2i}, where i is a positive integer varying from 1 to ∞ . Similarly, by reflecting from the plane yz (x = -d) initially, we have the images L^1_2, N^1_2, L^1_4, N^1_4 ..... L^1_{2i}, N^1_{2i}. From the theory of images, no image can have an effect on a point situated in the same medium.

The potential at a point is inversely proportional to its distance from the source or image. Since we are only interested in the x direction, we may replace the co-ordinates (x,y,z) of a point by the co-ordinates (x,r) where $r = \sqrt{y^2 + z^2}$.

The potential V_1, in the region $x \geqslant 0$ is:-

$$V_1 = \frac{{}_1S_1}{[r^2+(x-A)^2]^{1/2}} + \frac{{}_1M_2}{[r^2+(x+A)^2]^{1/2}} + \frac{{}_1L_2}{[r^2+(x-A+2d)^2]^{1/2}}$$
$$+ \frac{{}_1L_4}{[r^2+(x-A+4d)^2]^{1/2}} + \cdots + \frac{{}_1L'_2}{[r^2+(x+A+2d)^2]^{1/2}} + \frac{{}_1L'_4}{[r^2+(x+A+4d)^2]^{1/2}} + \cdots$$
$$= \frac{{}_1S_1}{[r^2+(x-A)^2]^{1/2}} + \frac{{}_1M_2}{[r^2+(x+A)^2]^{1/2}} + \sum_{i=1}^{i=\infty} \frac{{}_1L_{2i}}{[r^2+(x-A+2id)^2]^{1/2}}$$
$$+ \sum_{i=1}^{i=\infty} \frac{{}_1L'_{2i}}{[r^2+(x+A+2id)^2]^{1/2}} \qquad 9$$

Similarly,

$$V_2 = \frac{{}_2S_1}{[r^2+(x-A)^2]^{1/2}} + \sum_{i=1}^{i=\infty} \frac{{}_2L_{2i}}{[r^2+(x-A+2id)^2]^{1/2}} + \sum_{i=1}^{i=\infty} \frac{{}_2L'_{2i}}{[r^2+(x+A+2id)^2]^{1/2}}$$
$$+ \sum_{i=1}^{i=\infty} \frac{{}_2N_{2i}}{[r^2+(2id-x-A)^2]^{1/2}} + \sum_{i=1}^{i=\infty} \frac{{}_2N'_{2i}}{[r^2+(2id-x+A)^2]^{1/2}} \qquad 10$$

and

$$V_3 = \frac{{}_3S_1}{[r^2+(x-A)^2]^{1/2}} + \frac{{}_3M_2}{[r^2+(x+A)^2]^{1/2}} + \sum_{i=1}^{i=\infty} \frac{{}_3N_{2i}}{[r^2+(2id-x-A)^2]^{1/2}}$$
$$+ \sum_{i=1}^{i=\infty} \frac{{}_3N'_{2i}}{[r^2+(2id-x+A)^2]^{1/2}} \qquad 11$$

The subscript before each letter refers to the medium in which the effect is to be investigated.

Since the symbol $\sum_{i=1}^{i=\infty}$ will be repeated many times the symbol $\sum$ only will be used to imply the range from i = 1 to i = ∞ . The range will be stated if it differs.

The solutions must satisfy the following conditions (21):-

1. The potential at all points must satisfy Laplace's equation defining the steady state of electrical flow, i.e.:-

$$\frac{\partial^2 V}{\partial x^2} + \frac{\partial^2 V}{\partial y^2} + \frac{\partial^2 V}{\partial z^2} = 0 \qquad 12$$

2. The potential function must suffer no discontinuity at the boundary plane, i.e. when x = 0, $V_1 = V_2$ and when x = -d, $V_2 = V_3$.

13

3. At the boundary plane, the component of the current density normal to this plane must be the same computed from either side, i.e.

when x = 0, $(i_1)_x = (i_2)_x$,

and x = -d, $(i_2)_x = (i_3)_x$.

Ohm's Law, in its differential form is

$$i_x = -\frac{1}{\rho} \cdot \frac{\partial V}{\partial x}$$

$$\therefore \quad \frac{1}{\rho_1} \cdot \frac{\partial V_1}{\partial x} = \frac{1}{\rho_2} \cdot \frac{\partial V_2}{\partial x} \text{ at } x = 0 \qquad 14$$

and

$$\frac{1}{\rho_2} \cdot \frac{\partial V_2}{\partial x} = \frac{1}{\rho_1} \cdot \frac{\partial V_3}{\partial x} \text{ at } x = -d \qquad 15$$

It can be shown that Laplace's equation 12 holds for each equation, 9 , 10 , and 11 , since the sum of the double partial derivatives with respect to x, y and z is zero. All

the terms are of the same form:-

$$f(x,y,z) = \frac{1}{[r^2+(x-c)^2]^{1/2}} = \frac{1}{[y^2+z^2+(x-c)^2]^{1/2}}$$

$$\therefore \frac{\partial f}{\partial x} = -\frac{(x-c)}{[y^2+z^2+(x-c)^2]^{3/2}}$$

$$\text{and } \frac{\partial^2 f}{\partial x^2} = -\frac{[y^2+z^2+(x-c)^2]^{3/2} - 3(x-c)^2[y^2+z^2+(x-c)^2]^{1/2}}{[y^2+z^2+(x-c)^2]^3}$$

$$\text{also } \frac{\partial^2 f}{\partial y^2} = -\frac{[y^2+z^2+(x-c)^2]^{3/2} - 3y^2[y^2+z^2+(x-c)^2]^{1/2}}{[y^2+z^2+(x-c)^2]^3}$$

$$\text{and } \frac{\partial^2 f}{\partial z^2} = -\frac{[y^2+z^2+(x-c)^2]^{3/2} - 3z^2[y^2+z^2+(x-c)^2]^{1/2}}{[y^2+z^2+(x-c)^2]^3}$$

$$\therefore \frac{\partial^2 f}{\partial x^2} + \frac{\partial^2 f}{\partial y^2} + \frac{\partial^2 f}{\partial z^2} = -\frac{3[y^2+z^2+(x-c)^2]^{3/2} - 3[y^2+z^2+(x-c)^2]^{3/2}}{[y^2+z^2+(x-c)^2]^3} = 0$$

This result will be identical for all terms in all equations, so that Laplace's equation is satisfied throughout.

We now proceed to evaluate the effects of the various images in terms of ${}_1S_1$, the current source, by means of equations 13, 14 and 15.

At $x = 0$, $V_1 = V_2$

$$\therefore \frac{{}_1S_1}{[r^2+A^2]^{1/2}} + \frac{{}_1M_2}{[r^2+A^2]^{1/2}} + \sum \frac{{}_1L_{2i}}{[r^2+(2id-A)^2]^{1/2}} + \sum \frac{{}_1L'_{2i}}{[r^2+(2id+A)^2]^{1/2}}$$

$$= \frac{{}_2S_1}{[r^2+A^2]^{1/2}} + \sum \frac{{}_2L_{2i}}{[r^2+(2id-A)^2]^{3/2}} + \sum \frac{{}_2L'_{2i}}{[r^2+(2id+A)^2]^{1/2}}$$

$$+ \sum \frac{{}_2N_{2i}}{[r^2+(2id-A)^2]^{1/2}} + \sum \frac{{}_2N'_{2i}}{[r^2+(2id+A)^2]^{1/2}}$$

By equating those terms whose denominators are equal we obtain:-

$${}_1S_1 + {}_1M_2 = {}_2S_1 \qquad 16$$

$${}_1L_{2i} = {}_2L_{2i} + {}_2N_{2i} \qquad 17$$

$${}_1L'_{2i} = {}_2L'_{2i} + {}_2N'_{2i} \qquad 18$$

Again, at $x = -d$, $V_2 = V_3$,

$$\therefore \frac{{}_2S_1}{[r^2+(-d-A)^2]^{1/2}} + \sum \frac{{}_2L_{2i}}{[r^2+(2i-1\,d-A)^2]^{1/2}} + \sum \frac{{}_2L'_{2i}}{[r^2+(2i-1\,d+A)^2]^{1/2}}$$

$$+ \sum \frac{{}_2N_{2i}}{[r^2+(2i+1\,d-A)^2]^{1/2}} + \sum \frac{{}_2N'_{2i}}{[r^2+(2i+1\,d+A)^2]^{1/2}} = \frac{{}_3S_1}{[r^2+(-d-A)^2]^{1/2}}$$

$$+ \frac{{}_3M_2}{[r^2+(-d+A)^2]^{1/2}} + \sum \frac{{}_3N_{2i}}{[r^2+(2i+1\,d-A)^2]^{1/2}} + \sum \frac{{}_3N'_{2i}}{[r^2+(2i+1\,d+A)^2]^{1/2}}$$

This gives:-

$${}_2S_1 + {}_2L'_2 = {}_3S_1 \qquad 19$$

$${}_2L_2 = {}_3M_2 \qquad 20$$

$${}_2L_{2i} + {}_2N_{2(i-1)} = {}_3N_{2(i-1)} \text{ for } i = 2,3,4,\text{etc.} \qquad 21$$

$${}_2L'_{2i} + {}_2N'_{2(i-1)} = {}_3N'_{2(i-1)} \text{ for } i = 2,3,4,\text{etc.} \qquad 22$$

Under the conditions required by the equation 14 at $x = 0$,

$$\frac{1}{\rho_1}\left\{ - \frac{{}_1S_1(x-A)}{[r^2+(x-A)^2]^{3/2}} - \frac{{}_1M_2(x+A)}{[r^2+(x+A)^2]^{3/2}} - \sum \frac{{}_1L_{2i}(x-A+2id)}{[r^2+(x-A+2id)^2]^{3/2}} \right.$$

$$\left. - \sum \frac{{}_1L'_{2i}(x+A+2id)}{[r^2+(x+A+2id)^2]^{3/2}} \right\} = \frac{1}{\rho_2}\left\{ - \frac{{}_2S_1(x-A)}{[r^2+(x-A)^2]^{3/2}} - \sum \frac{{}_2L_{2i}(x-A+2id)}{[r^2+(x-A+2id)^2]^{3/2}} \right.$$

$$\left. - \sum \frac{{}_2L'_{2i}(x+A+2id)}{[r^2+(x+A+2id)^2]^{3/2}} + \sum \frac{{}_2N_{2i}(2id-x-A)}{[r^2+(2id-x-A)^2]^{3/2}} + \sum \frac{{}_2N'_{2i}(2id-x+A)}{[r^2+(2id-x+A)^2]^{3/2}} \right\}$$

which gives:-

$$\frac{1}{\rho_1}\left\{ \frac{{}_1S_1 \cdot A}{[r^2+A^2]^{3/2}} - \frac{{}_1M_2 \cdot A}{[r^2+A^2]^{3/2}} + \sum \frac{{}_1L_{2i}(A-2id)}{[r^2+(A-2id)^2]^{3/2}} - \sum \frac{{}_1L'_{2i}(A+2id)}{[r^2+(A+2id)^2]^{3/2}} \right\}$$

$$= \frac{1}{\rho_2}\left\{ \frac{{}_2S_1 \cdot A}{[r^2+A^2]^{3/2}} + \sum \frac{{}_2L_{2i}(A-2id)}{[r^2+(A-2id)^2]^{3/2}} - \sum \frac{{}_2L'_{2i}(A+2id)}{[r^2+(A+2id)^2]^{3/2}} \right.$$

$$\left. - \sum \frac{{}_2N_{2i}(A-2id)}{[r^2+(A-2id)^2]^{3/2}} + \sum \frac{{}_2N'_{2i}(A+2id)}{[r^2+(A+2id)^2]^{3/2}} \right\}$$

whence,

$$\frac{{}_1S_1}{\rho_1} - \frac{{}_1M_2}{\rho_1} = \frac{{}_2S_1}{\rho_2} \qquad 23$$

$$\frac{{}_1L_{2i}}{\rho_1} = \frac{{}_2L_{2i}}{\rho_2} - \frac{{}_2N_{2i}}{\rho_2} \qquad 24$$

$$\frac{{}_1L'_{2i}}{\rho_1} = \frac{{}_2L'_{2i}}{\rho_2} - \frac{{}_2N'_{2i}}{\rho_2} \qquad 25$$

Similarly by equation 15 we obtain

$$\frac{{}_2S_1}{\rho_2} - \frac{{}_2L'_2}{\rho_2} = \frac{{}_3S_1}{\rho_1} \qquad 26$$

$$-\frac{{}_2L_2}{\rho_2} = \frac{{}_3M_2}{\rho_1} \qquad 27$$

$$-\frac{{}_2L_{2i}}{\rho_2} + \frac{{}_2N_{2(i-1)}}{\rho_2} = \frac{{}_3N_{2(i-1)}}{\rho_1} \quad \text{for } i = 2,3,4, \text{etc.} \qquad 28$$

$$-\frac{{}_2L'_{2i}}{\rho_2} + \frac{{}_2N'_{2(i-1)}}{\rho_2} = \frac{{}_3N'_{2(i-1)}}{\rho_1} \quad \text{for } i = 2,3,4, \text{etc.} \qquad 29$$

To solve these equations in terms of ${}_1S_1$ let

$$k = \frac{\rho_2 - \rho_1}{\rho_2 + \rho_1}$$

Then $1 + k = \frac{2\rho_2}{\rho_2 + \rho_1}$ and $1 - k = \frac{2\rho_1}{\rho_2 + \rho_1}$

From 16 and 23,

$$\frac{2}{\rho_1} \cdot {}_1S_1 = \frac{{}_2S_1}{\rho_1} + \frac{{}_2S_1}{\rho_2}$$

$$\therefore \; {}_2S_1 = \frac{2\rho_2}{\rho_2 + \rho_1} \cdot {}_1S_1 = (1+k) \cdot {}_1S_1$$

and $${}_1M_2 = k \cdot {}_1S_1$$

From 19 and 26

$${}_3S_1 = (1-k) \cdot {}_2S_1 = (1-k^2) \cdot {}_1S_1$$

and $${}_2L'_2 = -k(1+k) {}_1S_1$$

From 20 and 27

$${}_2L_1 = {}_3M_2 = 0$$

From 17 and 24

$$ {}_2L_{2i} = \frac{1}{1-k} \cdot {}_1L_{2i} $$

and $$ {}_2N_{2i} = -k \cdot {}_2L_{2i} = \frac{-k}{1-k} \cdot {}_1L_{2i} $$

Similarly from 18 and 25

$$ {}_2L'_{2i} = \frac{1}{1-k} \cdot {}_1L'_{2i} $$

and $$ {}_2N'_{2i} = -k \cdot {}_2L'_{2i} = \frac{-k}{1-k} \cdot {}_1L'_{2i} $$

From 21 and 28

$$ {}_3N_{2(i-1)} = \left(1 - \frac{1}{k}\right) \cdot {}_2L_{2i} $$

and $$ {}_2N_{2(i-1)} = -\frac{1}{k} \cdot {}_2L_{2i} = \frac{1}{1-k} \cdot {}_3N_{2(i-1)} $$

From 22 and 29

$$ {}_3N'_{2(i-1)} = \left(1 - \frac{1}{k}\right) \cdot {}_2L'_{2i} $$

and $$ {}_2N'_{2(i-1)} = -\frac{1}{k} \cdot {}_2L'_{2i} = \frac{1}{1-k} \cdot {}_3N'_{2(i-1)} $$

$$ \therefore {}_2N'_{2i} = -k \cdot {}_2L'_{2i} = k^2 \cdot {}_2N'_{2(i-1)} = -k^3 \cdot {}_2L'_{2(i-1)} $$

$$ = k^4 \cdot {}_2N'_{2(i-2)} = -k^5 \cdot {}_2L'_{2(i-2)} = \ldots\ldots $$

$$ \ldots\ldots\ldots = k^{2n} \cdot {}_2N'_{2(i-n)} = -k^{2n+1} \cdot {}_2L'_{2(i-n)} . $$

Let $i-n = 1$, or $n = i-1$.

$$ \therefore {}_2N'_{2i} = -k^{2i-1} \cdot {}_2L'_2 = k^{2(i-1)} \cdot {}_2N'_2 . $$

But $$ {}_2L'_2 = -k(1+k) \cdot {}_1S_1 $$

$$ \therefore {}_2N'_{2i} = k^{2i}(1+k) \cdot {}_1S_1 $$

and $$ {}_2L'_{2i} = -k^{2i-1}(1+k) \cdot {}_1S_1 $$

Also $$ {}_1L'_{2i} = (1-k) \cdot {}_2L'_{2i} $$

$$ = -k^{2i-1}(1-k^2) \cdot {}_1S_1 $$

$$ {}_3N'_{2(i-1)} = (1-k) \cdot {}_2N'_{2(i-1)} = \frac{1-k}{k^2} \cdot {}_2N'_{2i} $$

$$ = \frac{1}{k^2} \cdot {}_3N'_{2i} $$

$$\therefore\ {}_3N'_{2i} = (1-k)\ {}_2N'_{2i} = k^{2i}(1-k^2)\ {}_1S_1$$

Similarly, $${}_2N_{2i} = -k^{2i-1}\ {}_2L'_2 = 0$$

$$\therefore\ {}_2N_{2i} = {}_2L_{2i} = {}_1L_{2i} = {}_3N_{2i} = 0$$

Equations 9, 10 and 11 now become

$$V_1 = {}_1S_1\left\{\frac{1}{[r^2+(x-A)^2]^{1/2}} + \frac{k}{[r^2+(x+A)^2]^{1/2}} - \sum\frac{k^{2i-1}(1-k^2)}{[r^2+(2id+x+A)^2]^{1/2}}\right\} \qquad 30$$

$$V_2 = {}_1S_1\left\{\frac{1+k}{[r^2+(x-A)^2]^{1/2}} - \sum\frac{k^{2i-1}(1+k)}{[r^2+(2id+x+A)^2]^{1/2}} + \sum\frac{k^{2i}(1+k)}{[r^2+(2id-x+A)^2]^{1/2}}\right\} \qquad 31$$

$$V_3 = {}_1S_1\left\{\frac{1-k^2}{[r^2+(x-A)^2]^{1/2}} + \sum\frac{k^{2i}(1-k^2)}{[r^2+(2id-x+A)^2]^{1/2}}\right\} \qquad 32$$

The equations 30, 31 and 32 can be simplified if all current sources are considered to be located on the x - axis, giving y = z = r = 0. It is important that the positive value of the denominator is always taken.

$$\therefore\ V_1 = {}_1S_1\left\{\frac{1}{|x-A|} + \frac{k}{|x+A|} - \sum\frac{k^{2i-1}(1-k^2)}{|2id+x+A|}\right\} \qquad 33$$

$$V_2 = {}_1S_1\left\{\sum_{i=0}^{\infty}\frac{k^{2i}(1+k)}{|2id-x+A|} - \sum\frac{k^{2i-1}(1+k)}{|2id+x+A|}\right\} \qquad 34$$

and $$V_3 = {}_1S_1\left\{\sum_{i=0}^{\infty}\frac{k^{2i}(1-k^2)}{|2id-x+A|}\right\} \qquad 35$$

By the same method, we may consider the case where the current source S is located within the second medium. The images are as shown in Fig. 20.

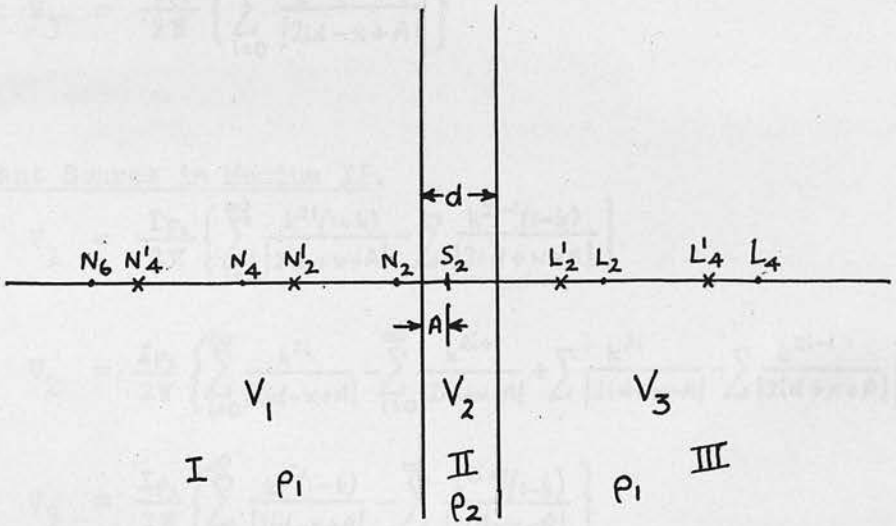

Fig. 20 Images due to a Point Source in Medium II

The relevant equations are:-

$$V_1 = {}_2S_2\left\{\sum_{i=0}^{\infty}\frac{k^{2i}(1-k^2)}{|2id+x-A|} - \sum\frac{k^{2i-1}(1-k)}{|2id+x+A|}\right\} \qquad 36$$

$$V_2 = {}_2S_2\left\{\sum_{i=0}^{\infty}\frac{k^{2i}}{|2id-x+A|} - \sum_{i=0}^{\infty}\frac{k^{2i+1}}{|2id-x-A|} + \sum\frac{k^{2i}}{|2id+x-A|} - \sum\frac{k^{2i-1}}{|2id+x+A|}\right\} \qquad 37$$

and $$V_3 = {}_2S_2\left\{\sum_{i=0}^{\infty}\frac{k^{2i}(1-k)}{|2id-x+A|} - \sum_{i=0}^{\infty}\frac{k^{2i+1}(1-k)}{|2id-x-A|}\right\} \qquad 38$$

In a semi-infinite medium, where the source is situated on the plane dividing the medium from air of infinite resistivity, then

$${}_1S_1 = \frac{I\rho_1}{2\pi}$$

Thus the operative equations for point sources situated at the surface are:-

Current Source in Medium I.

$$V_1 = \frac{I\rho_1}{2\pi}\left\{\frac{1}{|x-A|} + \frac{k}{|x+A|} - \sum\frac{k^{2i-1}(1-k^2)}{|2id+x+A|}\right\} \qquad 39$$

$$V_2 = \frac{I\rho_1}{2\pi}\left\{\sum_{i=0}^{\infty}\frac{k^{2i}(1+k)}{|2id-x+A|} - \sum\frac{k^{2i-1}(1+k)}{|2id+x+A|}\right\} \qquad 40$$

$$V_3 = \frac{I\rho_1}{2\pi}\left\{\sum_{i=0}^{\infty}\frac{k^{2i}(1-k^2)}{|2id-x+A|}\right\} \qquad 41$$

and

Current Source in Medium II.

$$V_1 = \frac{I\rho_2}{2\pi}\left\{\sum_{i=0}^{\infty}\frac{k^{2i}(1-k)}{|2id+x-A|}-\sum\frac{k^{2i-1}(1-k)}{|2id+x+A|}\right\} \qquad 42$$

$$V_2 = \frac{I\rho_2}{2\pi}\left\{\sum_{i=0}^{\infty}\frac{k^{2i}}{|2id-x+A|}-\sum_{i=0}^{\infty}\frac{k^{2i+1}}{|2id-x-A|}+\sum\frac{k^{2i}}{|2id+x-A|}-\sum\frac{k^{2i-1}}{|2id+x+A|}\right\} \qquad 43$$

$$V_3 = \frac{I\rho_2}{2\pi}\left\{\sum_{i=0}^{\infty}\frac{k^{2i}(1-k)}{|2id-x+A|}-\sum_{i=0}^{\infty}\frac{k^{2i+1}(1-k)}{|2id-x-A|}\right\} \qquad 44$$

These equations, 39 to 44, can be used to calculate the apparent resistivity curve using any disposition of the electrodes.

Wenner Configuration.

(a) Longitudinal Traverses

In this analysis,

let a = electrode interval,

d = thickness of vertical sheet,

x = distance of centre of electrode system from centre of sheet,

ρ_1 = resistivity of first and third media,

ρ_2 = resistivity of sheet,

$k = \frac{\rho_2-\rho_1}{\rho_2+\rho_1}$

C_1 and C_2 = current electrodes,

and P_1 and P_2 = potential electrodes.

Curves for traverses over sheets of various widths will

be derived, the thickness of the sheet being related to the electrode interval. The following values of d/a will be used - 0.01, 0.1, 0.5, 1, 1.5, 2, 2.5, 3, 4 and 5. These will give a range covering most of the cases possible in nature so that one can interpolate the shape of the curve for any other case.

Since the resistivity profile in the case of a vertical object is symmetrical about the centre of the sheet, only one half of each curve need be calculated. The origin is taken at the centre of the sheet.

A. Thickness of Sheet $\leqslant$ a, d/a $\leqslant$ 1.

Fig. 21 shows all the positions for which calculations are necessary.

(I). The potential effects will all be given by equation 39 :-

Due to C_1

$$V'_{P_1} = \frac{I\rho_1}{2\pi}\left\{\frac{1}{a} + \frac{k}{2x-2a-d} - \sum\frac{k^{2i-1}(1-k^2)}{2i-1\,d+2x-2a}\right\}$$

$$V'_{P_2} = \frac{I\rho_1}{2\pi}\left\{\frac{1}{2a} + \frac{k}{2x-a-d} - \sum\frac{k^{2i-1}(1-k^2)}{2i-1\,d+2x-a}\right\}$$

Due to C_2

$$V''_{P_1} = -\frac{I\rho_1}{2\pi}\left\{\frac{1}{2a} + \frac{k}{2x+a-d} - \sum\frac{k^{2i-1}(1-k^2)}{2i-1\,d+2x+a}\right\}$$

$$V''_{P_2} = -\frac{I\rho_1}{2\pi}\left\{\frac{1}{a} + \frac{k}{2x+2a-d} - \sum\frac{k^{2i-1}(1-k^2)}{2i-1\,d+2x+2a}\right\}$$

But $V = (V'_{P_1} - V'_{P_2}) - (V''_{P_1} - V''_{P_2})$

$$= \frac{I\rho_a}{2\pi a} \quad \text{where } \rho_a = \text{apparent resistivity.}$$

$$\therefore \rho_a/\rho_1 = 1 + k\left(\frac{1}{2\frac{x}{a} - \frac{d}{a} - 2} + \frac{1}{2\frac{x}{a} - \frac{d}{a} + 2} - \frac{1}{2\frac{x}{a} - \frac{d}{a} - 1} - \frac{1}{2\frac{x}{a} - \frac{d}{a} + 1}\right)$$

$$-(1-k^2)\left\{\sum\frac{k^{2i-1}}{2i-1\,\frac{d}{a}+2\frac{x}{a}-2} - \sum\frac{k^{2i-1}}{2i-1\,\frac{d}{a}+2\frac{x}{a}-1} - \sum\frac{k^{2i-1}}{2i-1\,\frac{d}{a}+2\frac{x}{a}+1} + \sum\frac{k^{2i-1}}{2i-1\,\frac{d}{a}+2\frac{x}{a}+2}\right\}$$

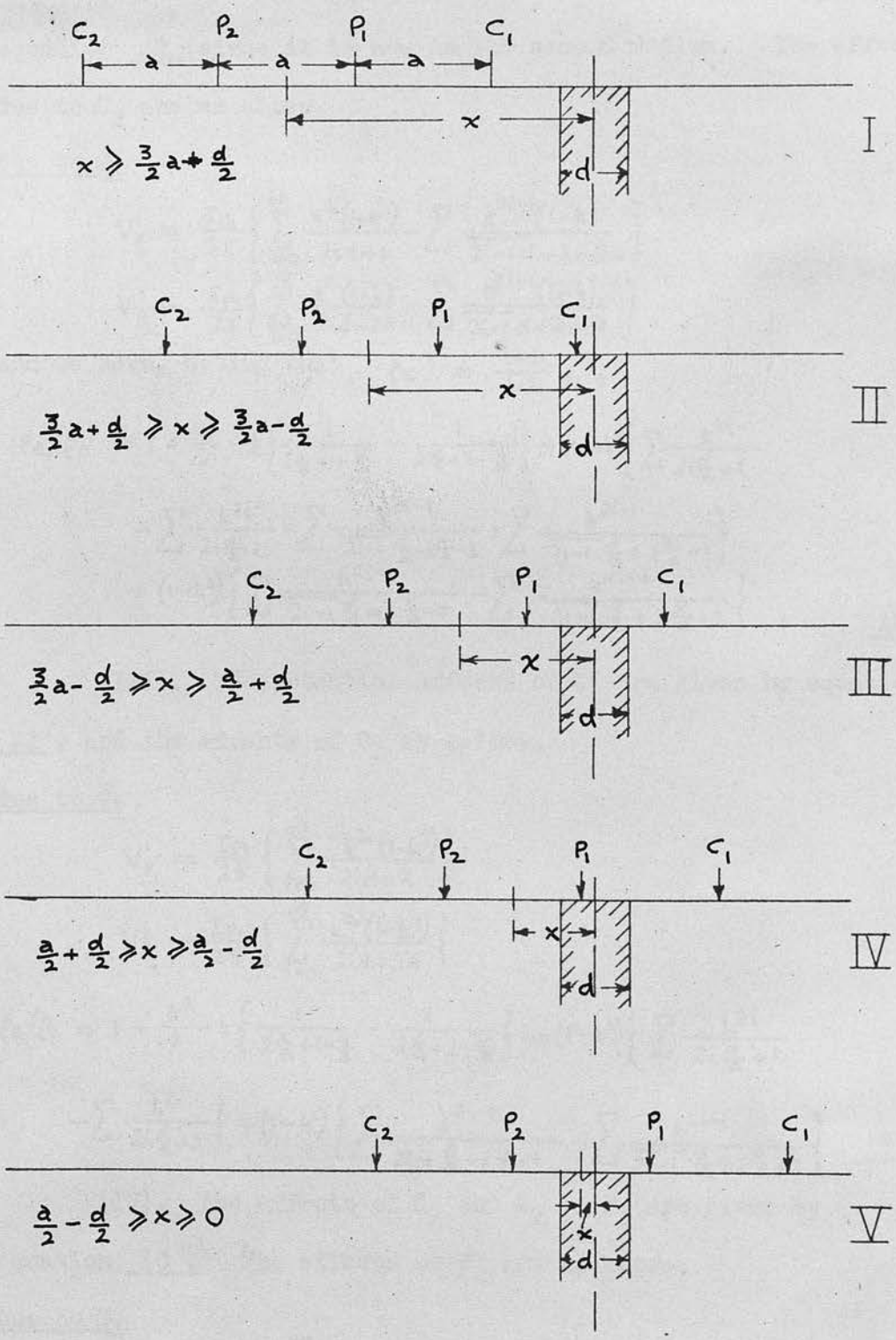

Fig.21 Electrode Set-up, Thickness of Sheet less than Electrode Interval

(II). The potential effects of C_1 are now given by equation 42 since it is now in the second medium. The effects due to C_2 are as above.

Due to C_1

$$V'_{P_1} = \frac{I\rho_2}{2\pi}\left\{\sum_{i=0}^{\infty}\frac{k^{2i}(1-k)}{2id+a} - \sum\frac{k^{2i-1}(1-k)}{2i-1\,d+2x-2a}\right\}$$

$$V'_{P_2} = \frac{I\rho_2}{2\pi}\left\{\sum_{i=0}^{\infty}\frac{k^{2i}(1-k)}{2id+2a} - \sum\frac{k^{2i-1}(1-k)}{2i-1\,d+2x-a}\right\}$$

and we have, noting that $\rho_2 = \frac{1+k}{1-k}\rho_1$,

$$\rho_a/\rho_1 = 1 + \frac{k}{2} - k\left\{\frac{1}{2\frac{x}{a}+1-\frac{a}{a}} - \frac{1}{2\frac{x}{a}+2-\frac{a}{a}}\right\} + (1+k)\left\{\sum\frac{k^{2i}}{2i\frac{a}{a}+1}\right.$$

$$\left. - \sum\frac{k^{2i}}{2i\frac{a}{a}+2} - \sum\frac{k^{2i-1}}{2i-1\,\frac{a}{a}+2\frac{x}{a}-2} + \sum\frac{k^{2i-1}}{2i-1\,\frac{a}{a}+2\frac{x}{a}-1}\right\}$$

$$+ (1-k^2)\left\{\sum\frac{k^{2i-1}}{2i-1\,\frac{a}{a}+2\frac{x}{a}+1} - \sum\frac{k^{2i-1}}{2i-1\,\frac{a}{a}+2\frac{x}{a}+2}\right\} \qquad 46$$

(III). The potential effects of C_1 are given by equation 41, and the effects of C_2 as before.

Due to C_1

$$V'_{P_1} = \frac{I\rho_1}{2\pi}\left\{\sum_{i=0}^{\infty}\frac{k^{2i}(1-k^2)}{2id+a}\right\}$$

$$V'_{P_2} = \frac{I\rho_1}{2\pi}\left\{\sum_{i=0}^{\infty}\frac{k^{2i}(1-k^2)}{2id+2a}\right\}$$

$$\rho_a/\rho_1 = 1 - \frac{k^2}{2} - k\left\{\frac{1}{2\frac{x}{a}+1-\frac{a}{a}} - \frac{1}{2\frac{x}{a}+2-\frac{a}{a}}\right\} - (1-k^2)\left\{\sum\frac{k^{2i}}{2i\frac{a}{a}+1}\right.$$

$$\left. - \sum\frac{k^{2i}}{2i\frac{a}{a}+2}\right\} + (1-k^2)\left\{\sum\frac{k^{2i-1}}{2i-1\,\frac{a}{a}+2\frac{x}{a}+1} - \sum\frac{k^{2i-1}}{2i-1\,\frac{a}{a}+2\frac{x}{a}+2}\right\} \qquad 47$$

(IV). The effects of C_1 and C_2 on P_1 are given by equation 40. The effects on P_2 are as above.

Due to C_1

$$V'_{P_1} = \frac{I\rho_1}{2\pi}\left\{\sum_{i=0}^{\infty}\frac{k^{2i}(1+k)}{2id+a} - \sum\frac{k^{2i-1}(1+k)}{2i-1\,d+2a-2x}\right\}$$

Due to C_2

$$V''_{P_1} = -\frac{I\rho_1}{2\pi}\left\{\sum_{i=0}^{\infty}\frac{k^{2i}(1+k)}{2id+2a} - \sum\frac{k^{2i-1}(1+k)}{2i-1\,d+2x+a}\right\}$$

$$\therefore \rho_a/\rho_1 = 1 + \frac{k}{2} + \frac{k^2}{2} + \frac{k}{2\frac{x}{a}+2-\frac{d}{a}} + \sum \frac{k^{2i}(1+k)}{2i\frac{d}{a}+1} - \sum \frac{k^{2i}(2+k-k^2)}{2i\frac{d}{a}+2}$$

$$-(1+k)\left\{\sum \frac{k^{2i-1}}{2i-1\ \frac{d}{a}+2-2\frac{x}{a}} - \sum \frac{k^{2i-1}}{2i-1\ \frac{d}{a}+2\frac{x}{a}+1} + \sum \frac{k^{2i-1}(1-k^2)}{2i-1\ \frac{d}{a}+2\frac{x}{a}+2}\right\} \quad 48$$

(V). The effects of C_1 on P_1 and C_2 on P_2 are given by equation 39 and of C_1 on P_2 and C_2 on P_1 by equation 41.

Due to C_1

$$V'_{P_1} = \frac{I\rho_1}{2\pi}\left\{\frac{1}{a} + \frac{k}{2a-2x-d} - \sum \frac{k^{2i-1}(1-k^2)}{2i-1\ d+2a-2x}\right\}$$

Due to C_2

$$V''_{P_1} = -\frac{I\rho_1}{2\pi}\left\{\sum_{i=0}^{\infty} \frac{k^{2i}(1-k^2)}{2id+2a}\right\}$$

$$\therefore \rho_a/\rho_1 = 2 + k^2 + k\left\{\frac{1}{2-2\frac{x}{a}-\frac{d}{a}} + \frac{1}{2+2\frac{x}{a}-\frac{d}{a}}\right\} - 2\sum \frac{k^{2i}(1-k^2)}{2i\frac{d}{a}+2}$$

$$-(1-k^2)\left\{\sum \frac{k^{2i-1}}{2i-1\ \frac{d}{a}+2-2\frac{x}{a}} + \sum \frac{k^{2i-1}}{2i-1\ \frac{d}{a}+2+2\frac{x}{a}}\right\} \quad 49$$

B. Thickness of Sheet $2a \geqslant d \geqslant a$.

The positions for which calculations are required are as shown in Fig. 22.

As will be seen, the first, second and fourth of these conditions have been considered and equations determined as shown by the Roman numbers I, II and IV. We have yet to investigate the cases denoted by VI and VII.

(VI). The effect of C_1 on P_1 is given by equation 43 and on P_2 by 42. The effect of C_2 on P_1 is derived from equation 40 and of C_2 on P_2 by 39.

Due to C_1

$$V'_{P_1} = \frac{I\rho_2}{2\pi}\left\{\sum_{i=0}^{\infty} \frac{k^{2i}}{2id+a} - \sum_{i=0}^{\infty} \frac{k^{2i+1}}{2i+1\ d+2a-2x} + \sum \frac{k^{2i}}{2id-a} - \sum \frac{k^{2i-1}}{2i-1\ d-2a+2x}\right\}$$

$$V'_{P_2} = \frac{I\rho_2}{2\pi}\left\{\sum_{i=0}^{\infty} \frac{k^{2i}(1+k)}{2id+2a} - \sum \frac{k^{2i-1}(1-k)}{2i-1\ d+2x-a}\right\}$$

Due to C_2

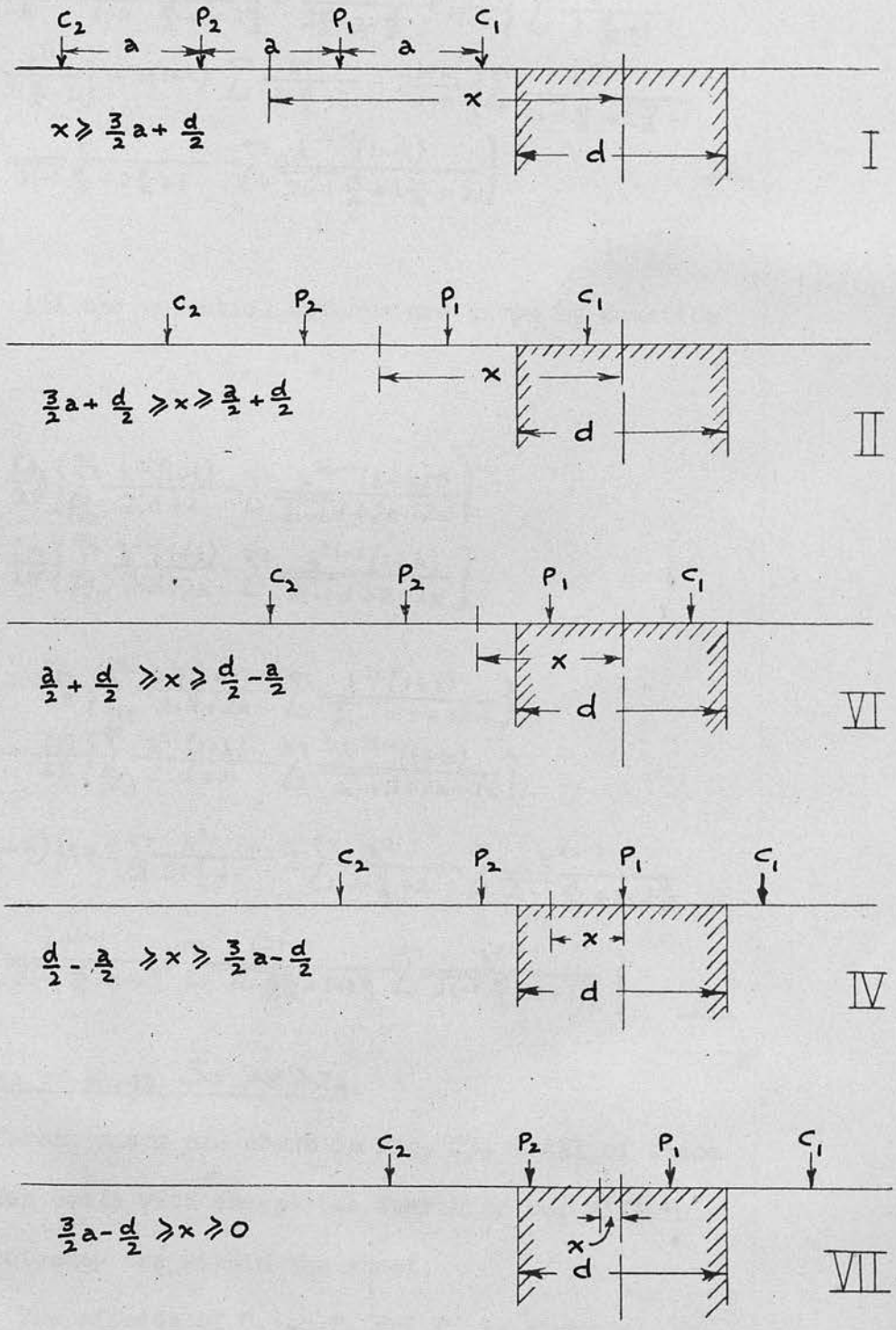

Fig. 22, Electrode Set-up, Thickness of Sheet greater than Electrode Interval but less than Twice Electrode Interval

$$V''_{P_1} = -\frac{I\rho_1}{2\pi}\left\{\sum_{i=0}^{\infty}\frac{k^{2i}(1+k)}{2id+2a} - \sum\frac{k^{2i-1}(1+k)}{2i-1\ d+2x+a}\right\}$$

$$V''_{P_2} = -\frac{I\rho_1}{2\pi}\left\{\frac{1}{a} + \frac{k}{2x+2a-d} - \sum\frac{k^{2i-1}(1-k^2)}{2i-1\ d+2x+2a}\right\}$$

$$\therefore \rho_a/\rho_1 = \frac{2k}{1-k} - \frac{1+k}{1-k}\cdot\frac{k}{\frac{d}{a}+2-2\frac{x}{a}} + \frac{k}{2\frac{x}{a}+2-\frac{d}{a}} + \frac{1+k}{1-k}\left\{\sum\frac{k^{2i}}{2i\frac{d}{a}+1}\right.$$

$$\left.+\sum\frac{k^{2i}}{2i\frac{d}{a}-1}\right\} - 2(1+k)\sum\frac{k^{2i}}{2i\frac{d}{a}+2} - \frac{1+k}{1-k}\left\{\sum\frac{k^{2i-1}}{2i-1\ \frac{d}{a}+2\frac{x}{a}-1}\right.$$

$$\left.+\sum\frac{k^{2i-1}}{2i-1\ \frac{d}{a}+2\frac{x}{a}+1} - \sum\frac{k^{2i-1}(1-k)}{2i-1\ \frac{d}{a}+2\frac{x}{a}+2}\right\} \qquad 50$$

(VII). All the potential effects are given by equation 40.

Due to C_1

$$V'_{P_1} = \frac{I\rho_1}{2\pi}\left\{\sum_{i=0}^{\infty}\frac{k^{2i}(1+k)}{2id+a} - \sum\frac{k^{2i-1}(1+k)}{2i-1\ d+2a-2x}\right\}$$

$$V'_{P_2} = \frac{I\rho_1}{2\pi}\left\{\sum_{i=0}^{\infty}\frac{k^{2i}(1+k)}{2id+2a} - \sum\frac{k^{2i-1}(1+k)}{2i-1\ d+a-2x}\right\}$$

Due to C_2

$$V''_{P_1} = -\frac{I\rho_1}{2\pi}\left\{\sum_{i=0}^{\infty}\frac{k^{2i}(1+k)}{2id+2a} - \sum\frac{k^{2i-1}(1+k)}{2i-1\ d+a+2x}\right\}$$

$$V''_{P_2} = -\frac{I\rho_1}{2\pi}\left\{\sum_{i=0}^{\infty}\frac{k^{2i}(1+k)}{2id+a} - \sum\frac{k^{2i-1}(1+k)}{2i-1\ d+2a+2x}\right\}$$

Hence

$$\rho_a/\rho_1 = (1+k)\left\{1+2\sum\frac{k^{2i}}{2i\frac{d}{a}+1} - 2\sum\frac{k^{2i}}{2i\frac{d}{a}+2} - \sum\frac{k^{2i-1}}{2i-1\ \frac{d}{a}+2-2\frac{x}{a}}\right.$$

$$\left.+\sum\frac{k^{2i-1}}{2i-1\ \frac{d}{a}+1-2\frac{x}{a}} + \sum\frac{k^{2i-1}}{2i-1\ \frac{d}{a}+1+2\frac{x}{a}} - \sum\frac{k^{2i-1}}{2i-1\ \frac{d}{a}+2+2\frac{x}{a}}\right\} \qquad 51$$

C. Thickness of Sheet $3a \geqslant d \geqslant 2a$.

The different cases are shown in Fig. 23. All of these have already been dealt with except the fourth or No, VIII in which three electrodes are within the sheet.

(VIII). The effects of C_1 on P_1 and P_2 is given by equation 43, and of C_2 on P_1 and P_2 by equation 40.

Due to C_1

$$V'_{P_1} = \frac{I\rho_2}{2\pi}\left\{\sum_{i=0}^{\infty}\frac{k^{2i}}{2id+a} - \sum_{i=0}^{\infty}\frac{k^{2i+1}}{2i+1\ d+2a-2x} + \sum\frac{k^{2i}}{2id-a} - \sum\frac{k^{2i-1}}{2i-1\ d-2a+2x}\right\}$$

$$V'_{P_2} = \frac{I\rho_2}{2\pi}\left\{\sum_{i=0}^{\infty}\frac{k^{2i}}{2id+2a} - \sum_{i=0}^{\infty}\frac{k^{2i+1}}{2i+1\ d+a-2x} + \sum\frac{k^{2i}}{2id-2a} - \sum\frac{k^{2i-1}}{2i-1\ d-a+2x}\right\}$$

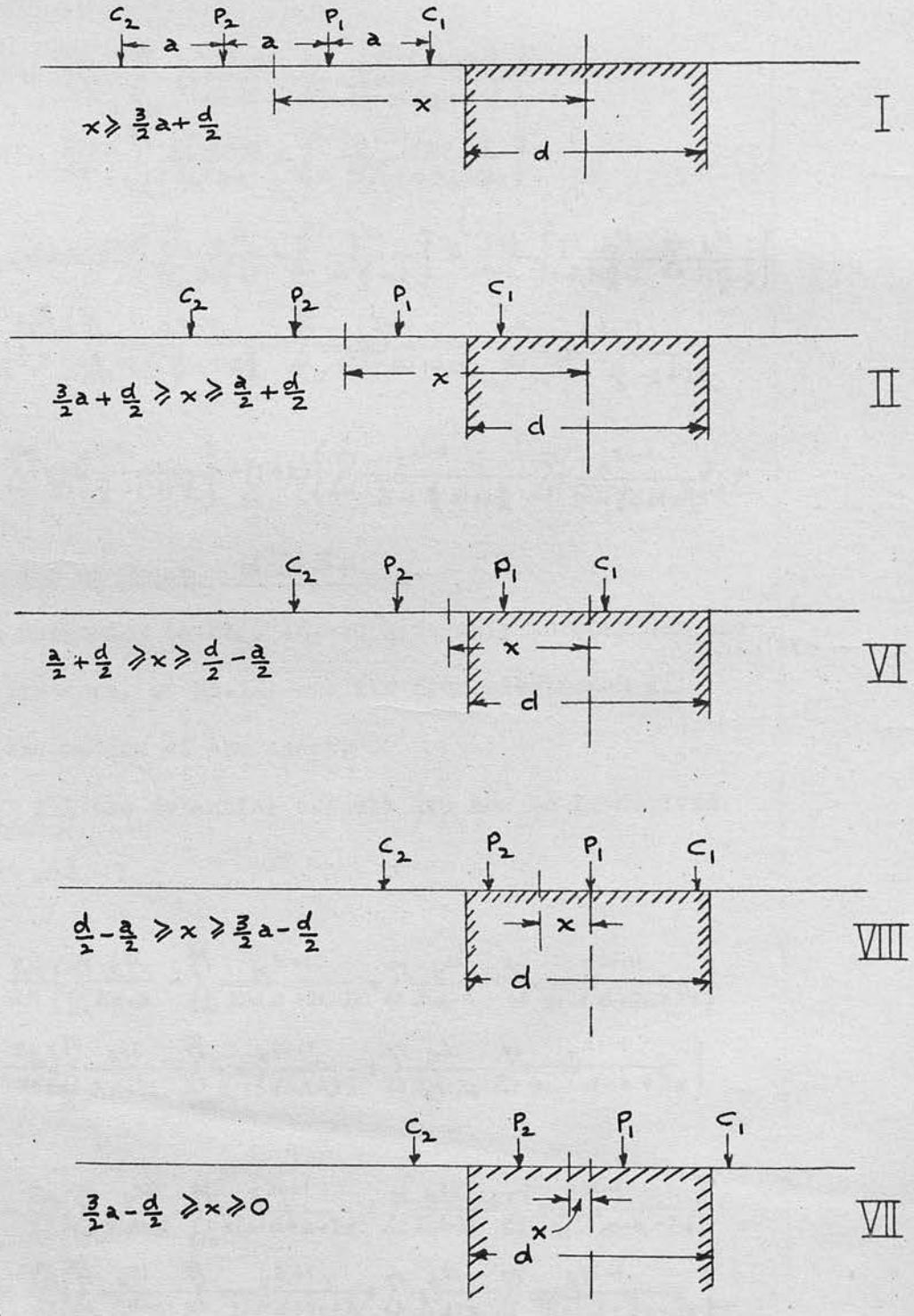

Fig.23, Electrode Set-up, Thickness of Sheet greater than Twice Electrode Interval but less than Three Times.

Due to C_2

$$V''_{P_1} = -\frac{I\rho_1}{2\pi}\left\{\sum_{i=0}^{\infty}\frac{k^{2i}(1+k)}{2id+2a} - \sum\frac{k^{2i-1}(1+k)}{2i-1\,d+a+2x}\right\}$$

$$V''_{P_2} = -\frac{I\rho_1}{2\pi}\left\{\sum_{i=0}^{\infty}\frac{k^{2i}(1+k)}{2id+a} - \sum\frac{k^{2i-1}(1+k)}{2i-1\,d+2a+2x}\right\}$$

$$\therefore \rho_a/\rho_1 = \left(\frac{2+k+k^2}{1-k}\right)\left\{\sum_{i=0}^{\infty}\frac{k^{2i}}{2i\frac{d}{a}+1} - \sum_{i=0}^{\infty}\frac{k^{2i}}{2i\frac{d}{a}+2}\right\} + \frac{1+k}{1-k}\left\{\sum\frac{k^{2i}}{2i\frac{d}{a}-1} - \sum\frac{k^{2i}}{2i\frac{d}{a}-2}\right\}$$

$$- \frac{1+k}{1-k}\left\{\sum_{i=0}^{\infty}\frac{k^{2i+1}}{2i+1\,\frac{d}{a}+2-2\frac{x}{a}} - \sum_{i=0}^{\infty}\frac{k^{2i+1}}{2i+1\,d+1-2\frac{x}{a}} - \sum\frac{k^{2i-1}}{2i-1\,\frac{d}{a}-2+2\frac{x}{a}}\right.$$

$$\left. - \sum\frac{k^{2i-1}}{2i-1\,\frac{d}{a}-1+2\frac{x}{a}}\right\} - (1+k)\left\{\sum\frac{k^{2i-1}}{2i-1\,\frac{d}{a}+1+2\frac{x}{a}} - \sum\frac{k^{2i-1}}{2i-1\,\frac{d}{a}+2+2\frac{x}{a}}\right\}$$ 52

D. Thickness of Sheet $d \geqslant 3a$.

Again referring to Fig. 24, we have only to consider one case. The last one, or No.IX, has its four electrodes all situated in the medium of the sheet.

(IX). All the potential effects are now to be derived from equation 43.

Due to C_1

$$V'_{P_1} = \frac{I\rho_2}{2\pi}\left\{\sum_{i=0}^{\infty}\frac{k^{2i}}{2id+a} - \sum_{i=0}^{\infty}\frac{k^{2i+1}}{2i+1\,d+2a-2x} + \sum\frac{k^{2i}}{2id-a} - \sum\frac{k^{2i-1}}{2i-1\,d-2a+2x}\right\}$$

$$V'_{P_2} = \frac{I\rho_2}{2\pi}\left\{\sum_{i=0}^{\infty}\frac{k^{2i}}{2id+2a} - \sum_{i=0}^{\infty}\frac{k^{2i+1}}{2i+1\,d+a-2x} + \sum\frac{k^{2i}}{2id-2a} - \sum\frac{k^{2i-1}}{2i-1\,d-a+2x}\right\}$$

Due to C_2

$$V''_{P_1} = -\frac{I\rho_2}{2\pi}\left\{\sum_{i=0}^{\infty}\frac{k^{2i}}{2id+2a} - \sum_{i=0}^{\infty}\frac{k^{2i+1}}{2i+1\,d+a+2x} + \sum\frac{k^{2i}}{2id-2a} - \sum\frac{k^{2i-1}}{2i-1\,d-a-2x}\right\}$$

$$V''_{P_2} = -\frac{I\rho_2}{2\pi}\left\{\sum_{i=0}^{\infty}\frac{k^{2i}}{2id+a} - \sum_{i=0}^{\infty}\frac{k^{2i+1}}{2i+1\,d+2a+2x} + \sum\frac{k^{2i}}{2id-a} - \sum\frac{k^{2i-1}}{2i-1\,d-2a-2x}\right\}$$

$$\therefore \rho_a/\rho_1 = \frac{1+k}{1-k}\left\{2\left[\sum_{i=0}^{\infty}\frac{k^{2i}}{2i\frac{d}{a}+1} - \sum_{i=0}^{\infty}\frac{k^{2i}}{2i\frac{d}{a}+2} + \sum\frac{k^{2i}}{2i\frac{d}{a}-1} - \sum\frac{k^{2i}}{2i\frac{d}{a}-2}\right]\right.$$

$$- \sum_{i=0}^{\infty}\frac{k^{2i+1}}{2i+1\,\frac{d}{a}+2-2\frac{x}{a}} - \sum_{i=0}^{\infty}\frac{k^{2i+1}}{2i+1\,\frac{d}{a}+1-2\frac{x}{a}} + \sum_{i=0}^{\infty}\frac{k^{2i+1}}{2i+1\,\frac{d}{a}+1+2\frac{x}{a}}$$

$$- \sum_{i=0}^{\infty}\frac{k^{2i+1}}{2i+1\,\frac{d}{a}+2+2\frac{x}{a}} - \sum\frac{k^{2i-1}}{2i-1\,\frac{d}{a}-2+2\frac{x}{a}} + \sum\frac{k^{2i-1}}{2i-1\,\frac{d}{a}-1+2\frac{x}{a}}$$ 53

$$\left. + \sum\frac{k^{2i-1}}{2i-1\,\frac{d}{a}-1-2\frac{x}{a}} - \sum\frac{k^{2i-1}}{2i-1\,\frac{d}{a}-2+2\frac{x}{a}}\right\}$$

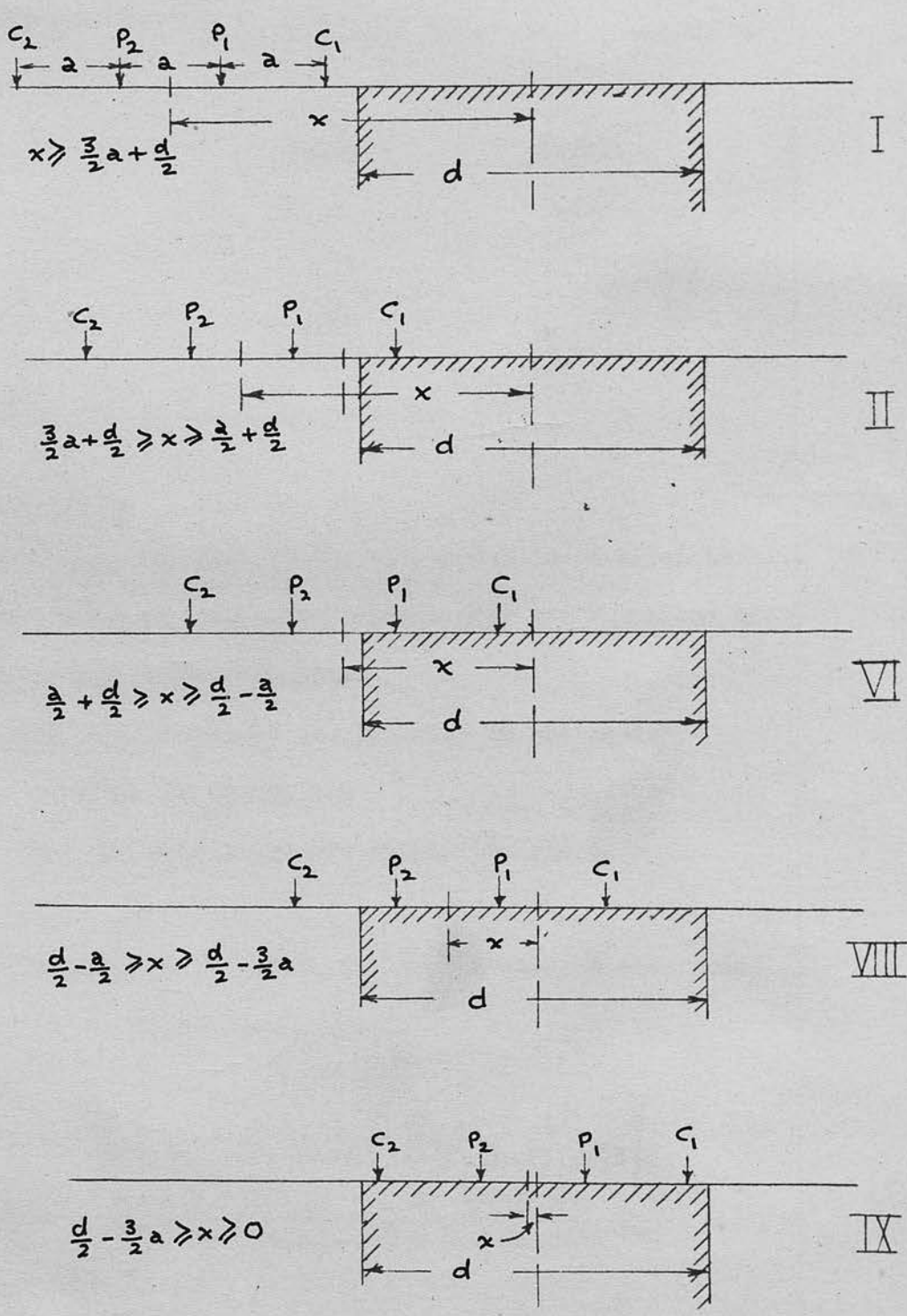

Fig. 24, Electrode Set-up, Thickness of Sheet greater than Three Times the Electrode Interval.

These equations have been evaluated for values of k = ± 0.3, ± 0.6 and ± 0.9, corresponding to the following values of ρ_a/ρ_1.

k	ρ_a/ρ_1	ρ_1/ρ_a
0.9	19	0.053
0.6	4	0.25
0.3	1.857	0.538
-0.3	0.538	1.857
-0.6	0.25	4
-0.9	0.053	19

The value of ρ_1 is taken as unity.

Transverse Traverses.

In this case, the line of the electrodes is parallel to the strike of the sheet, and there will be only two equations of apparent resistivity to be deduced:-

1. When the electrodes are situated in the medium outwith the sheet, and
2. When the electrodes are within the sheet.

1. The potentials at P_1 and P_2 due to the current electrodes C_1 and C_2 are given by equation 30.

Thus:-

$$V'_{P_1} = \frac{I\rho_1}{2\pi}\left\{\frac{1}{a} + \frac{k}{[a^2+(2x-d)^2]^{1/2}} - \sum \frac{k^{2i-1}(1-k^2)}{[a^2+(2x+\overline{2i-1}\,d)^2]^{1/2}}\right\}$$

$$V'_{P_2} = -\frac{I\rho_1}{2\pi}\left\{\frac{1}{2a} + \frac{k}{[4a^2+(2x-d)^2]^{1/2}} - \sum \frac{k^{2i-1}(1-k^2)}{[4a^2+(2x+\overline{2i-1}\,d)^2]^{1/2}}\right\}$$

By symmetry,

$$V''_{P_1} = -V'_{P_2},$$

$$V''_{P_2} = -V'_{P_1}.$$

$$\therefore \rho_a/\rho_1 = 1 + 2k\left\{\frac{1}{[1+(2\frac{x}{a}-\frac{d}{a})^2]^{1/2}} - \frac{1}{[4+(2\frac{x}{a}-\frac{d}{a})^2]^{1/2}}\right\}$$

$$-\frac{2(1-k^2)}{k}\left\{\sum \frac{k^{2i}}{[1+(2\frac{x}{a}+\overline{2i-1}\frac{d}{a})^2]^{1/2}} - \sum \frac{k^{2i}}{[4+(2\frac{x}{a}+\overline{2i-1}\frac{d}{a})^2]^{1/2}}\right\} \quad 54$$

2. When the electrodes are within the sheet of resistivity ρ_2, the potentials due to C_1 and C_2 are as in equation 37.

$$V'_{P_1} = \frac{I\rho_2}{2\pi}\left\{\sum_{i=0}^{\infty}\frac{k^{2i}}{[a^2+(2id)^2]^{1/2}} - \sum_{i=0}^{\infty}\frac{k^{2i+1}}{[a^2+(2i+1\,d-2x)^2]^{1/2}} + \sum\frac{k^{2i}}{[a^2+(2id)^2]^{1/2}} - \sum\frac{k^{2i-1}}{[a^2+(2i-1\,d+2x)^2]^{1/2}}\right\}$$

$$= \frac{1+k}{1-k}\cdot\frac{I\rho_1}{2\pi}\left\{\frac{1}{a} + 2\sum\frac{k^{2i}}{[a^2+(2id)^2]^{1/2}} - \sum_{i=0}^{\infty}\frac{k^{2i+1}}{[a^2+(2i+1\,d-2x)^2]^{1/2}} - \sum\frac{k^{2i-1}}{[a^2+(2i-1\,d+2x)^2]^{1/2}}\right\}$$

and $$V'_{P_2} = \frac{1+k}{1-k}\cdot\frac{I\rho_1}{2\pi}\left\{\frac{1}{2a} + 2\sum\frac{k^{2i}}{[4a^2+(2id)^2]^{1/2}} - \sum_{i=0}^{\infty}\frac{k^{2i+1}}{[4a^2+(2i+1\,d-2x)^2]^{1/2}} - \sum\frac{k^{2i-1}}{[4a^2+(2i-1\,d+2x)^2]^{1/2}}\right\}$$

also $$V''_{P_1} = -V'_{P_2},$$

and $$V''_{P_2} = -V'_{P_1}.$$

These give:-

$$\rho_a/\rho_1 = \frac{1+k}{1-k}\left\{1 + 4\left[\sum\frac{k^{2i}}{[1+(2i\frac{d}{a})^2]^{1/2}} - \sum\frac{k^{2i}}{[4+(2i\frac{d}{a})^2]^{1/2}}\right]\right.$$

$$- 2\left[\sum_{i=0}^{\infty}\frac{k^{2i+1}}{[1+(2i+1\,\frac{d}{a}-2\frac{x}{a})^2]^{1/2}} - \sum_{i=0}^{\infty}\frac{k^{2i+1}}{[4+(2i+1\,\frac{d}{a}-2\frac{x}{a})^2]^{1/2}}\right]$$

$$\left. - 2\left[\sum\frac{k^{2i-1}}{[1+(2i-1\,\frac{d}{a}+2\frac{x}{a})^2]^{1/2}} - \sum\frac{k^{2i-1}}{[4+(2i-1\,\frac{d}{a}+2\frac{x}{a})^2]^{1/2}}\right]\right\}$$

55

Summation of Infinite Terms.

The sums to infinity of equations 45 to 53 can all be expressed in the form:- $$\sum\frac{k^{2i}}{2i\frac{d}{a}+A}$$

and values of d/a from 0.01 to 5 are required.

Thus $\sum \frac{k^{2i}}{2i\frac{d}{a}+A} = \frac{a}{d}\sum \frac{k^{2i}}{2i+A\frac{a}{d}} = \frac{a}{d}\sum \frac{k^{2i}}{2i+y}$

where $y = A\frac{a}{d}$

For values of $k = \pm 0.3$ or ± 0.6 the easiest way is direct summation, but for values of $k = \pm 0.9$, the sum becomes only slowly convergent, and some 20 or more terms are required for a 1% accuracy, and 40 to 50 for 0.1%. This summation may be shortened by the following methods:-

(1) y = 0

If y = 0 then $\sum \frac{k^{2i}}{2i} = \frac{k^2}{2} + \frac{k^4}{4} + \frac{k^6}{6} + \cdots\cdots$

$= -\frac{1}{2}\log_e(1-k^2)$

$= \log_e \frac{1}{\sqrt{1-k^2}}$ 56

(2) y = an integer

$$\sum \frac{k^{2i}}{2i+y} = k^{-y}\sum \frac{k^{2i+y}}{2i+y}$$

Let y = 1

$$\therefore \sum \frac{k^{2i}}{2i+1} = \frac{1}{k}\left(\frac{k^3}{3} + \frac{k^5}{5} + \cdots\cdots\right)$$

$$= \frac{1}{k}\left(k + \frac{k^3}{3} + \frac{k^5}{5} \cdots\cdots - k\right)$$

$$= \frac{1}{k}\left(\log_e\sqrt{\frac{1+k}{1-k}} - k\right)$$

Let y = 2

$$\therefore \sum \frac{k^{2i}}{2i+2} = \frac{1}{k^2}\left(\frac{k^2}{2} + \frac{k^4}{4} + \frac{k^6}{6} + \cdots\cdots - \frac{k^2}{2}\right)$$

$$= \frac{1}{k^2}\left(\log_e \frac{1}{\sqrt{1-k^2}} - \frac{k^2}{2}\right)$$

Similarly

$$\sum \frac{k^{2i}}{2i+3} = \frac{1}{k^3}\left(\log_e \sqrt{\frac{1+k}{1-k}} - k - \frac{k^3}{3}\right)$$

and

$$\sum \frac{k^{2i}}{2i+4} = \frac{1}{k^4}\left(\log_e \frac{1}{\sqrt{1-k^2}} - \frac{k^2}{2} - \frac{k^4}{4}\right)$$

Generally,

if y is an odd number,

$$\sum \frac{k^{2i}}{2i+y} = \frac{1}{k^y}\left(\log_e \sqrt{\frac{1+k}{1-k}} - \sum_{i=1}^{i=\frac{y+1}{2}} \frac{k^{2i+1}}{2i+1}\right) \qquad 57$$

and if y is an even number

$$\sum \frac{k^{2i}}{2i+y} = \frac{1}{k^y}\left(\log_e \frac{1}{\sqrt{1-k^2}} - \sum_{i=1}^{i=\frac{y}{2}} \frac{k^{2i}}{2i}\right) \qquad 58$$

These equations are valuable for certain integral values of y where d/a is greater than about 0.1, but below this value the last term would still require an awkward summation. Also, in these cases where d/a is, say 5, then y will be 5, 10, 15 etc. and therefore equations 57 and 58 provide for only a few values with large intervals between, too much for direct interpolation.

(3) y is large (i.e. d/a is small).

Here, the Binomial theorem may be used in order to be able to neglect larger powers of 1/y.

Let $\sum \frac{k^{2i}}{2i+y} = z\sum \frac{k^{2i}}{1+2iz}$ where $z = \frac{1}{y}$

then $$z\sum \frac{k^{2i}}{1+2iz} = z\sum k^{2i}(1+2iz)^{-1}$$

$$= z\sum k^{2i}(1-2iz+4i^2z^2-8i^3z^3+\dots)$$

$$= z\sum k^{2i} - z^2\sum (2i)k^{2i} + z^3\sum (2i)^2 k^{2i} \dots$$

Let.

$$\sum k^{2i} = S_0,$$

$$\sum (2i)k^{2i} = S_1,$$

$$\sum (2i)^2 k^{2i} = S_2, \text{ etc.}$$

$$\therefore \quad S_0 = k^2 + k^4 + \dots = \frac{k^2}{1-k^2}$$

$$S_1 = 2k^2 + 4k^4 + 6k^6 + \dots$$

$$\therefore k^2 S_1 = \quad 2k^4 + 4k^6 + \dots$$

$$\therefore (1-k^2)S_1 = 2(k^2 + k^4 + k^6 + \dots)$$

$$= \frac{2k^2}{1-k^2}$$

$$\therefore S_1 = \frac{2k^2}{(1-k^2)^2}$$

when $k = 0.9$, $S_1 = 44.875$

When d/a is 0.01, the largest value of x/a we need concern ourselves with is 10, or $y = 1000$, $z = 0.001$.

Thus the term $z^2 \sum (2i) k^{2i} = .000001 \times \frac{2k^2}{(1-k^2)^2}$ which can be neglected.

If we work to 0.1% accuracy, then we can neglect the 2nd term for all values of x/a above 2.5.

$$S_2 = \sum (2i)^2 k^{2i}$$

$$= 4k^2 + 16k^4 + 36k^6 + 64k^8 + \ldots$$

$$\therefore k^2 S_2 = 4k^4 + 16k^6 + 36k^8 + \ldots$$

$$\therefore (1-k^2) S_2 = 4k^2 + 12k^4 + 20k^6 + 28k^8 + \ldots$$

$$\therefore (1-k^2) k^2 S_2 = 4k^4 + 12k^6 + 20k^8 + \ldots$$

$$\therefore (1-k^2)^2 S_2 = 4k^2 + 8k^4 + 8k^6 + 8k^8 + \ldots$$

$$= 8(k^2 + k^4 + \ldots) - 4k^2$$

$$= \frac{8k^2}{1-k^2} - 4k^2$$

$$\therefore S_2 = \frac{8k^2}{(1-k^2)^3} - \frac{4k^2}{(1-k^2)^2} = \frac{4k^2(1+k^2)}{(1-k^2)^3}$$

For $k = 0.9$, $S_2 = 855$.

For 1% accuracy, this is sufficient to x/a = 1.

Similarly, the next term

$$S_3 = \frac{8k^2(1+4k^2+k^4)}{(1-k^2)^4}$$

is enough, for values x/a down to 0.5.

The few values which would be required below this may be calculated from equations 57 and 58.

(4) y is not an integer

This is the most common case. For values of k of 0.9 or above, the convergence is slow, and so we must use a method which converts a slowly converging series into a more rapidly converging one. This may be done by Stirling's method of expressing a fraction as a series of inverse factors (22),

$$\text{e.g. } \frac{1}{n+y} = \frac{A_0}{n+m} + \frac{A_1}{n+m+2} + \frac{A_2}{n+m+4} + \dots$$

$$+ \dots + \frac{A_p}{n+m+2p} + \frac{B_{m,p}}{(n+y)(n+m)(n+m+2)\dots(n+m+2p)} \quad 59$$

Multiplying throughout,

$$(n+m)(n+m+2)\dots(n+m+2p) = (n+y)(n+m+2)\dots(n+m+2p)A_0 \dots$$
$$+ (n+y)(n+m)(n+m+4)\dots(n+m+2p)A_1 \dots$$
$$+ \dots + B_{m,p}.$$

The coefficients of A_0, A_1..... and $B_{m,p}$ may be evaluated:-

Let $n = -y$

$$\therefore B_{m,p} = (m-y)(m+2-y)\dots(m+2p-y)$$

Let $n = -m$

$$\therefore (y-m).2.4.\dots.2p.A_0 + B_{m,p} = 0$$

$$\therefore A_0 = \frac{(m+2-y)\dots(m+2p-y)}{2.4\dots2p}$$

Let $n = -m-2$,

$$\therefore (y-m-2)(-2).2\dots(2p-2)A_1 + B_{m,p} = 0$$

whence $A_1 = \dfrac{(m-y)(m+4-y)(m+6-y)\dots(m+2p-y)}{-2.2.4\dots(2p-2)}$

Let $n = -m-4$,

$$\therefore (y-m-4).-4.-2\dots(2p-4)A_2 + B_{m,p} = 0$$

$$\therefore A_2 = \frac{(m-y)(m+2-y)(m+6-y)\dots(m+2p-y)}{-4.-2.2\dots(2p-4)}, \text{ etc.}$$

Now taking n = 2i, and m = the next even integer (2q) greater than y or equal to y (i.e. m = 0, 2 ...) and summing with respect to i from i = 1,

$$\sum \frac{k^{2i}}{2i+y} = A_0 \sum \frac{k^{2i}}{2i+2q} + A_1 \sum \frac{k^{2i}}{2i+2q+2} + \ldots .$$

$$\ldots . + B_{m,p} \sum \frac{k^{2i}}{(2i+y)(2i+2q) \ldots . (2i+2q+2p)}$$

$$= A_0 . k^{-2q} \left(\sum \frac{k^{2i}}{2i} - \frac{k^{2q}}{2q} - \frac{k^{2q-2}}{2q-2} - \ldots . - \frac{k^2}{2} \right)$$

$$+ A_1 . k^{-2q-2} \left(\sum \frac{k^{2i}}{2i} - \frac{k^{2q+2}}{2q+2} - \frac{k^{2q}}{2q} - \ldots . - \frac{k^2}{2} \right)$$

$$+ \ldots . + \ldots .$$

$$+ \ldots . + B_{m,p} \sum \frac{k^{2i}}{(2i+y)(2i+2q) \ldots . (2i+2q+2p)} \qquad 60$$

The A terms are multiples of known sums, while the $B_{m,p}$ term contains a series whose convergence is improved by extra factors in the denominator. The assumed value of p depends on the last term.

In order to demonstrate the method of calculation and the number of terms required we may take the value of $\sum \frac{0.9^{2i}}{2i \times 0.5 + 1.7}$ By direct summation to five decimal places this is 0.85681.

$$\sum \frac{0.9^{2i}}{2i \times 0.5 + 1.7} = 2 \sum \frac{0.9^{2i}}{2i + 3.4}$$

$$\therefore \sum \frac{0.9^{2i}}{2i+3.4} = A_0 . 0.9^{-4} \left\{ \sum \frac{0.9^{2i}}{2i} - \frac{0.9^4}{4} - \frac{0.9^2}{2} \right\}$$

$$+ A_1 . 0.9^{-6} \left\{ \sum \frac{0.9^{2i}}{2i} - \frac{0.9^6}{6} - \frac{0.9^4}{4} - \frac{0.9^2}{2} \right\}$$

$$+ \ldots . .$$

$$\ldots . + B_{m,p} \sum \frac{0.9^{2i}}{(2i+3.4)(2i+4) \ldots (2i+4+2p)}$$

where $B_{m,p} = (4-3.4)(6-3.4)\ldots(4+2p-3.4)$

$$A_0 = \frac{(6-3.4)(8-3.4)\ldots(4+2p-3.4)}{2.2.4\ldots 2p}$$

$$A_1 = \frac{(4-3.4)(8-3.4)\ldots(4+2p-3.4)}{-2.2.4\ldots(2p-2)}, \text{ etc.}$$

Let $p = 1$

$$\therefore B_{4,1} = (4-3.4)(6-3.4) = 1.56$$

$$A_0 = \frac{6-3.4}{2} = 1.3$$

$$A_1 = \frac{4-3.4}{-2} = -0.3$$

$$\therefore \sum \frac{0.9^{2i}}{2i+3.4} = 1.3\sum \frac{0.9^{2i}}{2i+4} - 0.3\sum \frac{0.9^{2i}}{2i+6}$$

$$+1.56\left(\frac{0.9^2}{5.4\times 6\times 8} + \frac{0.9^4}{7.4\times 8\times 10} + \ldots\right)$$

$$= 1.3\times 0.39835 - 0.3\times 0.32513$$

$$+1.56\times 0.00520$$

$$= \underline{0.42843}$$

The B infinite factor requires eleven terms of which the last five can be performed mentally.

Now let $p = 2$

$$B_{4,2} = (4-3.4)(6-3.4)(8-3.4) = 7.176$$

$$A_0 = \frac{(6-3.4)(8-3.4)}{2.4} = 1.495$$

$$A_1 = \frac{(4-3.4)(8-3.4)}{-2.2} = -0.69$$

$$A_2 = \frac{(4-3.4)(6-3.4)}{-4.-2} = 0.195$$

$$\therefore \sum \frac{k^{2i}}{2i+3.4} = 1.495\sum \frac{0.9^{2i}}{2i+4} - 0.69\sum \frac{0.9^{2i}}{2i+6}$$

$$+0.195\sum\frac{0.9^{2i}}{2i+8}+7.176\left(\frac{0.9^2}{5.4\times6\times8\times10}\right.$$

$$\left.+\frac{0.9^4}{7.4\times8\times10\times12}+\ldots.\right)$$

$$=\underline{0.42840}$$

In this case only five terms are required to evaluate the infinite sum, and four of these can be calculated mentally. The infinite sums ($\sum\frac{k^{2i}}{2i+y}$) are, of course, previously calculated for the different values of y.

The values obtained by putting p = 1 and p = 2 are, therefore, 0.85686 and 0.85680 respectively, compared to the direct summation answer of 0.85681.

(5) Direct Summation

The method of direct summation can be used with small values of k but for k = 0.9 and above, it is too lengthy. Much of this work can be reduced by a calculating machine and Barlow's Tables of squares, square roots, reciprocals, etc. When k = 0.9 and d/a = 0.01, thirty-three terms have to be calculated and summed to give totals to 0.0001; one hundred and four are required to 0.00001. When d/a = 5, the terms needed are thirteen and thirty respectively. With k greater than 0.9, direct summation is out of the question, both from the point of view of the number of terms and of the accuracy of the sum when stopping at a certain term.

The error due to neglect of additional terms may be

considered thus :-

$$\sum_{i=n}^{\infty} \frac{k^{2i}}{2i+y} = \frac{k^{2n}}{2n+y} + \frac{k^{2n+2}}{2n+2+y} + \ldots\ldots$$

$$< \frac{k^{2n}}{2n+y} + \frac{k^{2n+2}}{2n+y} + \ldots\ldots$$

$$< \frac{1}{2n+y} \cdot \frac{k^{2n}}{1-k^2}$$

$$< \frac{1}{1-k^2} \cdot \frac{k^{2n}}{2n+y}$$

$\therefore$ the error is less than $\frac{1}{1-k^2}$ times the first neglected term.

Hence, when k = 0.95, error < 11 x first neglected term

k = 0.9 do. < 5 do.

k = 0.6 do. < 1.5 do.

k ≅ 0.3 do. < 1 do.

The terms of the form $\sum \frac{k^{2i}}{[1+(2i\frac{d}{a}+\frac{y}{a})^2]^{1/2}}$ derived from the transverse traverse equations 54 and 55 were summed directly, since more time would have been taken in deriving short-cut methods than was taken by direct summation.

The cases of y/a = 0, of course, could usually be derived or checked from Roman's Tables (23).

Discussion of Graphs

1. Longitudinal Traverses over Vertical Insulating Sheets.

These graphs are shown in Figs. 25 to 27. The changes in the shape of the curves as the thickness of the sheet increases is rather remarkable. When the thickness of the sheet is small compared with the electrode interval, the curves

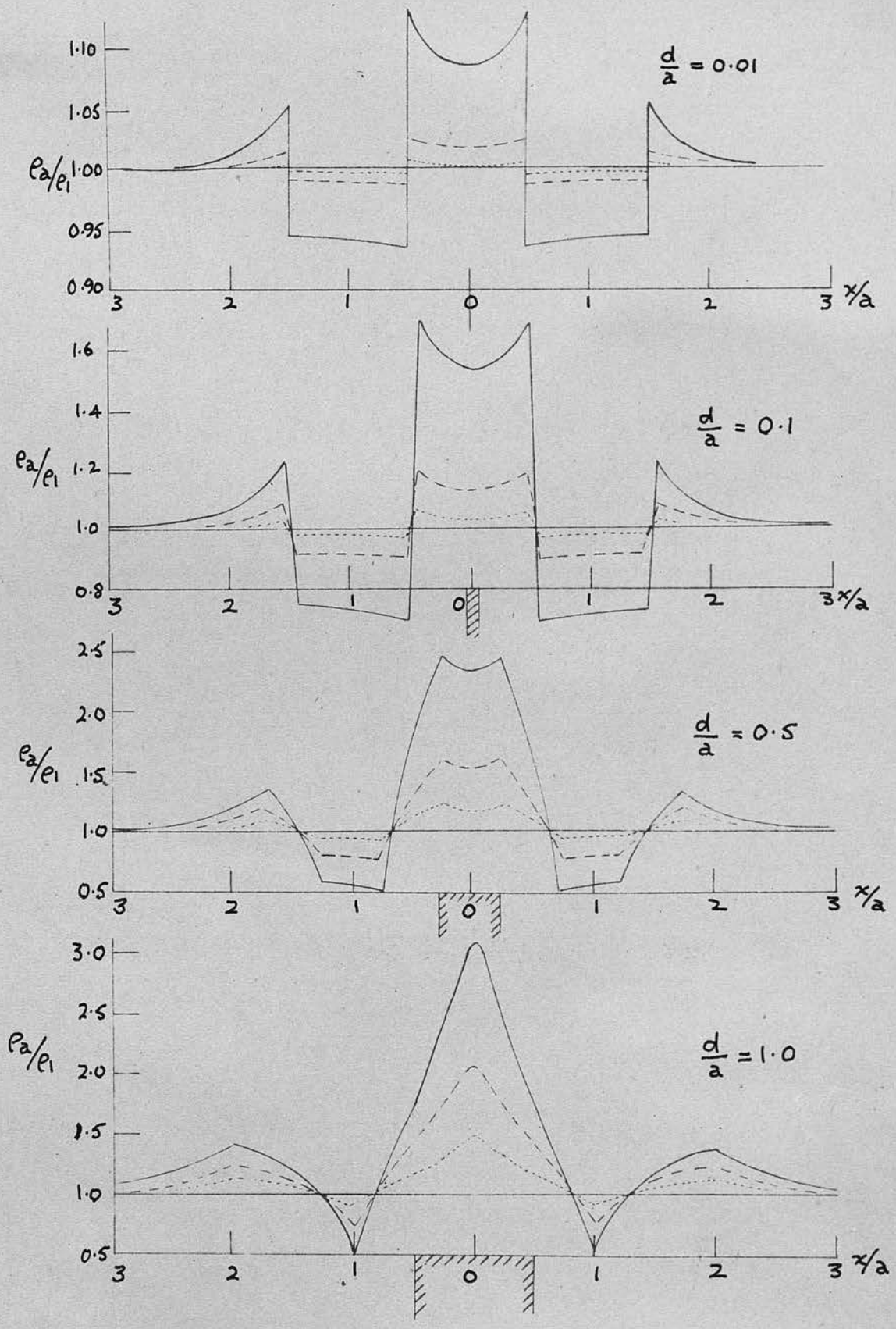

Fig. 25, Longitudinal Traverses over Vertical Insulators

——— k = 0.9
– – – – – k = 0.6
. . . . . k = 0.3

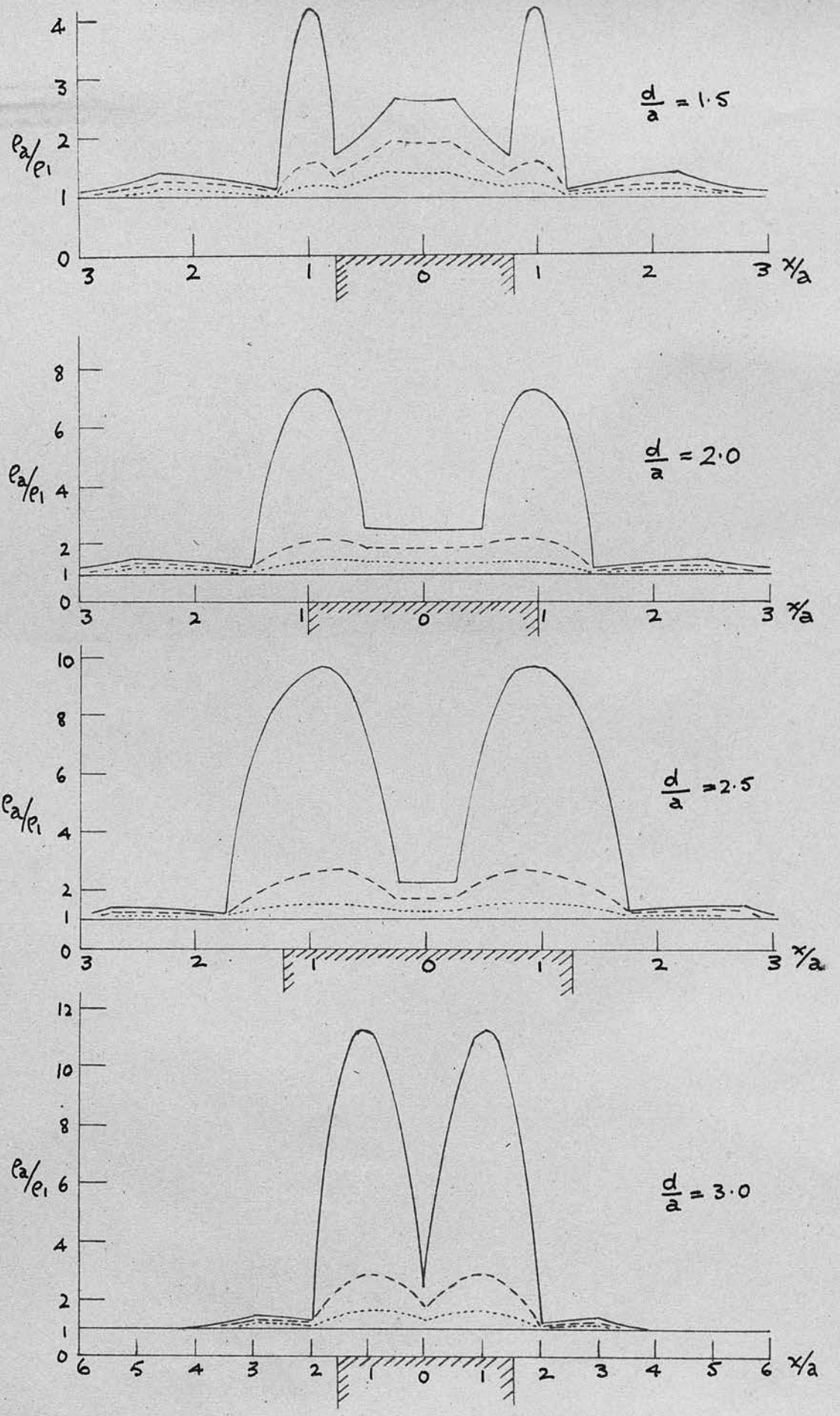

Fig. 26, Longitudinal Traverses over Vertical Insulators

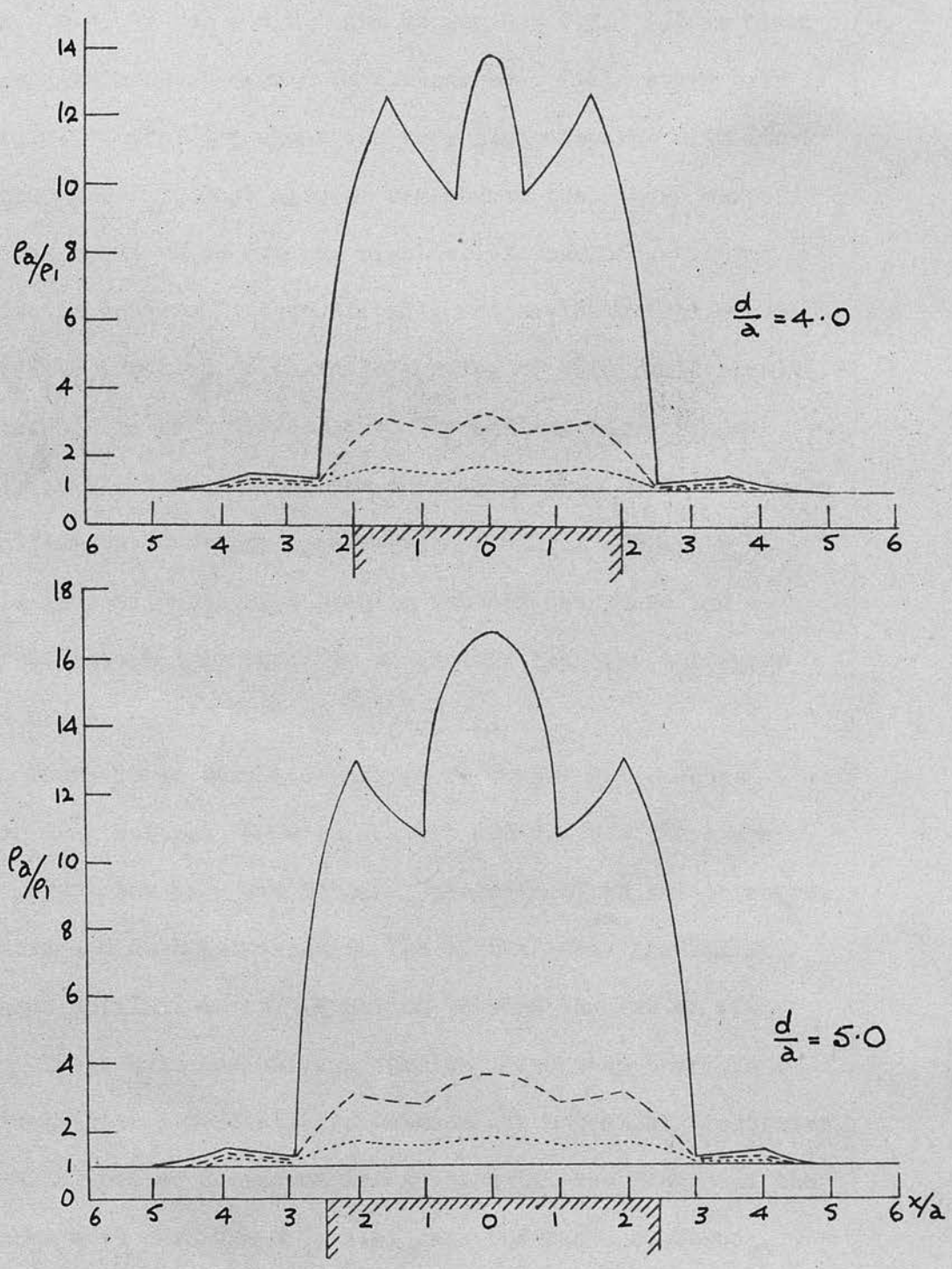

Fig. 27, Longitudinal Traverses over Vertical Insulators

——— k = 0·9,
– – – – – – k = 0·6,
····· k = 0·3.

are similar to those of Fig.13 for the very thin perfect insulator. The curve for d/a = 0.01 shows that the maximum anomaly in apparent resistivity is about 15% greater than normal when k = 0.9, 3% for k = 0.6 and 1% for k = 0.3. It is clear that such thin sheets would be obvious on a field curve only if the resistivity of the sheet was very high compared with its surroundings. It must also be remembered that these curves are for a sheet which extends right to the surface. Any increase in cover will automatically reduce the height of the resistivity profile, so that the proving of thin fault planes is likely to be very difficult. The maximum value rises rapidly as the thickness of the sheet increases, and the figure is modified to the single peak when d/a = 1. Hubbert's W profile (19) with the high peak is established where the electrode interval is equal to or greater than the thickness of the sheet.

There is an abrupt change of form when d/a becomes greater than unity. Between d/a = 1 and d/a = 2 there are three peaks, the side one becoming predominant as the thickness increases and as k increases. The central peak gradually decreases until it is only a hollow between the two on either side. These twin resistivity summits arise when there is a relatively high potential drop between the potential electrodes. The central hollow decreases in extent until the flanks of the two peaks meet when d/a = 3, i.e. when the whole electrode

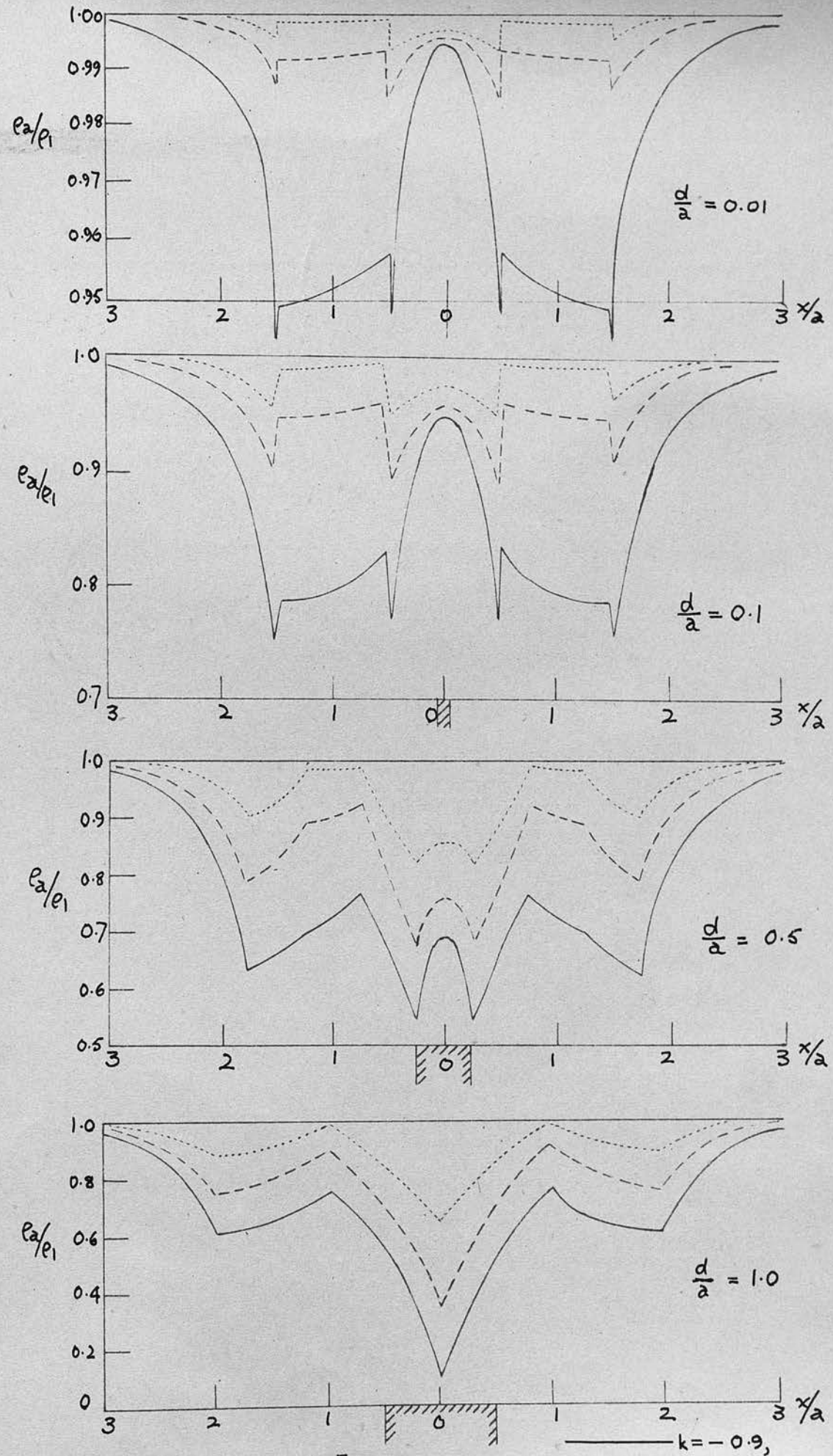

Fig 28, Longitudinal Traverses over Vertical Conductors.

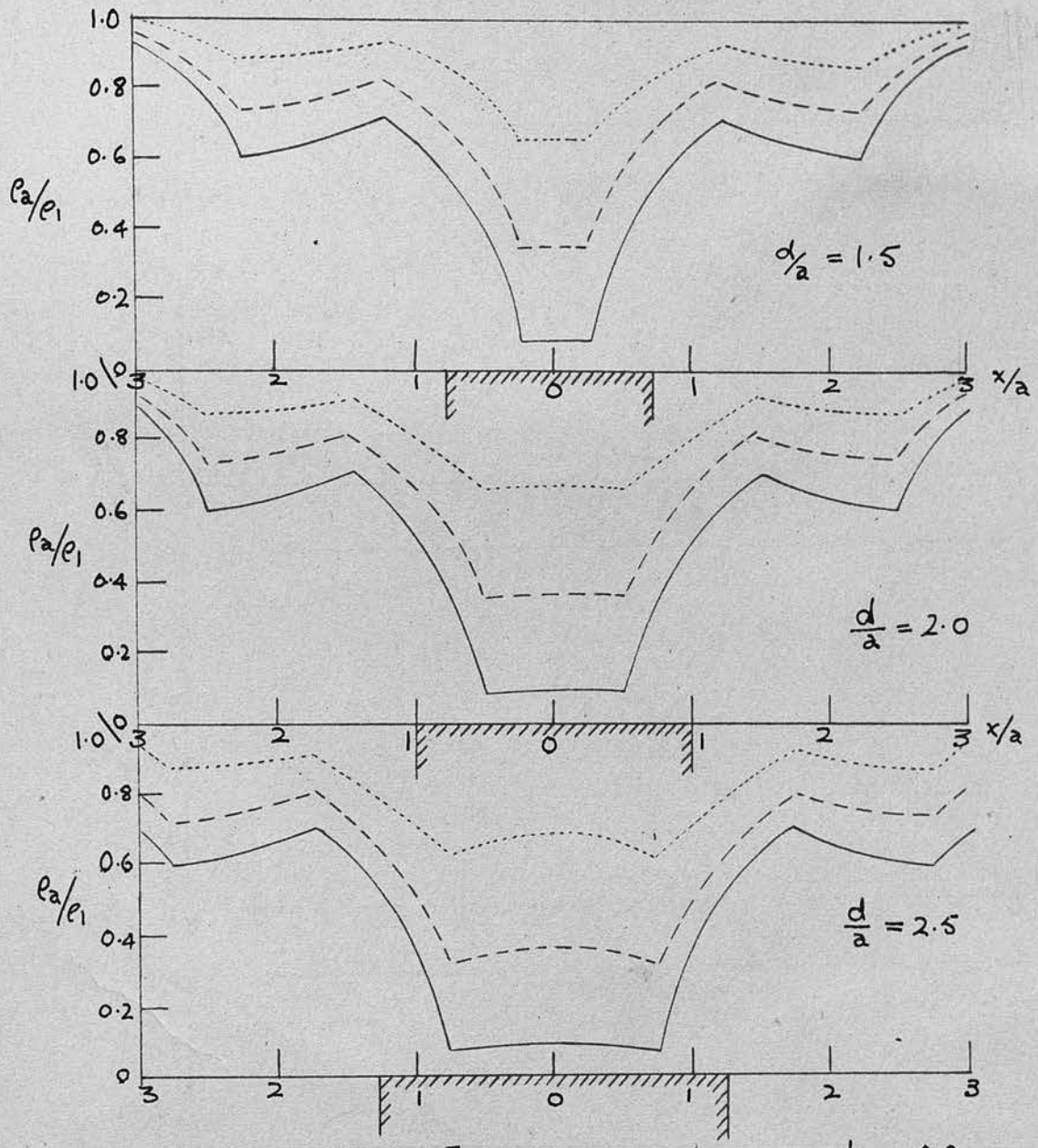

Fig. 29, Longitudinal Traverses over Vertical Conductors

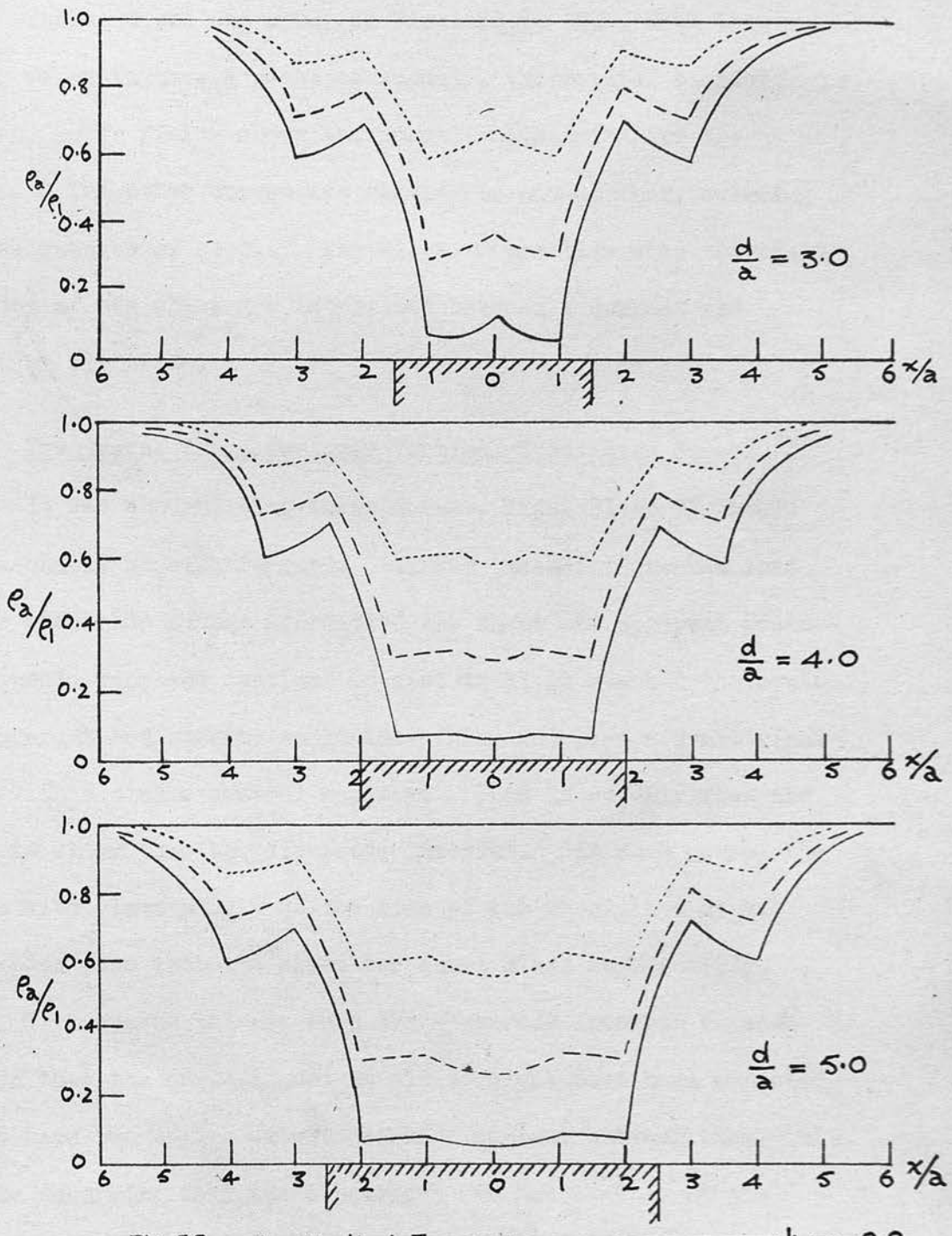

Fig. 30, Longitudinal Traverses over Vertical Conductors

system straddles the sheet. With greater thicknesses there is a maximum at the centre and smaller maxima at either side.

2. Longitudinal Traverses over Vertical Conducting Sheets.

These curves are shown in Figs. 28 to 30. With thin sheets we again have a W-shaped anomaly, the central maximum, however, never rising above the normal resistivity for the region. The other curves are similar to one another, evincing several changes of slope. The slope is positive when the sheet or sides of the sheet are interposed between a current and potential electrode.

3. Transverse Traverses over Vertical Insulating Sheets.

It was thought that these curves, Figs. 31 to 33, would be reasonably straightforward. It was taken for granted that as the electrode system approached the sheet the apparent resistivity would rise and continue to rise until it reached the centre. The apparent resistivity would then fall, and give a symmetrical curve with a single central maximum. This is so only when the sheet is wider than the electrode interval. In such cases, the resistivity rises slowly to the side of the sheet, and as the electrodes pass into the sheet the curve rises more sharply.

With sheets thinner than the electrode interval it will be seen that the curve is not at all as might have been expected. Now we have two maxima with a definite minimum between them, this minimum occurring when the electrodes are set exactly at the

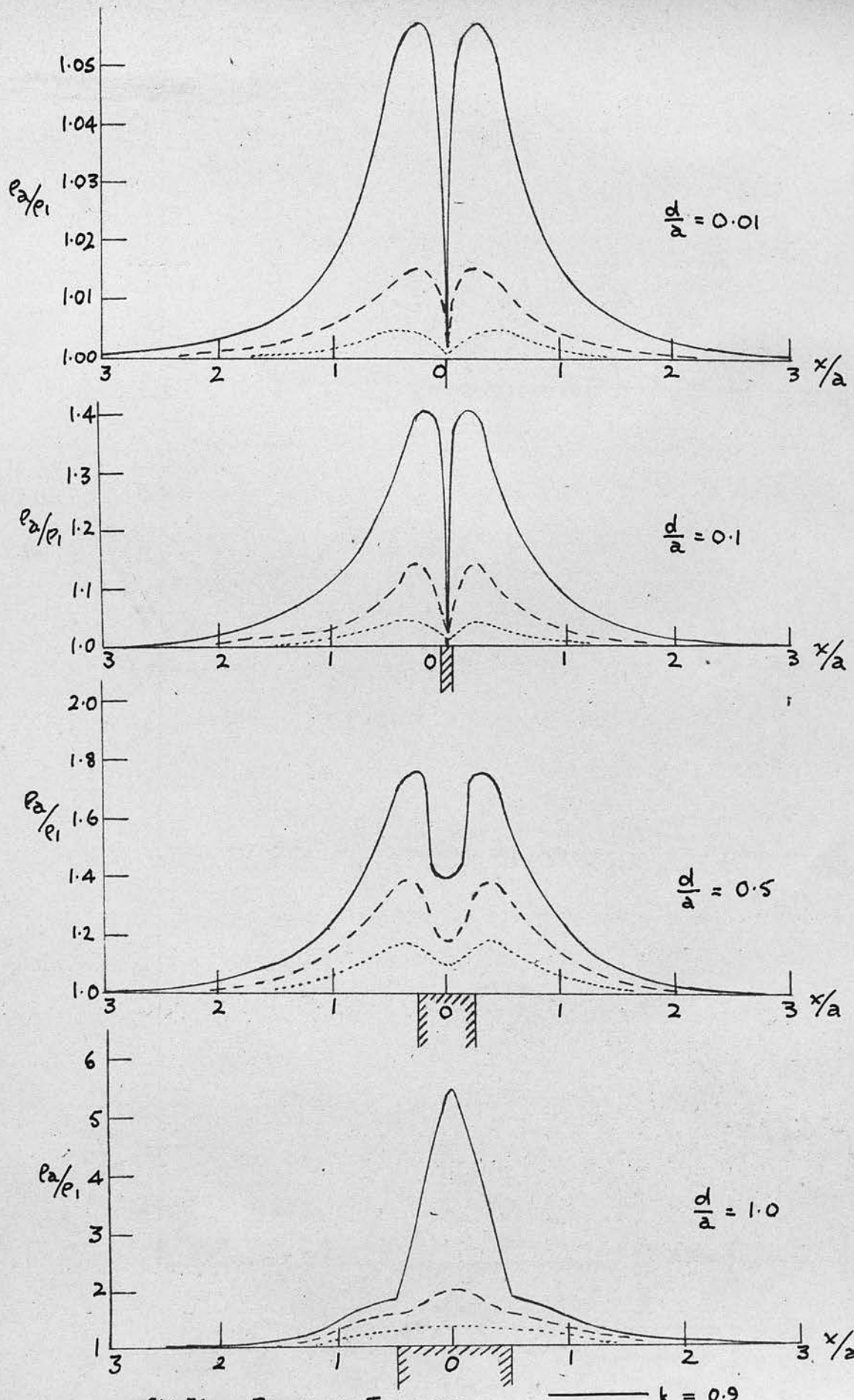

Fig. 31, Transverse Traverses over Vertical Insulators

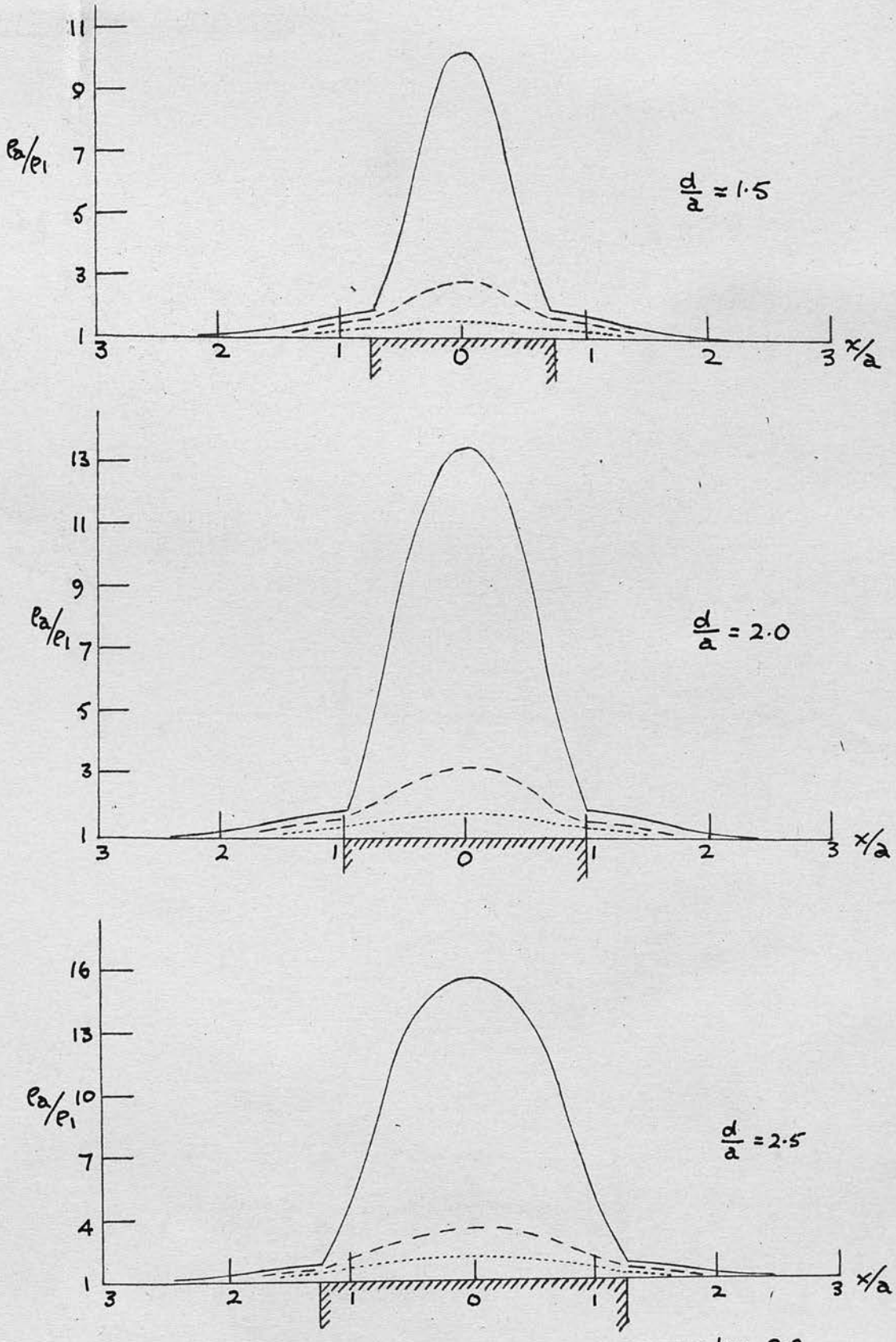

Fig. 32, Transverse Traverses over Insulating Sheets.

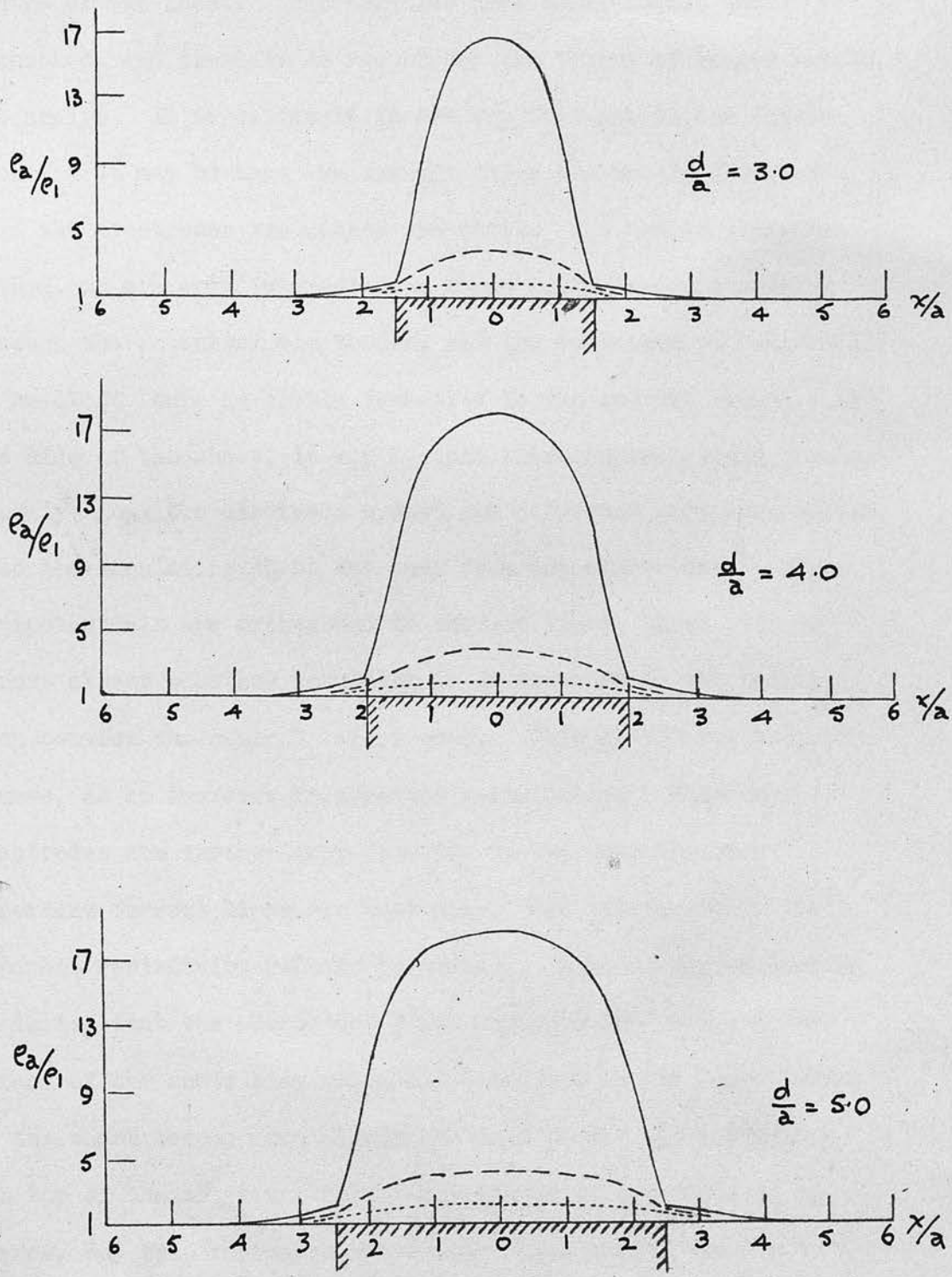

Fig. 33, Transverse Traverses over Vertical Insulators

centre of the sheet. The formulae have been checked and rechecked, and there is no reason why the theory of images should not apply. It is difficult to see why this phenomenon should occur. It may be that the current lines are barely diverted when the electrodes are within the sheet. In the resistivity method, we are only interested in those equipotentials passing through the potential electrodes, and the deviation of these will be small if there is little deviation in the current lines. At the side of the sheet, it may be that these current lines passing closely along the electrode system are refracted more than before into the insulating sheet and away from the electrodes. Since equipotentials are orthogonal to current lines, these will be thrust closer together resulting in an increase in the potential drop between the central electrodes. This is interpreted, of course, as an increase in apparent resistivity. When the electrodes are further away from the sheet, only the less important current lines are bent away, and consequently, the apparent resistivity returns to normal. Another way of looking at it is, that the electrodes first approach the side and the effect of the sheet side gradually decreases as the lower parts of the sheet become more highly inclined to the electrodes. The top of the sheet has relatively little effect while it is narrow, but this increases until with thick sheets the top is more predominant than the sides. These curves show, as with the longitudinal traverses, that apparent resistivity cannot be

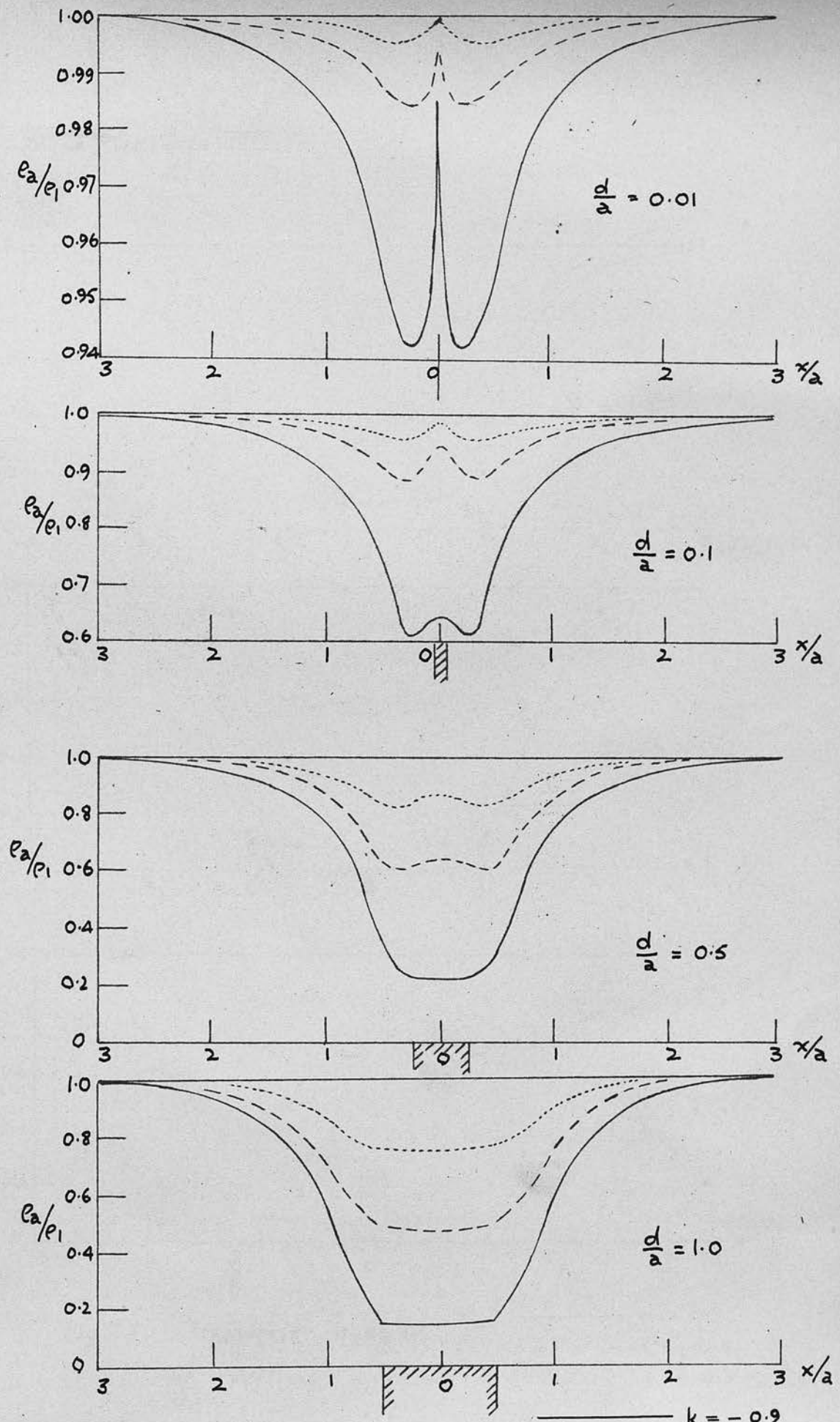

Fig. 34, Transverse Traverses over Vertical Conductors

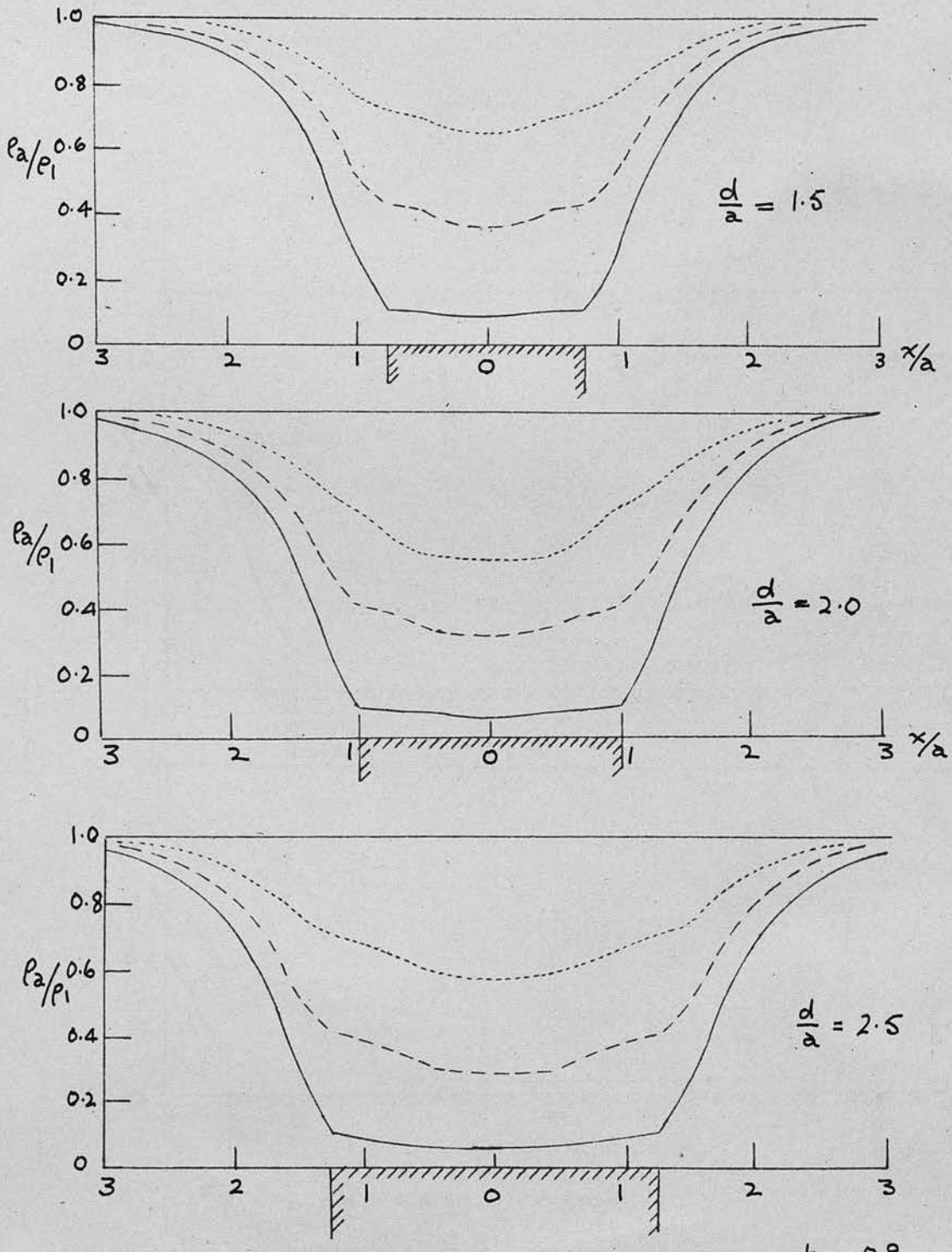

Fig. 35, Transverse Traverses over Vertical Conductors

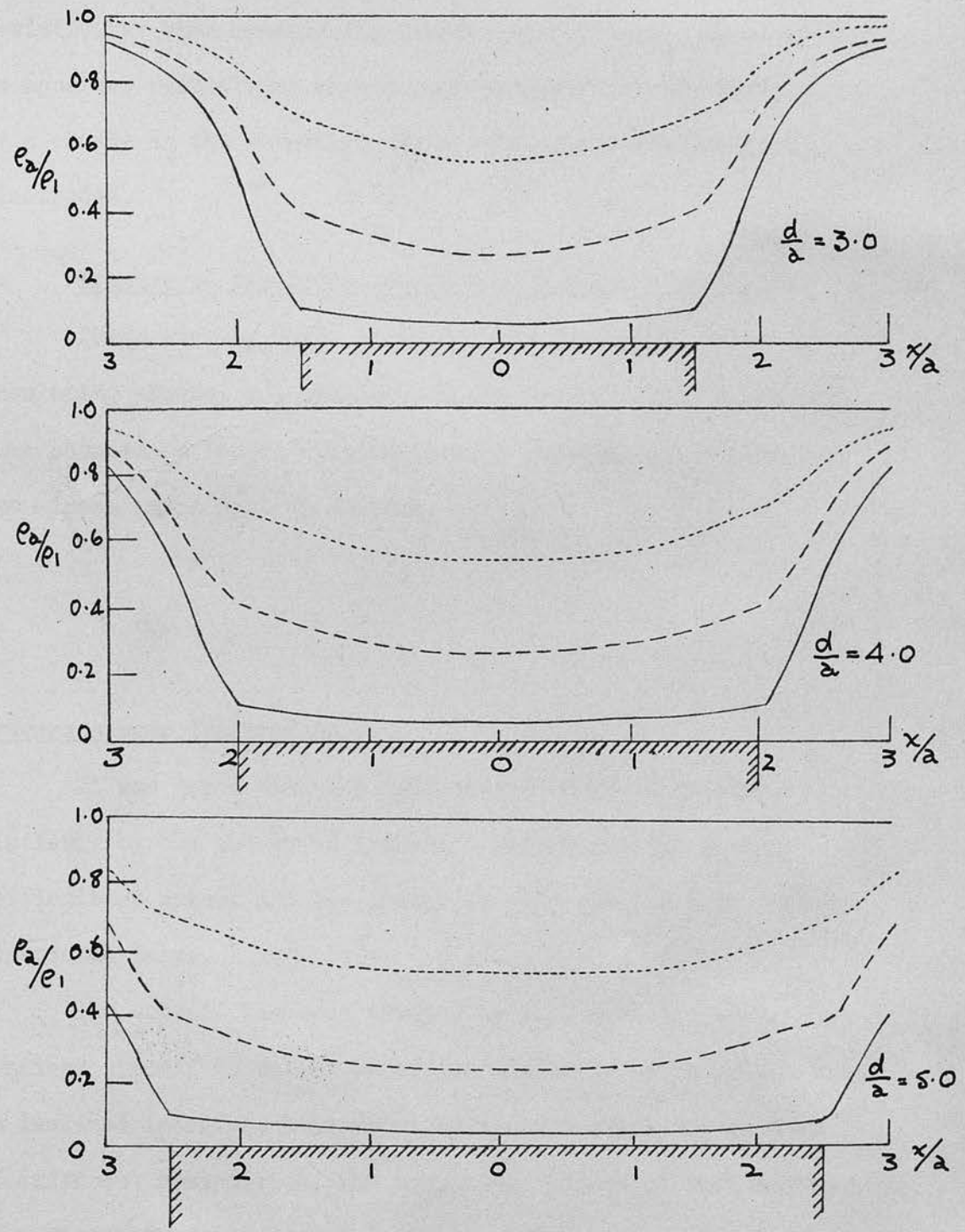

Fig. 36, Transverse Traverses over Vertical Conductors

regarded as an entirely satisfactory measure of underground resistivity when considering lateral variations. An alteration in apparent resistivity should be interpreted in the first place as a change in the potential difference across the potential electrodes.

4. Transverse Traverses over Vertical Conducting Sheets.

These curves, Figs. 34 to 36, are similar to those for insulating sheets, and similar remarks apply. Once again, the same phenomenon occurs with the thinner sheets, i.e. there are two minima and a central maximum.

Traverses over Inclined Sheets.

It was hoped that inclined sheets could be treated similarly by the theory of images. Unfortunately, several difficulties arise, and the theory is only available in certain restricted cases.

The subject has been treated by R.F. Aldredge (24). He confined himself to Wenner expanding electrode depth probes over an inclined interface between a top stratum overlying another of different resistivity, and showed the effect of such inclination on resistivity-depth curves. He was mainly interested in the errors caused by assuming such an interface to be horizontal, and goes on to demonstrate a method whereby dip may be determined. He does not consider dips greater than 15°. In traverses

we are often more interested in steeper dips of the order of say, 40° to 70° or so. As will be shown, Aldredge had good reason for this apparent neglect of steep dips.

As an example, let us take first of all an interface dipping at 45° and separating two media of resistivity ρ_1 on the down dip side and ρ_2 on the up dip side, as in Fig. 37.

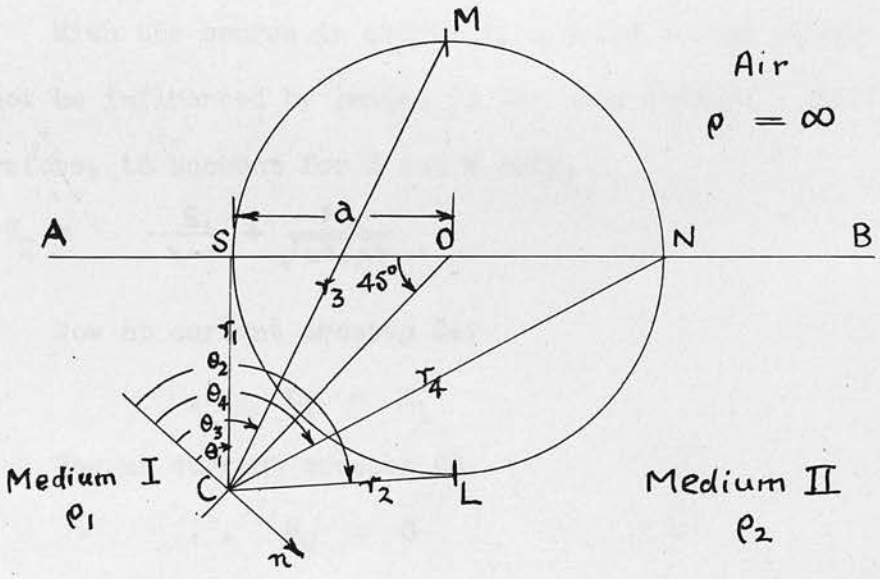

Fig. 37 Images for Inclined Interface

Let S be the current source situated at the surface of the first medium at a distance **a** from the point of intersection, O, of the interface OC and the surface AOB. The images of S are L, M and N which will all be situated on the circumference of a circle, the centre of which is O and radius OS. Let the potential at any point on the surface of medium I be V_1, and at any point on the surface of medium II be V_2. The points at

which the ~~the~~ potential is to be found are distant x from O.

The potential at a point in medium I will be due to the source S plus the images L, M and N as modified by their respective distances from the point.

Thus $V_1 = \frac{S_1}{x-a} + \frac{L_1}{\sqrt{x^2+a^2}} + \frac{M_1}{\sqrt{x^2+a^2}} + \frac{N_1}{x+a}$ 61

The subscripts denote the medium in which an effect is produced.

With the source in medium I, a point in the second medium cannot be influenced by images in the same medium. We have, therefore, to account for S and M only,

and $V_2 = \frac{S_2}{x-A} + \frac{M_2}{\sqrt{x^2+a^2}}$ 62

Now no current crosses OA.

$$\therefore \quad L_1 = M_1$$

Now no current crosses OB.

$$\therefore \quad M_2 = 0 .$$

At all points along OC, $V_1 = V_2$.

$$\therefore \quad S_2 = S_1 + L_1$$

$$\text{and } M_1 = -N_1$$

Taking any point C on the boundary OC, we require the current normal to the interface to be the same on both sides.

From equation 14

$$\frac{1}{\rho_1} \cdot \frac{\partial V_1}{\partial n} = \frac{1}{\rho_2} \cdot \frac{\partial V_2}{\partial n}$$

$$\therefore \frac{1}{\rho_1}\left(-\frac{S_1}{r_1^2}\cos\theta_1 - \frac{L_1}{r_2^2}\cos\theta_2 - \frac{M_1}{r_3^2}\cos\theta_3 - \frac{N_1}{r_4^2}\cos\theta_4\right)$$

$$= \frac{1}{\rho_2}\left(-\frac{S_2}{r_1^2}\cos\theta_1\right)$$

But, by symmetry about OC,

$$r_1 = r_2 \; ; \; \theta_1 = 180^\circ - \theta_2 \; ; \; r_3 = r_4 \text{ and } \theta_3 = 180^\circ - \theta_2$$

$$\therefore \frac{1}{\rho_1}\left\{-\frac{\cos\theta_1}{r_1^2}(S_1 - L_1) - \frac{\cos\theta_3}{r_2^2}(M_1 - N_1)\right\} = \frac{1}{\rho_2}\left(-\frac{S_2}{r_1^2}\cos\theta_1\right)$$

$$\therefore \frac{1}{\rho_1}(S_1 - L_1) = \frac{1}{\rho_2} S_2$$

$$\text{and} \quad M_1 = N_1 .$$

These equations can only be satisfied consistently if:-

1. $\rho_1 = \rho_2$, in which case $L_1 = M_1 = N_1 = 0$.

Hence there is no image solution in the general case (ρ_1, ρ_2);

2. ρ_2 is infinite, in which case the conditions become,

(a) no current across OA, $\therefore$ $L_1 = M_1$

(b) " " " OC, $\therefore$ $S_1 = L_1$

and $M_1 = N_1$

giving four equal sources.

The above expression for V_2 does not hold in this case, since the source S will have no effect inside a perfect insulator;

3. ρ_2 is zero, i.e. medium II is a perfect conductor,

(a) no current across OA, $\therefore$ $L_1 = M_1$

(b) V_1 constant (and $\therefore$ zero) along OC

$\therefore$ $L_1 = -S_1$

and $N_1 = -M_1$

This is equivalent to two equal sources and two equal sinks.

In this case $V_2 = 0$.

It will thus be seen that Aldredge's treatment is not a

rigorous one. The number of effective images for an inclined surface are given by him as $\pi/2\theta$ where θ is the angle of dip of the interface. In fact, these are the images on one side only, and we have exactly the same number symmetrical with them on the other side. Also, such an image solution is possible only with perfect conductors or perfect insulators. The sort of problems which possess sufficient symmetry to be amenable to image theory are illustrated in Fig. 38.

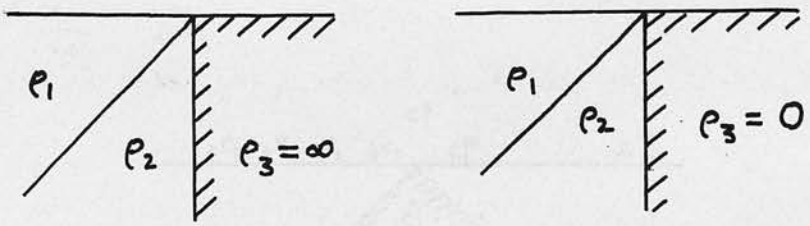

Fig.38 Problems which can be solved by Images

It will be agreed that these are of small practical utility.

As has been shown, the case of inclined sheets may be solved if these are either perfect conductors or insulators. However, the foregoing analysis is only applicable to the down dip side. With a traverse the electrodes must be able to move across the sheet, and so include the case where the angle between the sheet and the surface is between 90° and 180°. Since these sloping surfaces cannot be dealt with satisfactorily by

theory, laboratory experiments incorporating them are included in Chapter VI.

Traverses over Wedges.

An example of another combination with inclined surfaces which can be solved is that illustrated in Fig. 39, where a wedge of infinite resistivity or conductivity just touches the surface of the ground.

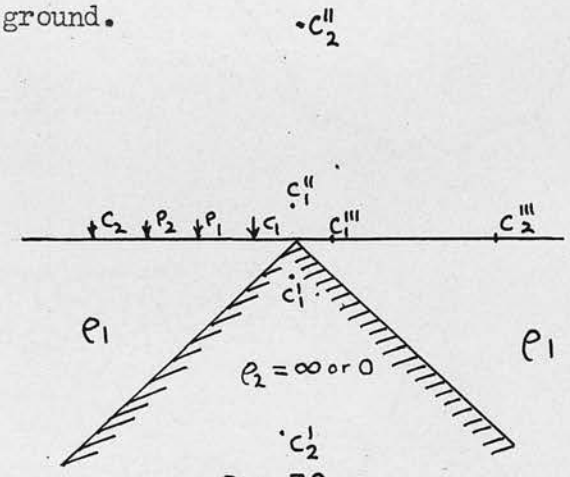

Fig. 39

Considering the electrodes approaching the wedge as above, the images are as shown. If the wedge has infinite resistivity then C_1, C_1', C_1'' and C_1''' are four equal sources. If a perfect conductor, C_1 and C_1''' are equal sources and C_1' and C_1'' are equal but opposite in sign, i.e. sinks.

Both longitudinal and transverse traverses have been calculated, and are illustrated graphically in Fig. 40. These, of course, are similar to those concerning vertical insulating and conducting sheets, but have more pronounced and broader effects. Such wedges, again, are of little value in practice,

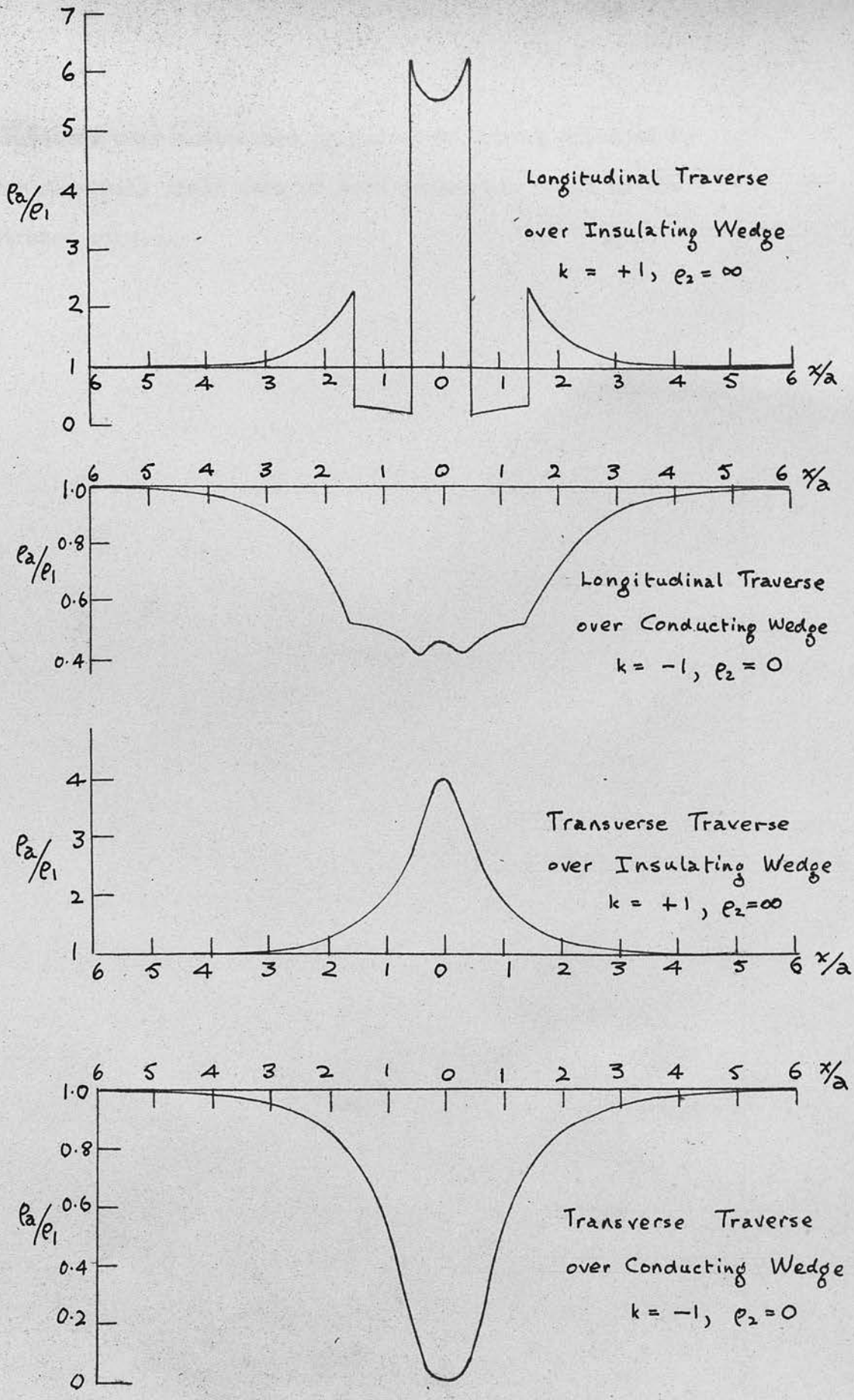

Fig. 40, Traverses over Wedges

but traverses over anticlines or masses of gravel embedded in boulder clay will yield more or less degenerate forms of the illustrated curves.

CHAPTER VI.

FIELD AND LABORATORY TRAVERSES

FIELD AND LABORATORY TRAVERSES

In order to confirm some of the results obtained from the foregoing theoretical analysis of apparent resistivity traverses over vertical conductors and insulators, a number of laboratory experiments were conducted to determine whether the theoretical results were borne out practically. The tank used for the experiment was a ractangular porcelain bath 110 cm. x 53 cm. x 36 cm. The tank was filled with water, and common salt dissolved in the water to provide a good conducting medium. The resistivity of the medium was brought down to about 30 ohm-cm. so that, using the Wenner configuration with a 5 cm. electrode interval, the value of the resistance measured was approximately 1 ohm. It was, of course, essential to have a small electrode interval in order that the tank itself should have a negligible effect. The Megger was used for these experiments, and since the maximum reading on it is 30 ohms, a highly conductive medium was required with such a small electrode separation. The electrodes were four nails filed to a very sharp point, and protruding from a piece of wood $\frac{1}{2}$ inch thick. This gave sufficient stability, and ensured that the electrodes remained fixed at their proper distances apart. The choice of materials to simulate the vertical sheets was, unfortunately, limited to those which, when compared with salt water, must either be regarded as perfect insulators or conductors. The curves given refer only to a perspex sheet which acted as a perfect insulator.

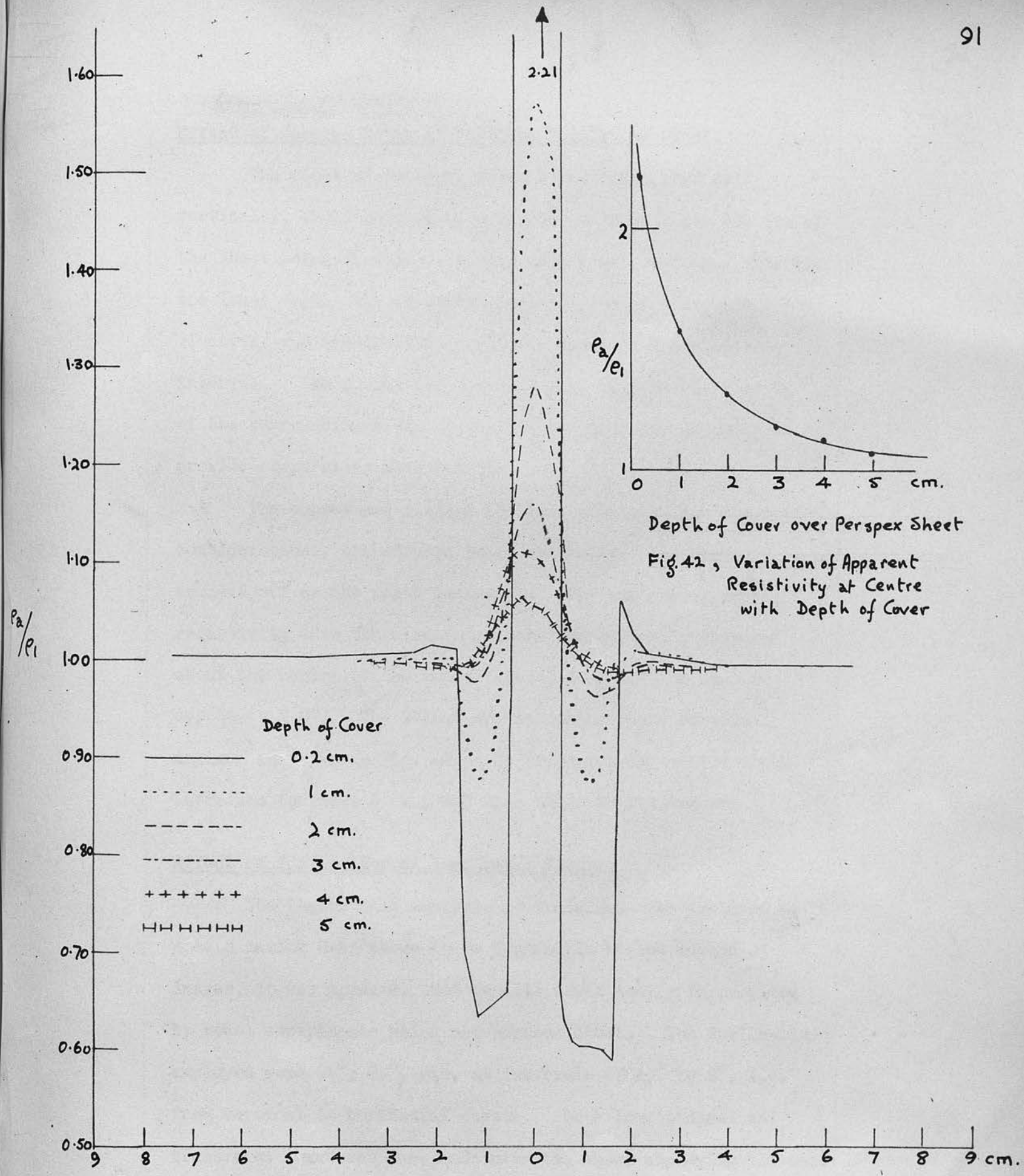

Fig. 41, Longitudinal Traverses over Perspex Sheet at Varying Depths

Fig. 42, Variation of Apparent Resistivity at Centre with Depth of Cover

Effect of Varying Depth of Vertical Insulating Sheet.

The sheet of perspex, about 2 mm. thick, was held vertically, and longitudinal traverses made over it, the top of the sheet being at depths varying from 2 mm. to 5 cm., i.e. at the least depth, the electrode interval was 25 times the depth of cover, and the greatest depth was equal to the electrode interval. The curves are shown in Fig. 41, the resistivity of the surrounding medium being reduced to unity in order to provide comparative measurements.

The curves are similar to those obtained from theoretical considerations, the effects being reduced and the curves rounded off as the depth increased. The maximum apparent resistivity when the electrodes were symmetrically disposed about the centre of the sheet reduced from 2.2 for shallow depths to 1.07. The effect of increasing depth on this maximum is shown in Fig. 42. It drops quickly as the depth increases to about 2 cm., and then tends to flatten out.

Effect of Inclination of Insulating Sheets.

The theoretical analysis of traverses over inclined sheets having been shown to be impossible by the method of images, it was apparent that results would easily be provided by model experiments using the perspex sheet. The inclinations employed were 90°, 75°, etc. at intervals of 15° to 0°, i.e. from vertical to horizontal sheets. Both longitudinal and transverse traverses were made over the sheet employing the same

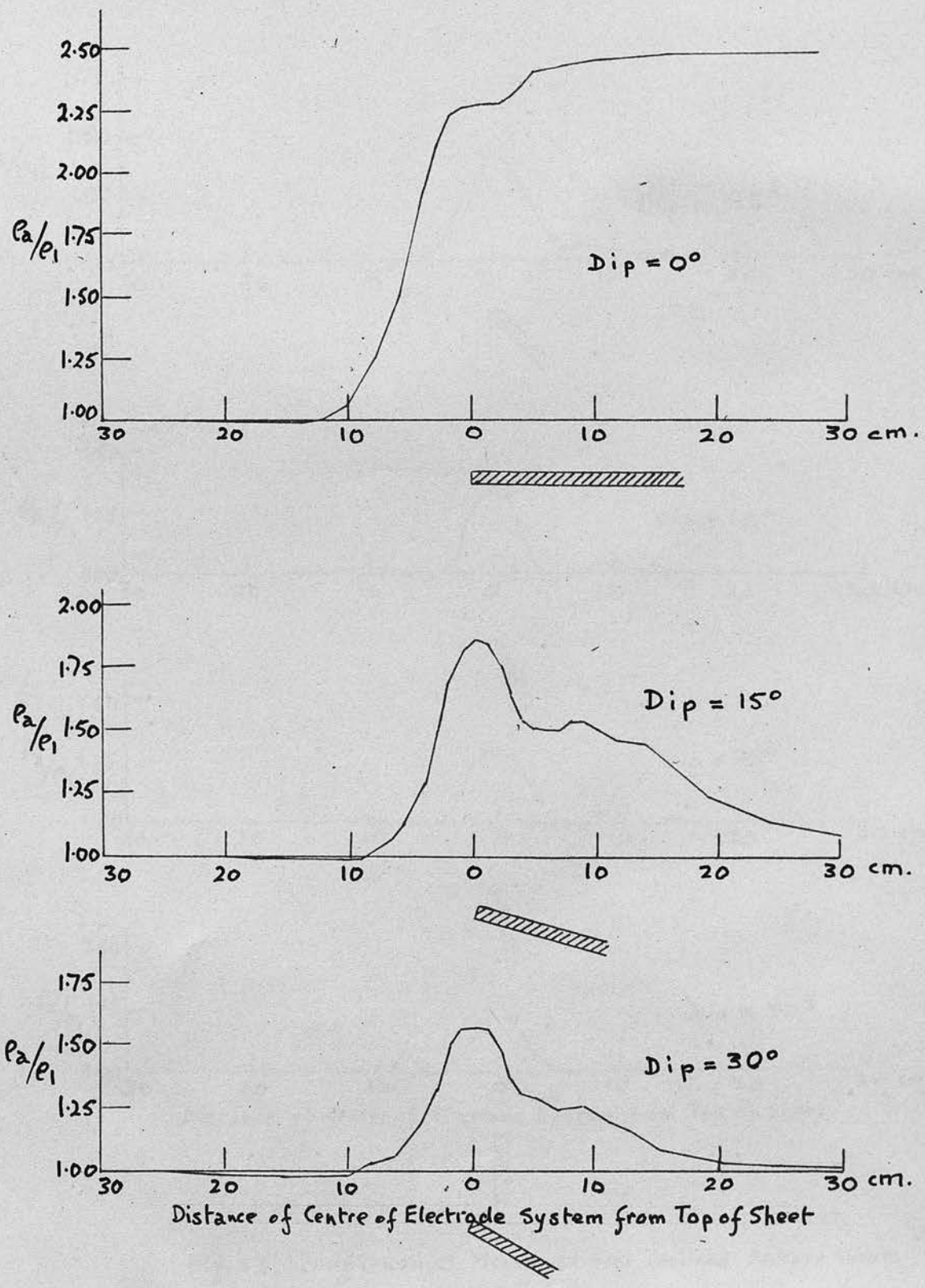

Fig. 43, Longitudinal Traverses over Inclined Perspex Sheets

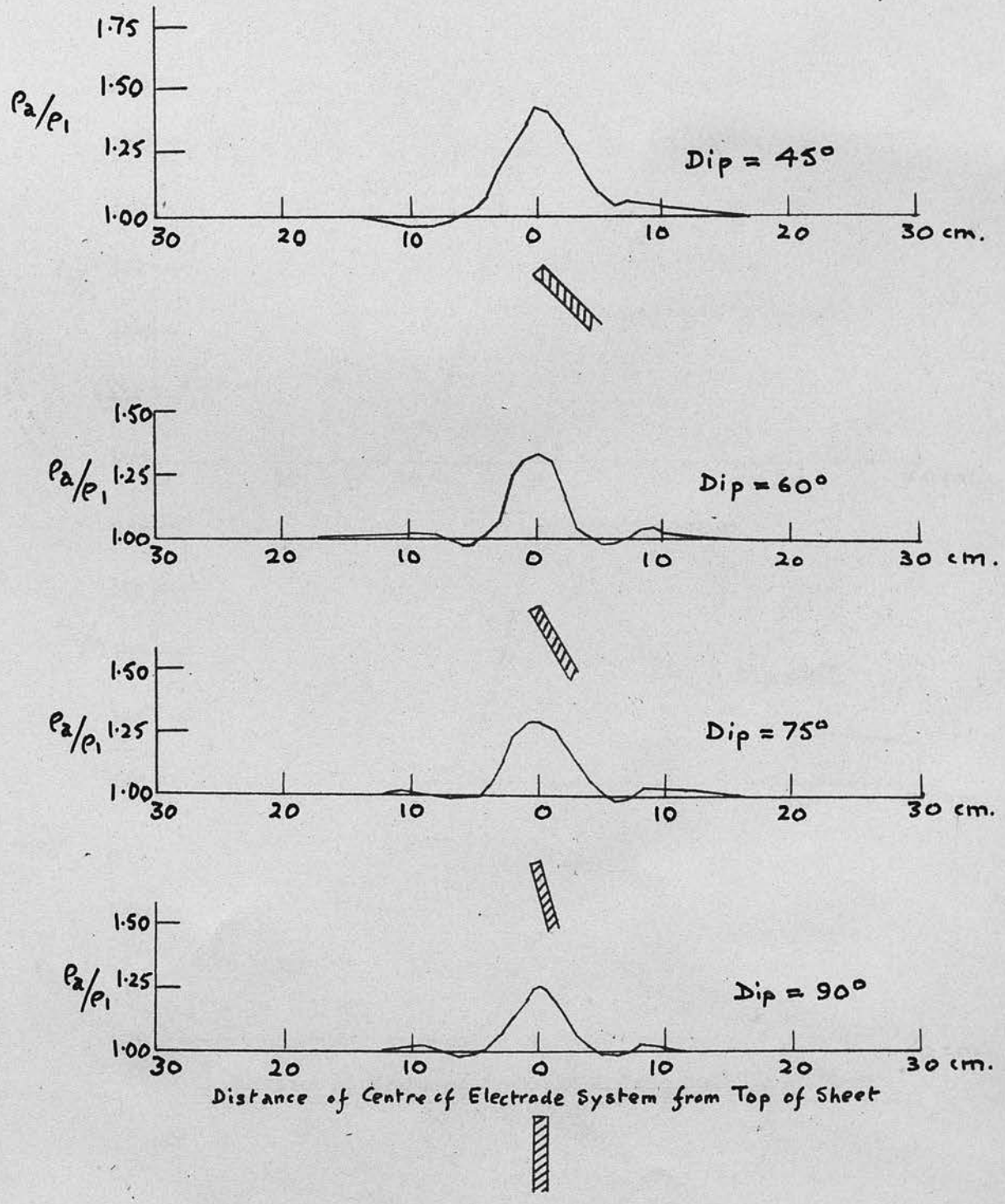

Fig. 43, Longitudinal Traverses over Inclined Perspex Sheets

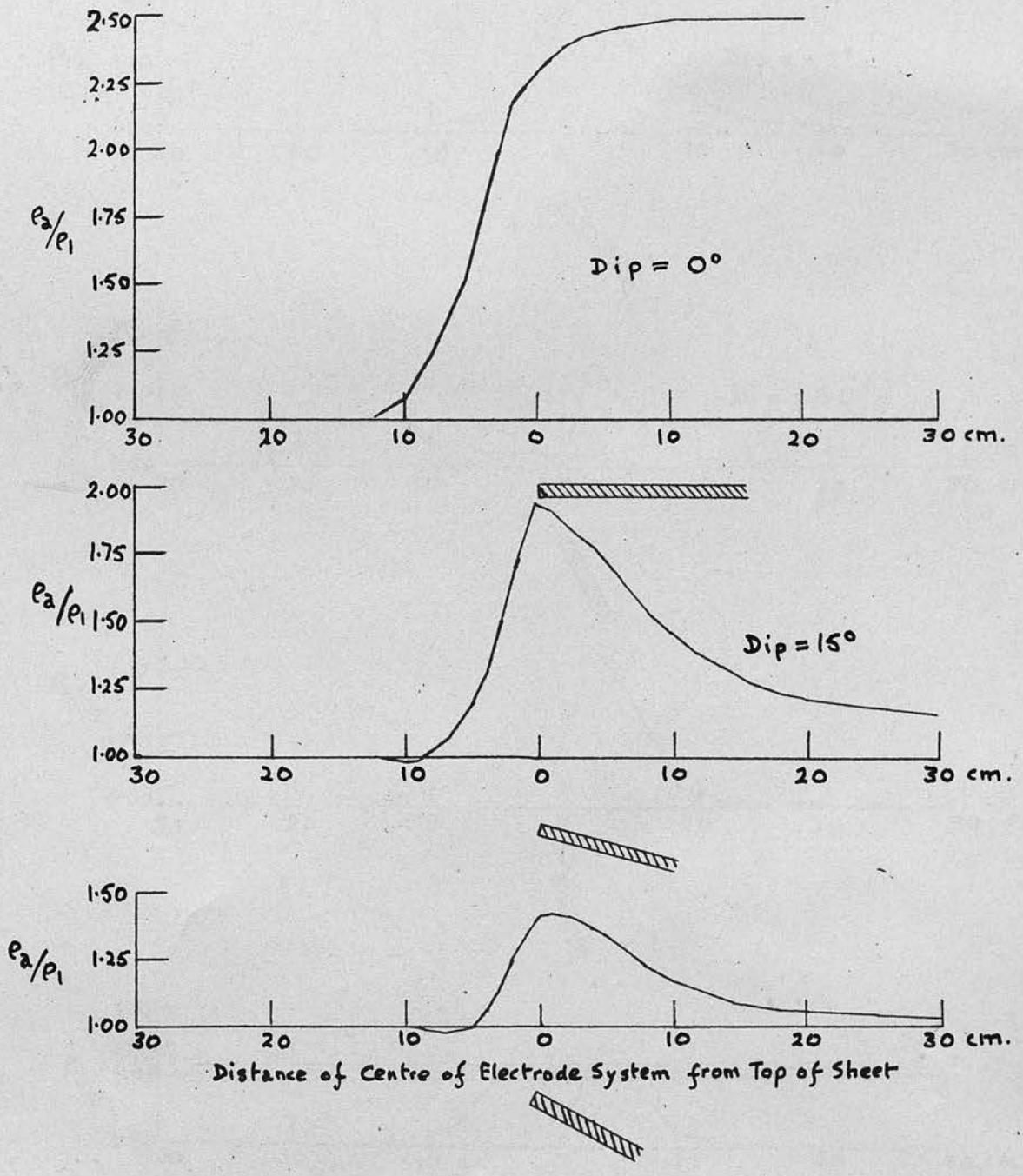

Fig.44, Transverse Traverses over Inclined Perspex Sheets

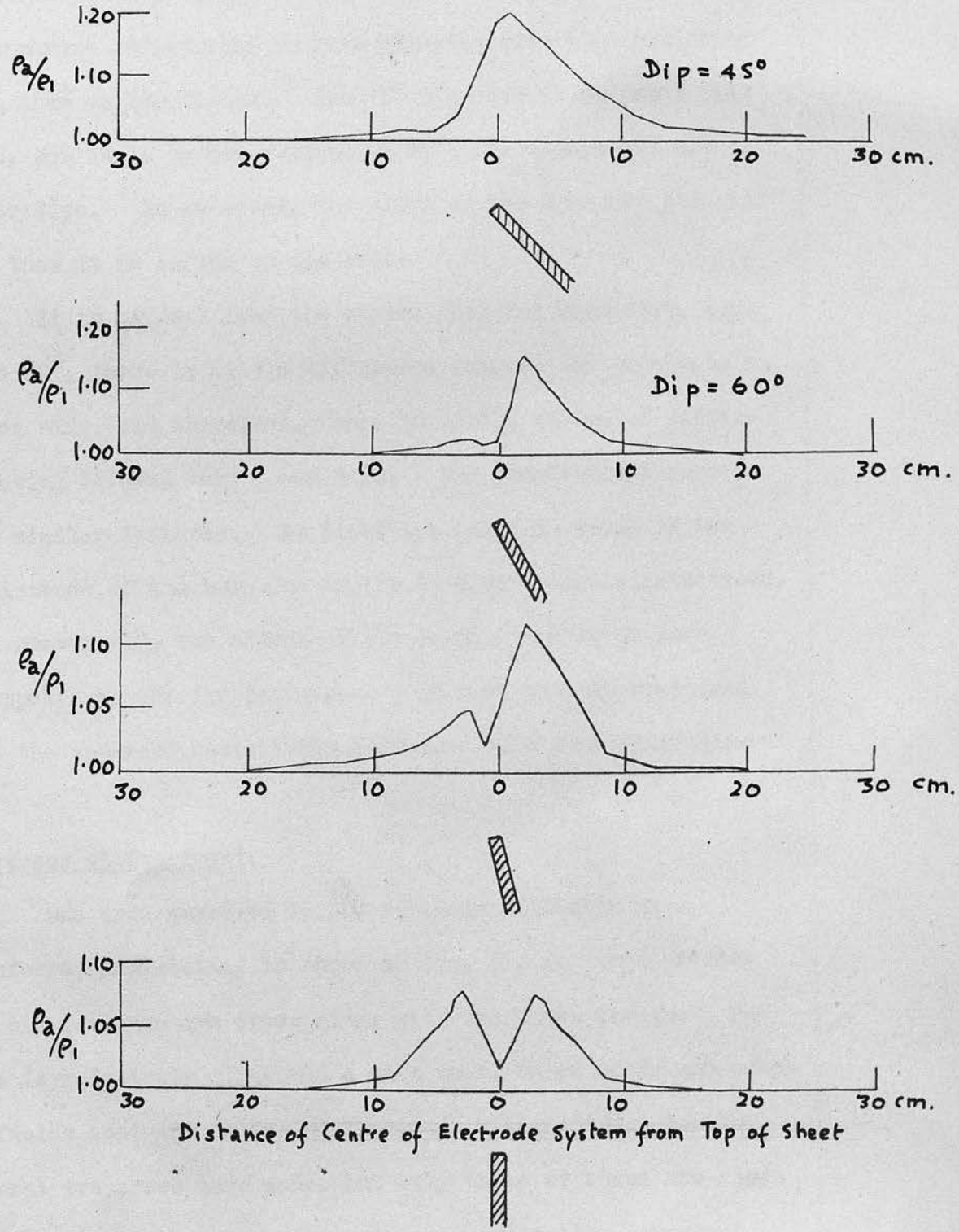

Fig. 44, Transverse Traverses over Inclined Perspex Sheets

5 cm. electrode interval. The curves for a depth to the top of the sheet of 2.5 cm. are shown in Figs. 43 and 44.

The transverse traverse over a 90° (vertical) sheet illustrates the peculiar anomaly discussed on page 73 , where the apparent resistivity is less directly over the insulating sheet than on its flanks. The 75° dip also illustrates this point, but it is hardly evident at 60°, and disappears at lesser dips. As expected, the slope on the down dip side is less than it is on the up dip side.

It is evident from the curves that for high dips, i.e. above 60°, there is little difference between the gradients on either side, and, therefore, there is little chance of differentiating between very steep dips. The longitudinal curves show similar features. An important point in these is the persistence of the bump due to the leading potential electrode, and, conversely, the effect of the lagging electrode soon disappears as the dip decreases. It must also be mentioned that the apparent resistivity increases with decreasing dip.

Traverses at Oxenfoord.

One area surveyed in the vicinity of Castle Mine, Oxenfoord, Midlothian, is shown in Fig. 45, in which present and old workings are drawn along with the known faults. The area is relatively flat, but a main road, thick woods and crops in fields kept the number of traverses within strict bounds. Several traverses were made, but only three of these are shown in Fig. 46, as they were the only ones indicating important

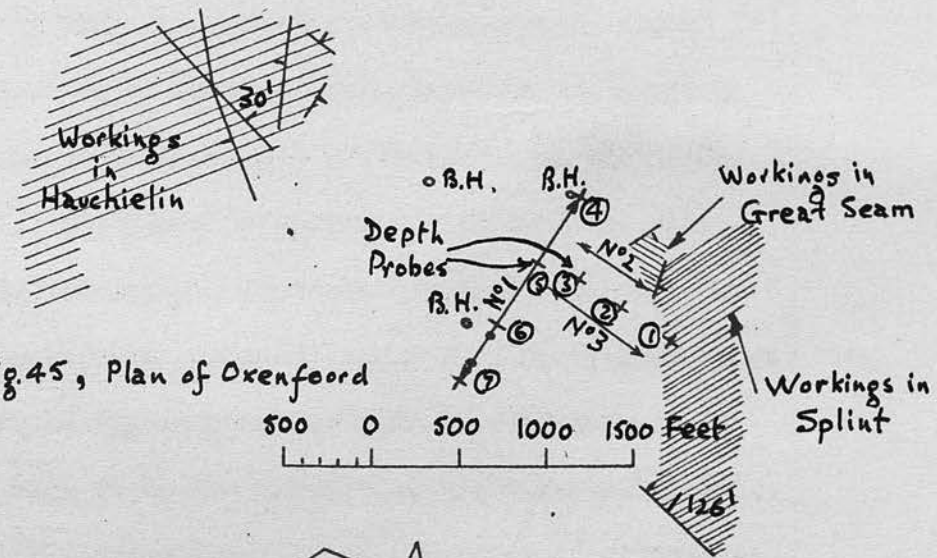

Fig. 45, Plan of Oxenfoord

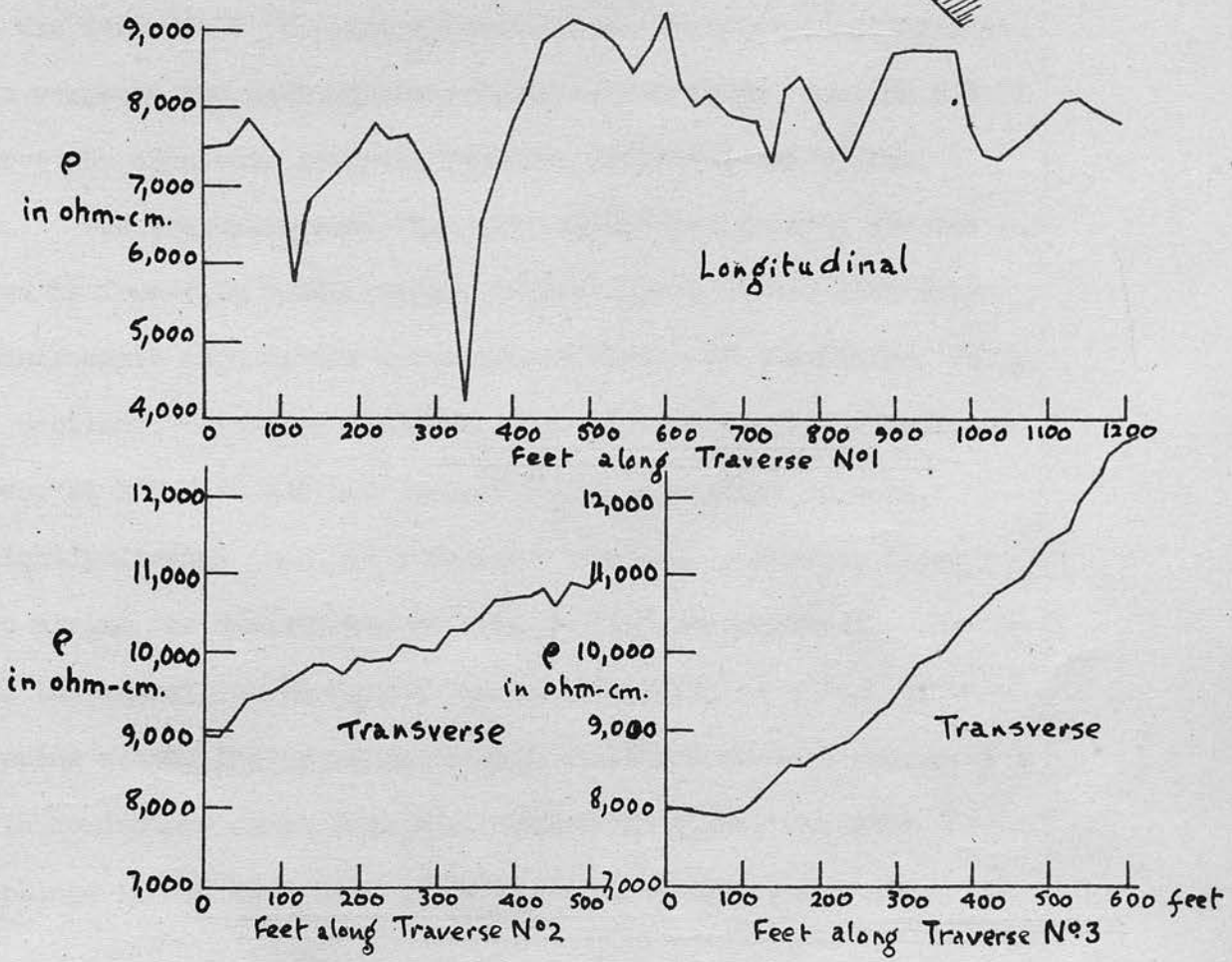

Fig. 46, Resistivity Traverses at Oxenfoord

features. In Nos. 1 and 3 the electrode separation was 200 feet, and in No.2 160 feet, the reason for the choice of 200 feet being that the depth of boulder clay varied from 60 to 120 feet, and it was necessary that the resistivity measurements should penetrate well under the rockhead. No.2 traverse had perforce to be reduced to 160 feet on account of obstacles in the field. As mentioned above, the type of traverse was dictated by the surface features in the area. No.1 was a longitudinal one since it could only be made along the verge of a main road. Nos. 2 and 3 were chosen as transverse traverses so that they could commence from the main road, and proceed at right angles thereto. It was impossible to start a longitudinal traverse right against the verge as the back current electrode had to be one and a half times the electrode interval from the centre of the system.

The traverses show that the average resistivity for the area is from 8 to 9,000 ohm-cm. This figure agrees with other measurements made in the Carboniferous rocks of the Midland Valley of Scotland. In No.1 traverse (Fig. 46) there are two definite lows, at 120 feet and 340 feet. Their separation is only slightly greater than the electrode interval. Between these two minima the resistivity returns to just below normal. Assuming the anomaly to be due to the interposition of a steeply dipping sheet, the curve is clearly analogous to that caused by a thin conductor, as in Fig. 28. Since the survey was made workings to the east have proved a fault of 126 feet throw,

throwing down the measures to the north. The 30 feet fault shown in the Hauchielin workings when joined to this fault passes almost exactly between the two lows of traverse No.1. There can thus be little doubt that the fault in this case acts as a conductor, and causes a sufficient change at the surface to be discovered by the resistivity method.

Nos. 2 and 3 transverse traverses were approaching present-day workings and crossed two known faults; the limit of the workings being then at the ends of the traverses. These workings were in the Splint Coal at a depth of 160 to 170 feet. Both traverses show steady rises as the workings are approached, indicating that the resistivity increases due to fracture of the strata and probably draining of water. The rise with 200 feet electrode separation in No.3 traverse is less than in No.2 traverse with shallower penetration. No.3 traverse, therefore, includes strata below the workings and not affected as the upper strata. The non-appearance of the faults in the resistivity curves may be because they are so thin as to have negligible effect at the surface, or that their resistivity is affected by the workings. The difference in resistivity found over these workings gives some reason to hope that there may be cases where the method could locate old workings. This is probable, but extensive tests by Cox and Price (3) in South Wales have shown that its application is restricted.

Traverses at Rig Colliery.

A series of traverses were made in the neighbourhood of Rig Mine, a small surface drift mine to the north of the Sanquhar coalfield, which constitutes an outlier of Carboniferous rocks resting unconformably on highly folded Ordovician strata. At Rig Mine the mine entries are about half a mile south of the River Nith and the seams being worked are shallow, sometimes less than 100 feet from the surface. This district lies about 20 miles from Cairnsmore of Carsphairn, part of a ridge which acted as a breeding ground for glaciers in the Southern Uplands. The geological map of this area shows many fluvio-glacial channels leading towards the Nith, as in Fig. 47. These contain rather coarse gravels in this case.

Four boreholes had been previously put down. Depth probes at these holes proved difficult to interpret as will be discussed in Chapter VIII , and so it was decided that the method of traversing should be attempted. One channel was already known near the main road, having been discovered by underground workings at depths of 80 to 100 feet. Since the depth was of the order of 100 feet, the electrode interval used was 200 feet, and all traverses made were longitudinal, readings being taken every 20 feet. Fortunately several lines of boreholes were available to test these traverses.

On plotting the two traverses it was found that there was a variation of resistivity across the channels. However, here the resistivity increases above the centre of the channel showing that the gravel has a higher resistivity than the local strata, a

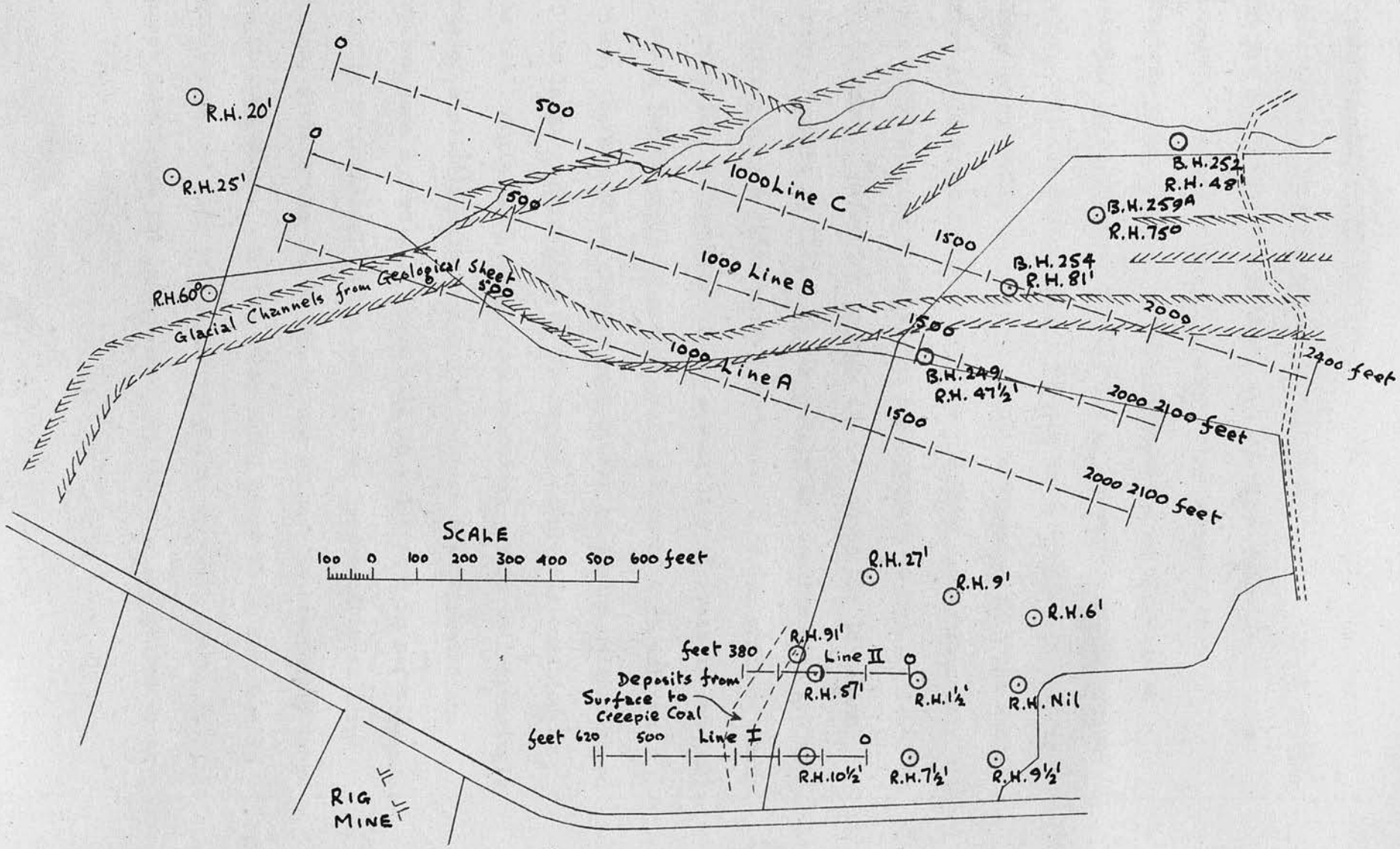

Fig. 47, Plan of Surface around Rig Colliery

rather unusual occurrence since alluvium commonly has a lower resistance. This may be due to the fresher water in the gravel, but Dr. Fisch (25) has offered the following solution to this paradox. He has found, like many other workers, that the greatest yield of water is often obtained from alluvial or diluvial deposits which exhibit the greatest electrical resistivity. As the conductivity of rocks is determined in the first place by the water content, it would be expected that the useful water yield would increase with the porosity and consequently with the electrical conductivity, but the opposite is usually found to be the case. Referring to Fig. 48, if, as in the left-hand corner, a space is filled as completely as possible with grains of uniform size A (with rhombic arrangement of the grains), then the porosity, independent of the actual size of grain is 26% (26). If now a larger grain is placed among a mass of such uniform grains, there must be greater pore spaces b, in the neighbourhood of the large grain B than in the region completely occupied by the small grains with small pore spaces a. This is increasingly true of a still greater grain C with which are connected the greater pore spaces c. There will be a decrease in porosity which is proportional to the cube of the radius of these large grains, since a quarter of the volume of each is completely lacking in pore space. On the other hand, there is an increase in porosity in the case of the larger grains as shown above, but this cannot cancel out the loss, since the increase is limited to the

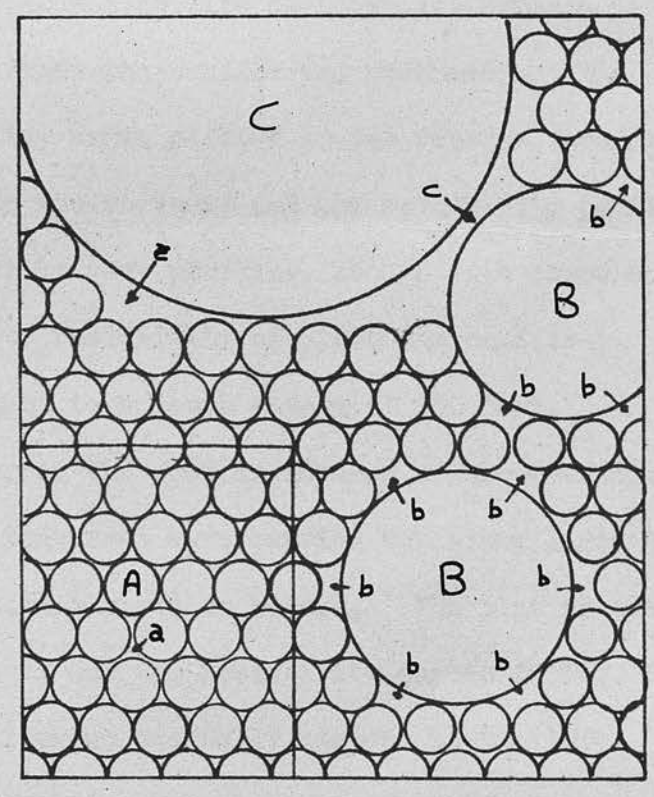

Fig.48, Grain Size and Effective Porosity

surface of the larger grain and therefore is proportional to the square of the radius. Therefore, for a mixture of different grain sizes, there is a smaller gross porosity than for a uniform grain size. Thus with similar water contents, a mixture of sizes will have a larger resistivity than a material having uniform size grains. The gravels found in this area are therefore liable to be more resistive than the normal boulder clay which usually contains less boulders in a matrix of stiff, unstratified clay.

As an increase in resistivity followed an increase in depth Fig. 49, which shows the surface and rockhead profile, includes the resistivity curve plotted in the reverse direction. The similarity between the rockhead and the resistivity profiles with the scales chosen is very striking, and in both cases an increase of 0.1 ohm (or resistivity of 3,800 ohm-cm.) is approximately equivalent to a depth change of 100 feet.

In order to survey the area in advance of the workings, similar longitudinal traverses were carried out along lines A, B and C, and the results plotted as before. The plan of the area is shown in Fig. 47 and the resistivity curves in Fig. 50. These show that the alluvium gradually deepens to the left. In line A there occurs the main channel shown on the geological map, and in addition a slightly shallower channel with centre at 1,400 feet. This secondary channel apparently diminishes and merges with the main channel between lines B and C. The surveys show that the channels are more extensive than previously thought

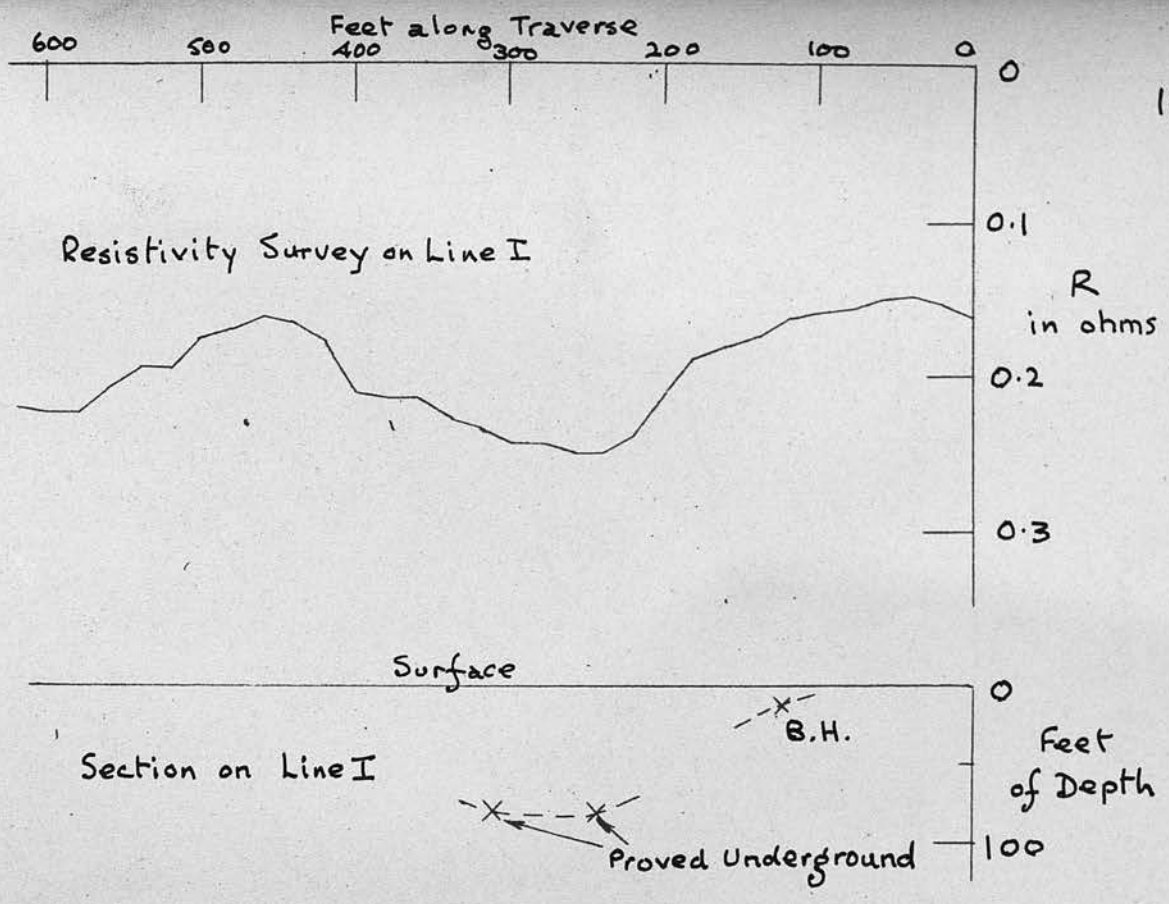

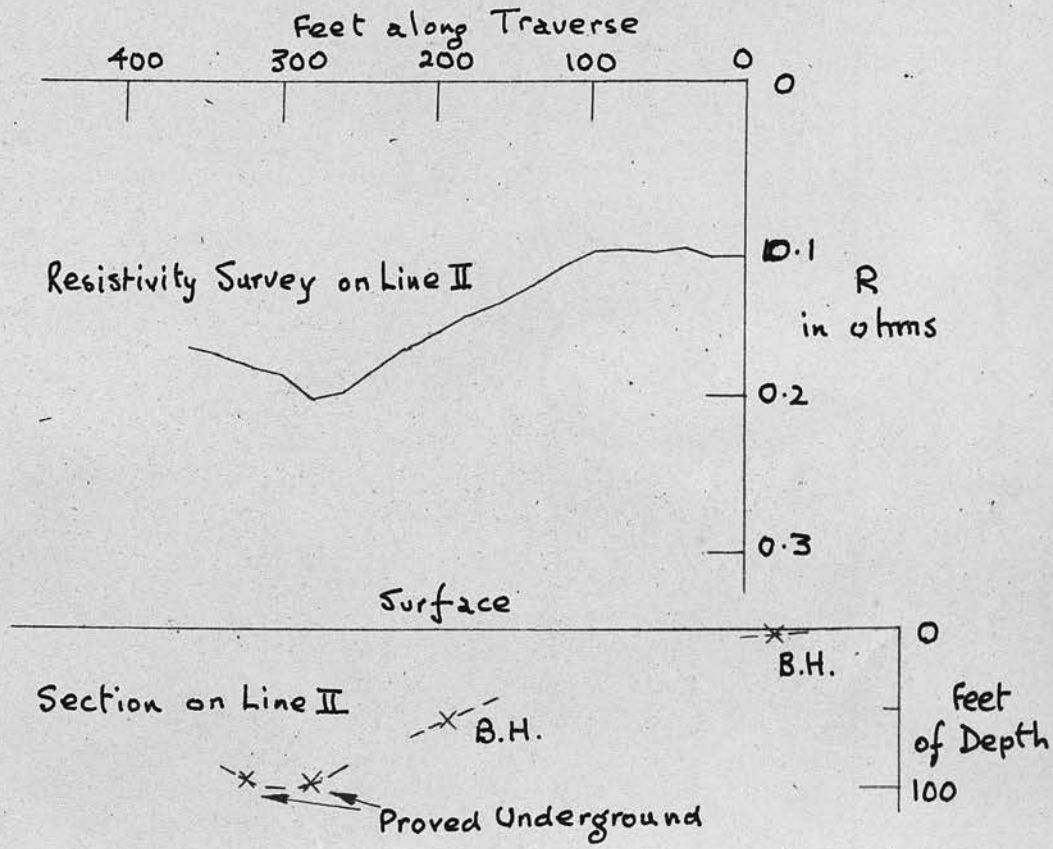

Fig.49, Longitudinal Traverses over Lines I and II at Rig Colliery

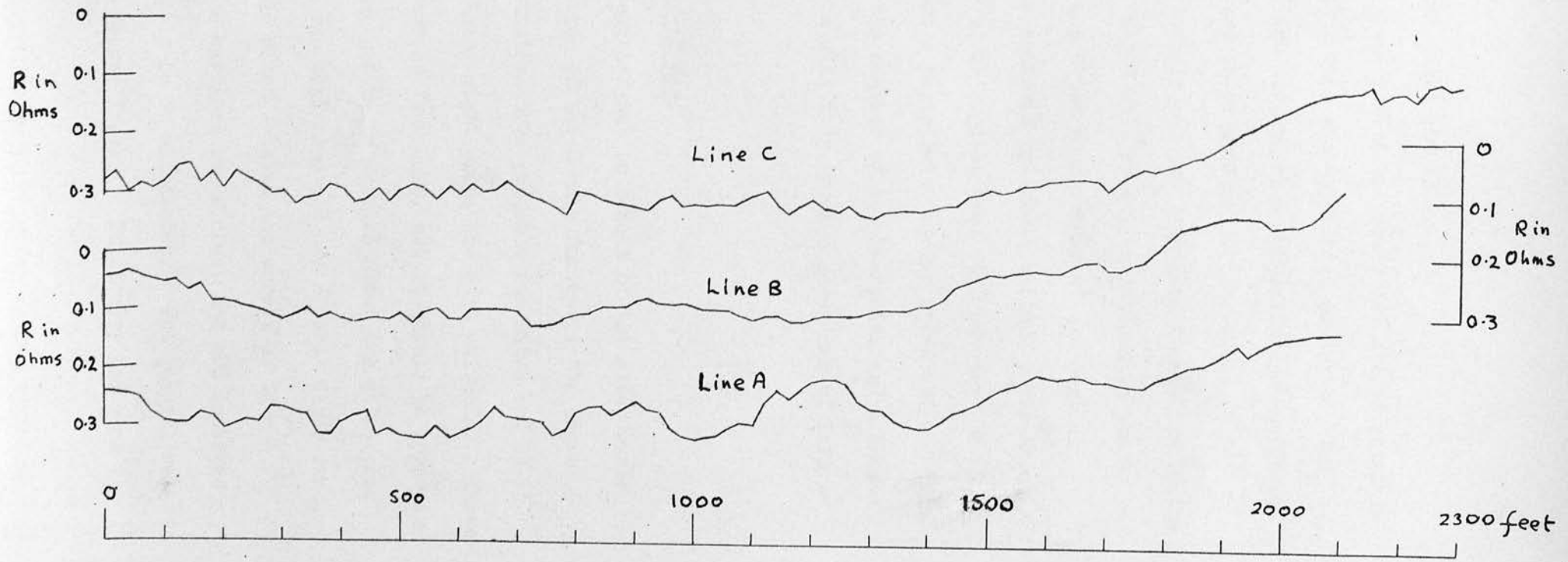

Fig. 50 Longitudinal Traverses A, B, and C at Rig Colliery.

and their depths are at least 100 feet.

These results testify that traverses can afford valuable information when depth probes are apparently useless. The difficulty is that we are dealing with undulating sub-surfaces while theory usually treats of horizontal interfaces. It follows that buried channels and the like lend themselves to the method of traversing, which will reveal variations in the depth to rockhead, but not a precise measurement of the depths. Precision will only be achieved by actual boring. The amount of boring required to prove a given area can, however, be reduced by carrying out a resistivity survey previously. This survey will indicate the centres of the channels, and a bore-hole sunk in the centre will then provide a maximum of information.

Traverses at the Water of May.

This work was carried out on behalf of the Fife County Council at the invitation of the County Surveyor, the aim of the survey being to examine three probable dam sites and to investigate which of these might prove the most suitable. Three long traverses were made in four days, but it should be borne in mind that the equipment had to be carried about two miles over very steep country at the beginning and end of each day's work. In addition, heavy rain often delayed the survey as the insulation of the cable carriers broke down, and odd leakages of current had frequently to be eliminated. The general wetness also invaded the Megger itself. Difficulty had been

experienced on a previous survey after a thunderstorm, and the Megger was returned to the manufacturer who found nothing wrong. Subsequent field trials gave no further erroneous indications until this present survey, the fault being finally located as due to water interfering with the variable resistance on the generator. On drying out at night the apparatus functioned normally. The trouble made itself evident when it was found to be impossible to balance the galvanometer.

The total amount of work done on the site comprised three longitudinal traverses with an electrode interval of 200 feet over the three suggested dam sites. Readings were taken every 20 feet, but these intervals were reduced to 5 feet at one place in order to verify a large anomaly. The No.1 dam site had been already explored by boreholes and trial pits as shown in Fig. 51. The diagram includes the evidence of the rockhead as deduced by these bores and pits, the profile of the ground and the resistance as read from the Megger. The resistance is plotted, as it is directly proportional to the resistivity. The average resistance in the area, where the country rock is of Old Red Sandstone andesite, of 0.4 ohms is equivalent to a resistivity of 15,320 ohm-cm.

It was hoped that the resistivity profile and the rockhead profile might show a distinct relationship, both being available for No.1 site. As will be seen, these two profiles have not the slightest resemblance to each other, and the profile due to the thickening cover of drift is concealed completely by an anomaly which includes a central maximum flanked by two minima. The two minima, 250 feet apart, are remarkably

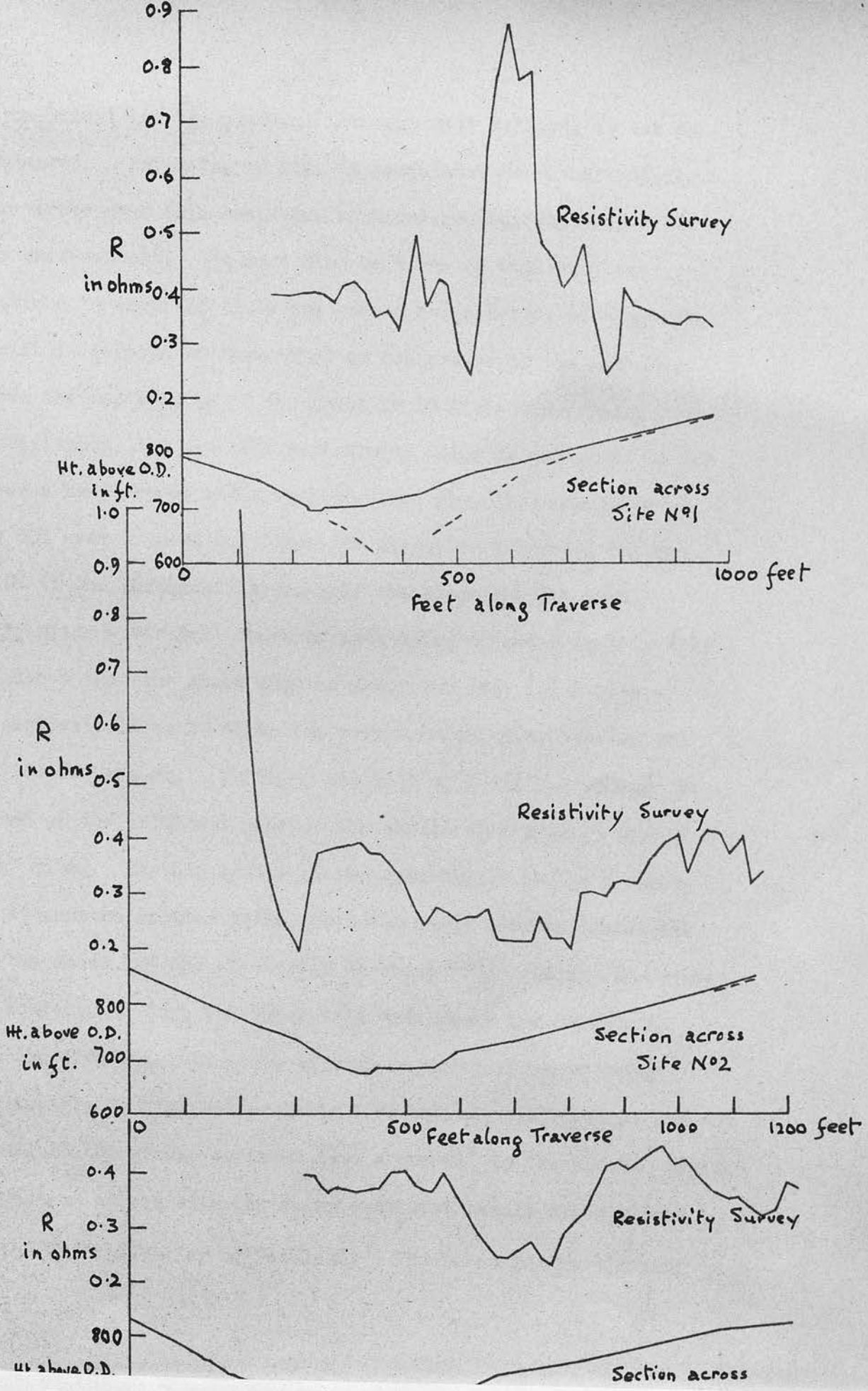
0·9
0·8
0·7
0·6
0·5
0·4
0·3
0·2
R
in ohms
Resistivity Survey
800
700
600
Ht. above O.D.
in ft.
Section across
Site No1
0
500
1000 feet
Feet along Traverse
1·0
0·9
0·8
0·7
0·6
0·5
0·4
0·3
0·2
R
in ohms
Resistivity Survey
800
700
600
Ht. above O.D.
in ft.
Section across
Site No2
0
500
Feet along Traverse
1000
1200 feet
0·4
0·3
0·2
R
in ohms
Resistivity Survey
800
Ht. above O.D.
Section across

symmetrical but the maximum, although well defined, is not so balanced. Referring to Fig. 25 calculated for longitudinal traverses over thin resistive vertical sheets, the comparison is self-evident. It must also be borne in mind that the maximum is about 2¼ times the normal resistivity, although the drift is perhaps 20 feet thick at the centre of the maximum. When the resistivity of the sheet is 19 times the country resistivity, the apparent resistivity value is increased by 10% over a sheet whose width is 0.01 times the electrode interval, by 60% over a sheet 0.1 times the electrode interval, but by 150% if the thickness is one-half the electrode interval. Suggesting a vertical sheet of insulating material in this case requires that the sheet must be about 100 feet thick with a resistivity 15 to 20 times the normal value, i.e. say 200,000 to 300,000 ohm-cm. Further, one half of a similar anomaly is found at the left-hand side of the resistivity profile over No.2 dam site. If this is due to the same highly inclined sheet, as it must be assumed to be, then the angle between the strike of the sheet and the electrodes is about 75°. It may therefore be conjectured that the sheet is a dyke about 100 feet thick running from slightly south of west to north of east. Its inclination is high and probably lies between the vertical and the normal to the ground surface, i.e. about 85° to the north. This suggestion agrees with the known east-west basalt dykes common in the Midland Valley of Scotland. The bores in the vicinity

were put down several months before, the rockhead was simply recorded as such, and there is no evidence now available as to the type of rock.

It follows that depths could not be estimated at the other dam sites due to this defection in No.1 site. However it is clear that Nos. 2 and 3 demonstrate that the resistivity of the drift is less than normal, and that the resistivity profile is valuable in defining the extent and form of the buried river channel. These show that the channel is wider at No.2 site than at No.3, but the latter profile shows steeper sides and perhaps deeper drift cover.

Although the surveys were not too successful in the definition of the channel base, they proved their value in the discovery of the dyke. No.3 site is assumed to be the most suitable one for the site of the future dam, since it is clear of the dyke and the buried channel is narrower there.

Traverses at Gilmerton.

Gilmerton Colliery is about four miles south of Edinburgh, and is sunk on the western outcrop of the Limestone Coal Group of the Carboniferous Limestone Series of Midlothian. The Midlothian coalfield is in the form of a syncline with a slight pitch to the north. The coals on the west side are very steep, varying from 60 to 80°, so that they are known locally as the "Edge Coals". The area concerned here is that to the

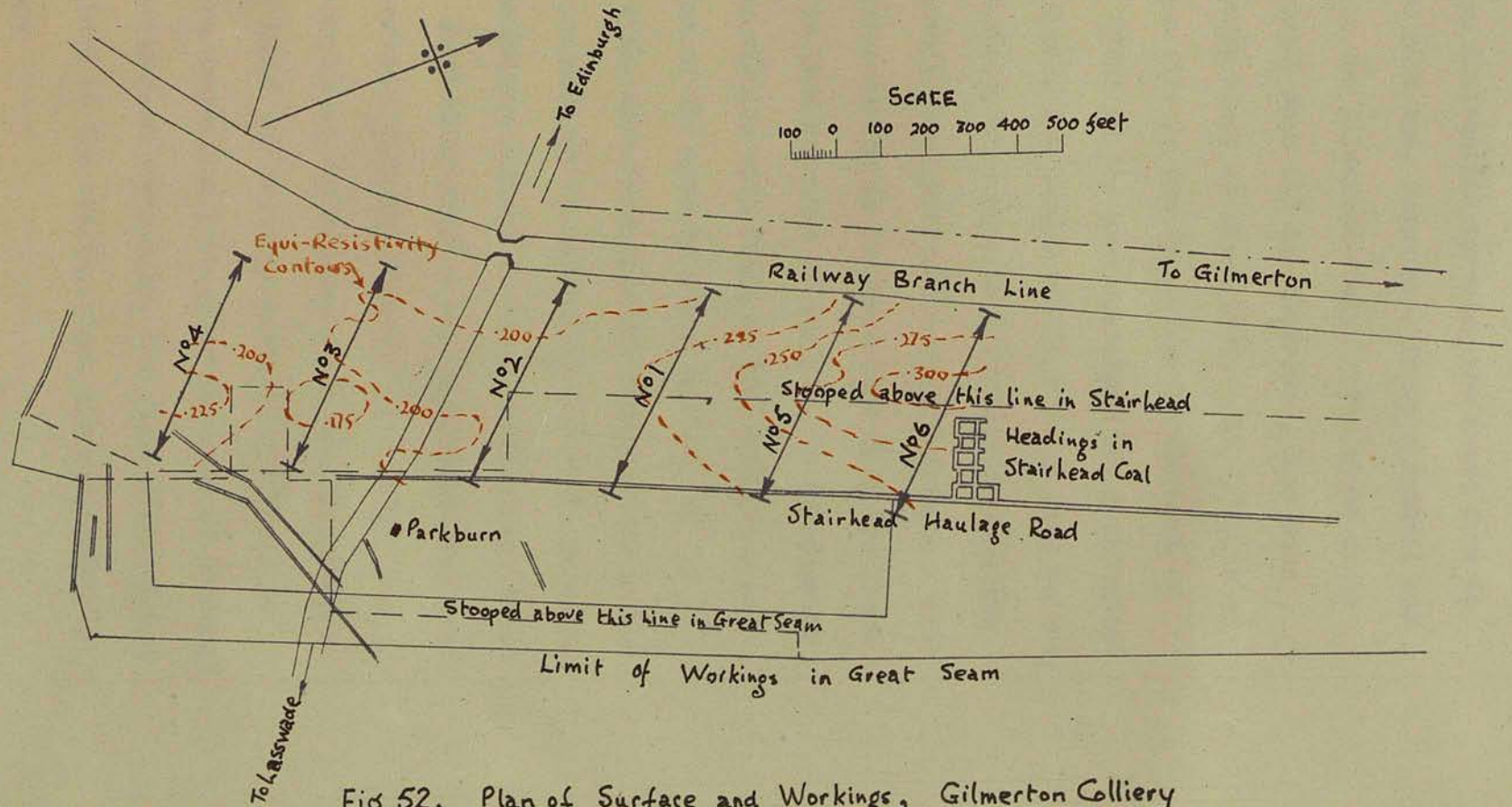

Fig. 52, Plan of Surface and Workings, Gilmerton Colliery

west of the shafts between these and the Sheriffhall fault. The latter is a large dislocation throwing the seams down to the north some 1,000 feet and, therefore, forms a natural and effective boundary to the Gilmerton field. The upper coals in the series, the Great Seam and the Stairhead, have been worked near the outcrop since at least 1780. An old plan of that date refers to a fire in the Great Seam to the west of Parkburn Cottages. Coal in the area concerned has been worked down to 1,000 feet depth, the deeper workings being very recent. Since the coals are steep, they have been worked by stoop and room methods with almost total extraction of the stoops. With so many seams in juxtaposition it has been easy to drive short cross-measures drifts from one seam to another, in consequence of which the area is riddled with roads in the coal seams and across them. A plan of the area is given in Fig. 52.

In February 1951, when headings were being driven in the Stairhead workings preparatory to developing the coals on either side into stoops, smoke was noticed in these headings and these had to be sealed. No further trouble was experienced for some months, and it was assumed that the fire had died out. In October, however, more smoke was discovered in the Blackchapel level some distance inbye the previous heating. Efforts to locate this fire were unavailing because of the maze of headings and mines and old wastes and eventually, the whole district had to be sealed right back at the shafts, since air was obviously reaching the heating.

With few facts available, it was difficult to find the seat of the fire, and at this stage it was suggested that a resistivity survey might conceivably provide some light on this subject. The survey was undertaken with little hope, but, at that time, any information at all might have been valuable. No signs of the fire might indicate that the fire was burning in the newer and deeper workings. The survey was undertaken during the week-end in order that four men and two surveyors could be spared without interfering with their normal work.

It was decided that the electrode interval should be as large as possible. With the wires available this allowed 900 feet between the outer current electrodes. The inner potential electrodes were kept at 280 feet to allow as many readings being taken as possible without moving the generator and the potentiometer units. The area concerned was crossed by a secondary roadway running in a north-westerly direction towards Edinburgh, while the northern boundary was a made-up railway embankment with a road behind it. Crossing these latter obstacles with a longitudinal traverse would have been difficult, and stopping in front of them would have meant surveying a much smaller area, since the centre of traverse would be 450 feet from either current electrode. To suit the surface features, it was, therefore, decided that the traverse should be a transverse one, but a transverse traverse with the line of electrodes at an angle of 70° to the direction of advance. This permitted maximum advance to the railway fence, and by judicious positioning of

the traverse lines never more than one wire would be lying on the roadway. It was deemed impracticable to lift the wires for passing traffic, since this would have slowed down the traverse, and probably required extra labour. At the end of two days work one wire was found to be broken but this caused only a short delay.

In all six traverses of 500 feet length with readings taken every 20 feet were made in two days. Three of the lines were ideal from the point of view of speed and convenience; they were level and free from obstructions. The other lines were more time-consuming, since they entailed moving wires along a roadway with intermittent traffic, and negotiating a burn, hedges and a steep embankment. The transverse method of traverse is also wasteful in time; it is easier and quicker to move the electrodes along their own line as in longitudinal traverses, because control is easier and less setting out is required.

The six curves obtained from these traverses are shown together in Fig. 53, the farthest south being drawn at the top of the diagram. Of these, the curves for lines 1 and 2 show little variation, and, therefore, there are no anomalous effects in their vicinity. Lines 3 and 4 are complementary. The decrease in resistivity below the normal represented by 0.2 ohm (7,660 ohm-cm.) in line 3 is almost mirrored by a similar increase above normal in line 4. The two lines are 300 feet

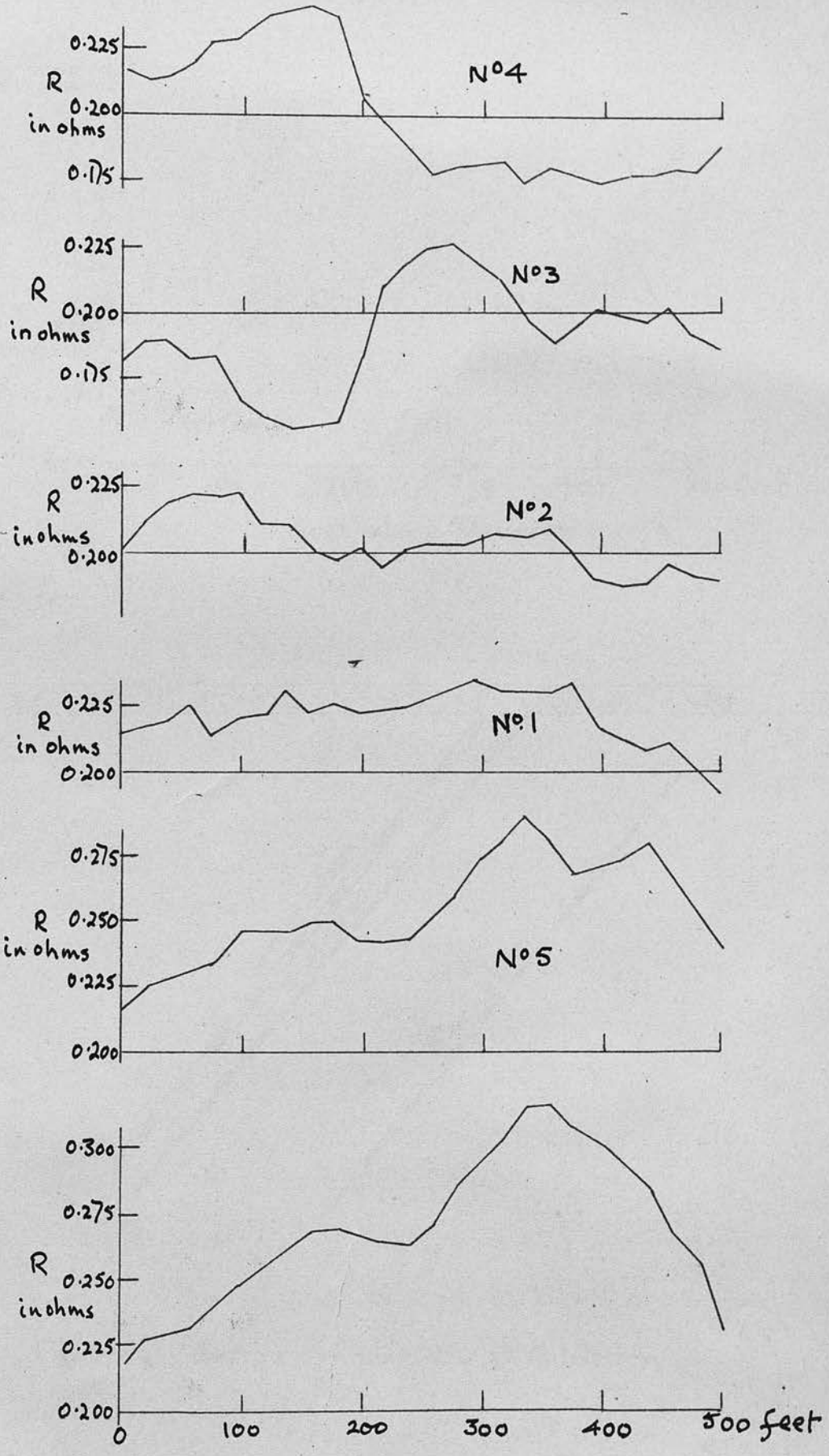

Fig. 53, Transverse Traverses at Gilmerton

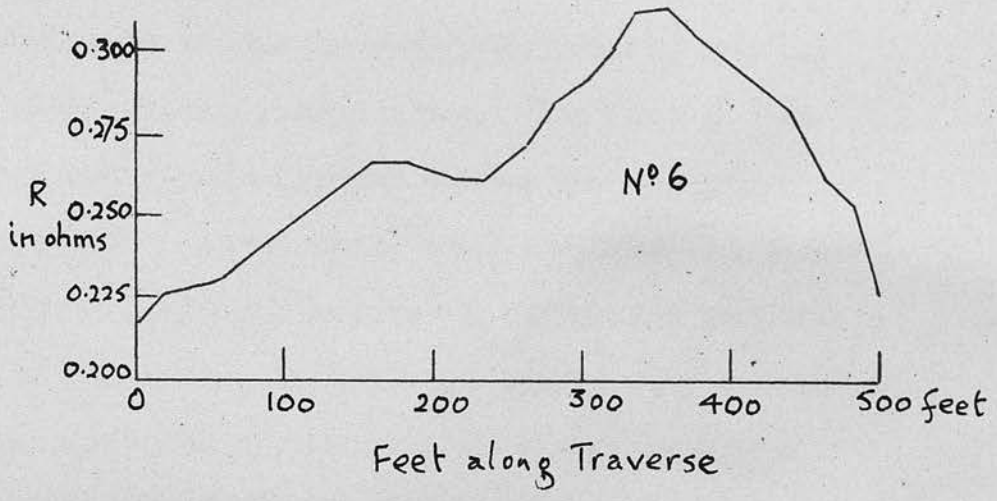

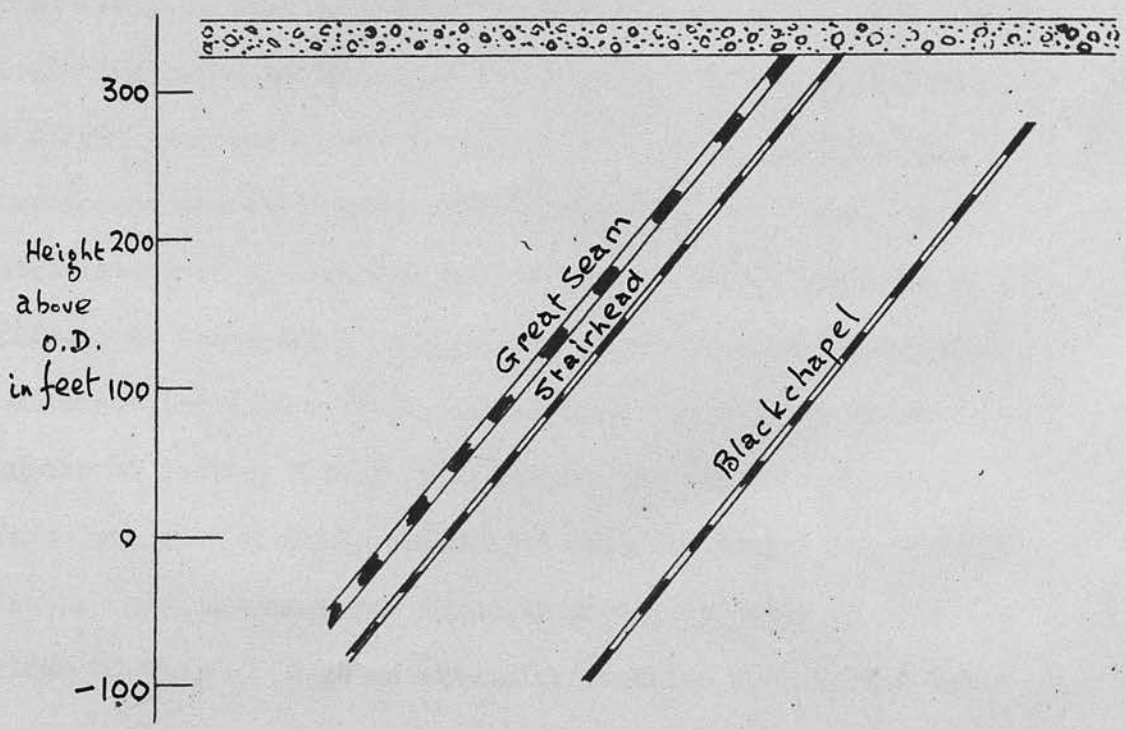

Fig. 54, Section on Line Nº6 at Gilmerton

apart and therefore line 4 would lie between the southerly current and potential electrodes of line 3. Line 3 would be situated between the similar northerly electrodes of line 4. There are, therefore, two possibilities. The first is that an insulating body of material lies between the potential electrodes of line 4, such material would give rise to a larger drop of potential than usual between the current and potential electrodes of line 3, and, it follows, a smaller drop between the potential electrodes of line 3. The effect would be a decrease in apparent resistivity as exhibited by the curve for line 3. Secondly, a conducting body near line 3 would react conversely in line 4. However, any such conductor near line 3 would influence ~~in~~ the curve for line 2. There is, actually, a slight increase at the beginning of line 2. Thus both hypotheses are explicable from the curves. Of these, the postulation of a conductor has no bearing on the location of a fire. An insulator at the beginning of line 4 is suspicious, but other facts have to be considered. As will be seen a number of faults, albeit small, cross the region indicated. These are most probably associated with the larger Sheriffhall fault, which although not actually proven is known to lie close to these. Such an extensive troubled area in the fault zone is almost certain to have a significant difference in resistivity to the normal undisturbed strata.

Lines 5 and 6 show much greater deviations from normality, both having peaks at 330 feet along the traverse, the peak

of line 6 being the highest. There is a slight increase in line 1. This, and the absence of any decrease in apparent resistivity could perhaps be explained by an insulating region gradually dying out towards them. Equi-resistivity contours are drawn on the plan. These, of course, cannot be regarded as precise as the lines are 300 feet apart, with readings along them at intervals of 20 feet. They do indicate the presence of a strongly non-conducting zone between lines 5 and 6 or to the north-east of 6. In addition it should be observed that the gradient of each of those two curves is steeper to the north-west and relatively small to the south-east. This is exactly what would be expected if the insulating body dipped to the south-east, and agrees reasonably well with the laboratory curves obtained over a dipping insulator. Approaching from the south-east the effect would be noticed some distance away, but past the maximum the resistivity would fall more rapidly. This corresponds to the vertical force magnetic curve obtained by traversing over a dipping magnet. Another factor is that line 6 is almost exactly over the headings in the Stairhead Seam where smoke was first observed. Fig. 54 compares the resistivity curve of line 6 with a section of the strata on the same line.

On this evidence it was suggested to the local colliery officials that, if the fire was near the surface, then the most likely site was in the waste above these headings. Since the

heating was so persistent, a shallow depth is likely as air could be drawn from the surface through the old wastes disturbed by the approaching workings. Since the stoppings were at least quarter of a mile from these headings, the hazards of reopening the seals and exploring the old wastes and the expense of the work, compelled the decision to leave the area sealed. The survey shows that the location of a shallow underground fire is not without the scope of earth-resistivity equipment. It is unfortunate that the suggested location could not be conclusively proved.

Traverses at Seton.

A series of magnetic surveys were made across an East-West quartz-dolerite dyke at Seton Mains in East Lothian. The dyke is well-known, and its position established by exposures, underground workings and previous magnetic surveys (27). The object of the survey was to give an accurate position to the National Coal Board at one point, where it was intended to drive mines to provide access to coal on the other side. The dyke comes very close to the surface, the maximum cover in the area being 20 feet but it is more usually about 10 feet with a thick dyke coming close to the surface, the depth of cover being much less than the thickness, the approximate rule, that the width of the dyke is equal to one-half of the width of the anomalous magnetic vertical force curve, may be used (28).

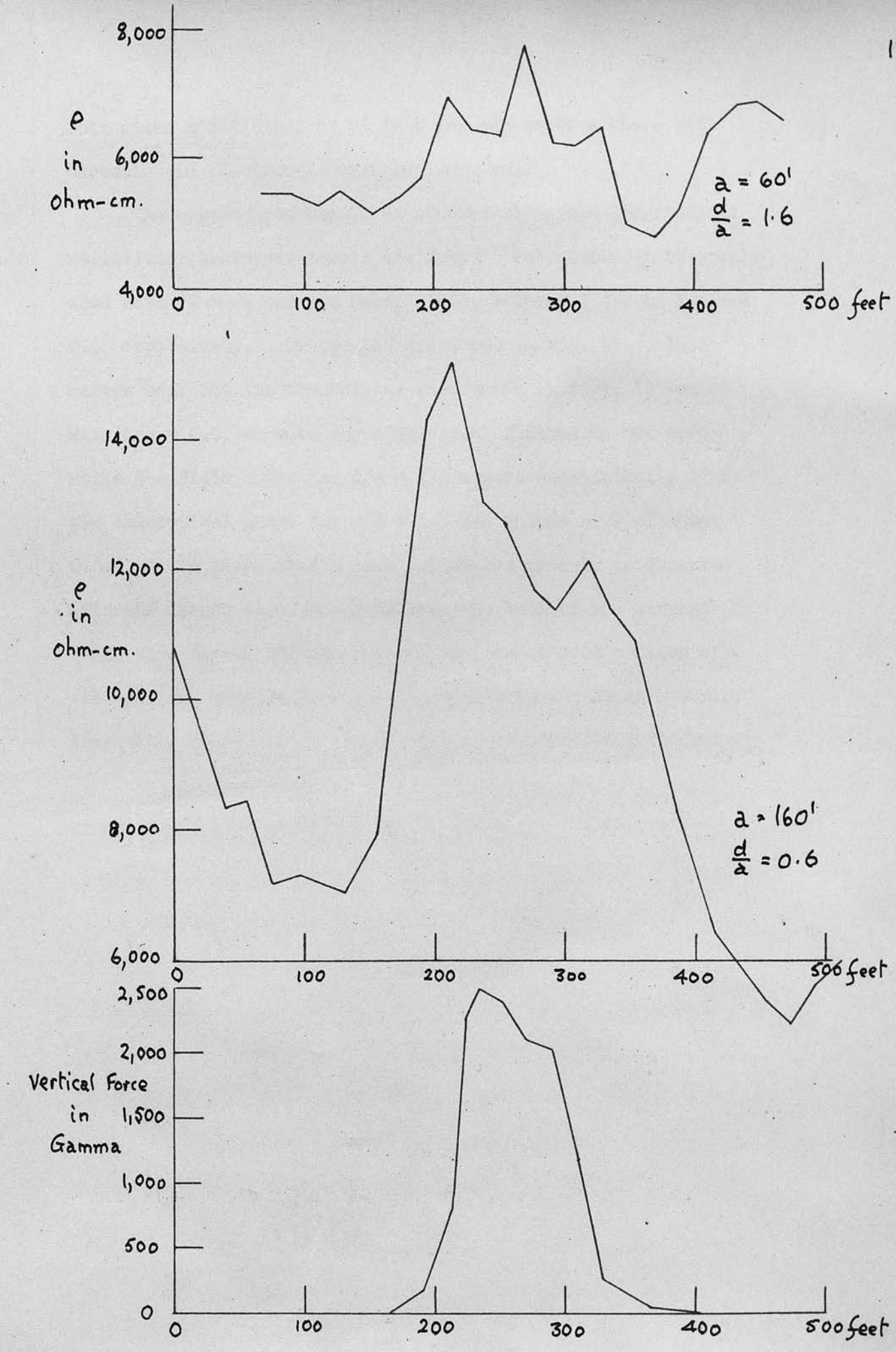

Fig. 55, Electrical and Magnetic Surveys over Seton Dyke

This gives a thickness of 95 feet for one section where both magnetic and electrical traverses were run.

An opportunity was taken of conducting two longitudinal resistivity traverses across the dyke. The electrode intervals used were 60 feet and 160 feet, giving values of d/a of 1.6 and 0.6 respectively. The graphs are shown in Fig. 55. These curves bear out the theoretical ones shown in Figs. 25 and 26. With d/a = 0.6, we have the single peak flanked by two troughs, while the field curve for d/a = 1.6 agrees substantially with the theoretical curve for d/a = 1.5 and values of k of about 0.6. It is clear that a more pronounced anomaly is observed with the larger electrode interval, the bulk of the current being then forced through more of the unweathered portion of the dyke and also below the surface alluvium. In an example like this, it should be stated that an earth-resistivity survey is not so easily carried out as a magnetic survey, it requires more labour and, further, does not yield as convenient results.

Traverses over the Acklington Dyke.

This example is taken from a paper by Granville Poole, Whetton and Taylor in which several traverses are described over fault and dyke structures in the North of England (6). The diagram illustrating the Acklington Dyke and resistivity traverses over it are reproduced in Fig. 56. The dyke is inclined at about 70°, and is 40 feet thick, while the

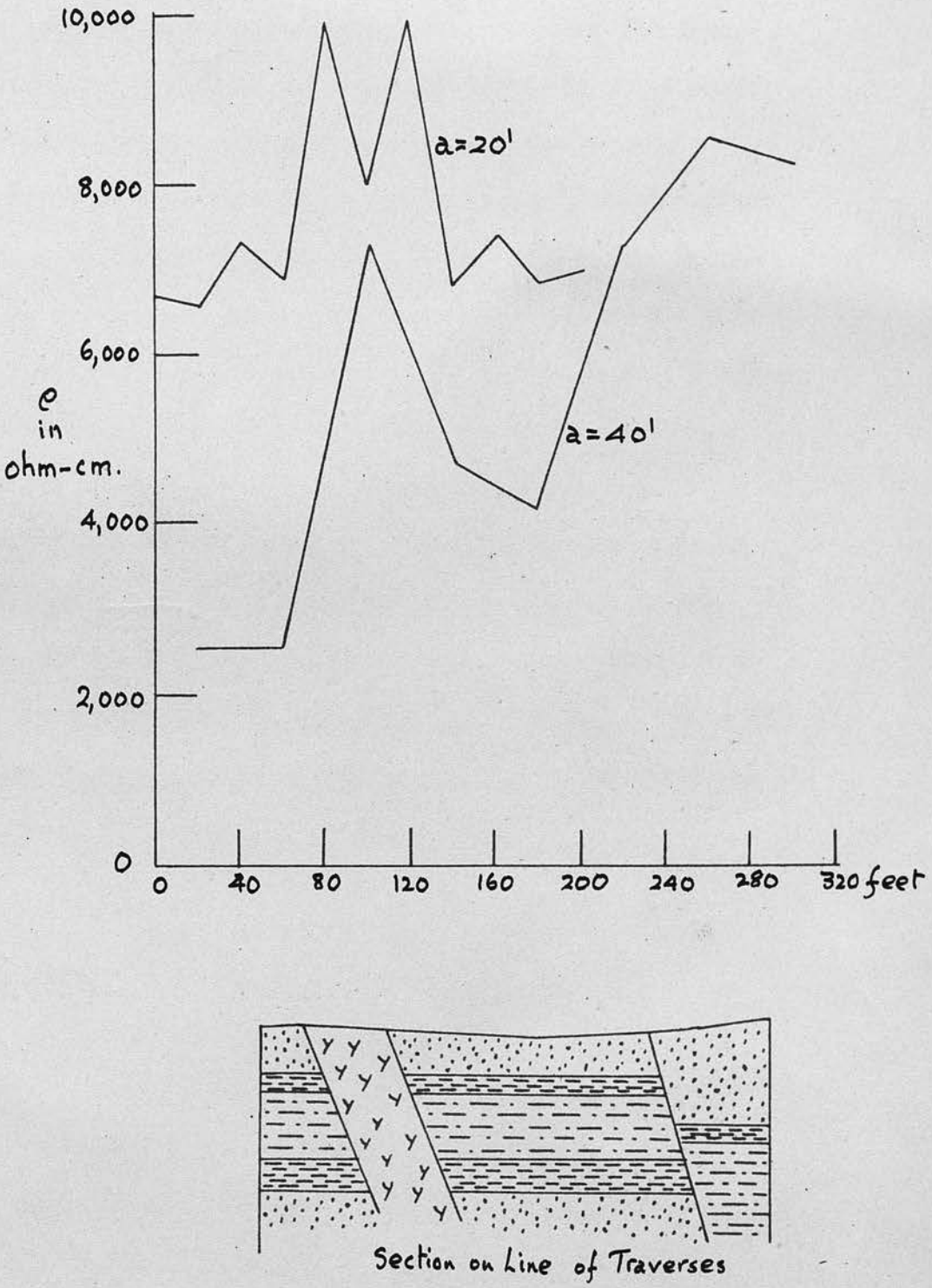

Fig. 56, Longitudinal Traverses over Acklington Dyke

surrounding strata is horizontal.

Two longitudinal step traverses were run over the dyke, one at 20 feet intervals and the other 40 feet; in other words, d/a is 2.0 for the first traverse and 1.0 for the second. Comparing these to Figs. 25 and 26 showing theoretical traverses over vertical insulators with similar values of d/a, the double peak for d/a = 2.0 is at once evident, and also the single peak for d/a = 1.0. In the paper itself, it is stated that "the edges of the intrusion are more resistant than the middle portion, this being due to differential weathering subsequent to segregation of the dyke material." Such a conclusion appears to be justified on the field curve for d/a = 2.0, but as has been shown, the curve is almost exactly the same as that for a highly-inclined dyke which is homogeneous throughout. There is thus no need to suggest differences in the dyke resistivity, as the curves bear out the theory presented here.

CHAPTER VII.

THEORY OF INTERPRETATION OF DEPTH MEASUREMENTS

THEORY OF INTERPRETATION OF DEPTH MEASUREMENTS

By far the greatest advantage derived from the resistivity method has been in its application to the measurement of depth of underlying strata, particularly the depth of alluvium down to the rockhead, information which is invaluable in shallow mining and in the determination of suitable dam sites. Other uses include the determination of the depth to the water table together with a probable indication of the likelihood of obtaining water from boreholes. Generally speaking the method is suited only to shallow exploration, and, indeed, the Megger Earth Tester is restricted to low depths.

Two-Layer Problems

If the electrodes are expanded about a central point, the electrodes being kept equidistant, then it is evident that deeper parts of the ground will increasingly affect the apparent resistivity. Were the ground homogeneous and isotropic, the resistivity would be unaltered with increasing penetration. It is common in glaciated countries to have the solid rockhead overlain by alluvium, a case which may often be regarded as composed of two distinct layers separated by an interface parallel to the surface, as in Fig. 57.

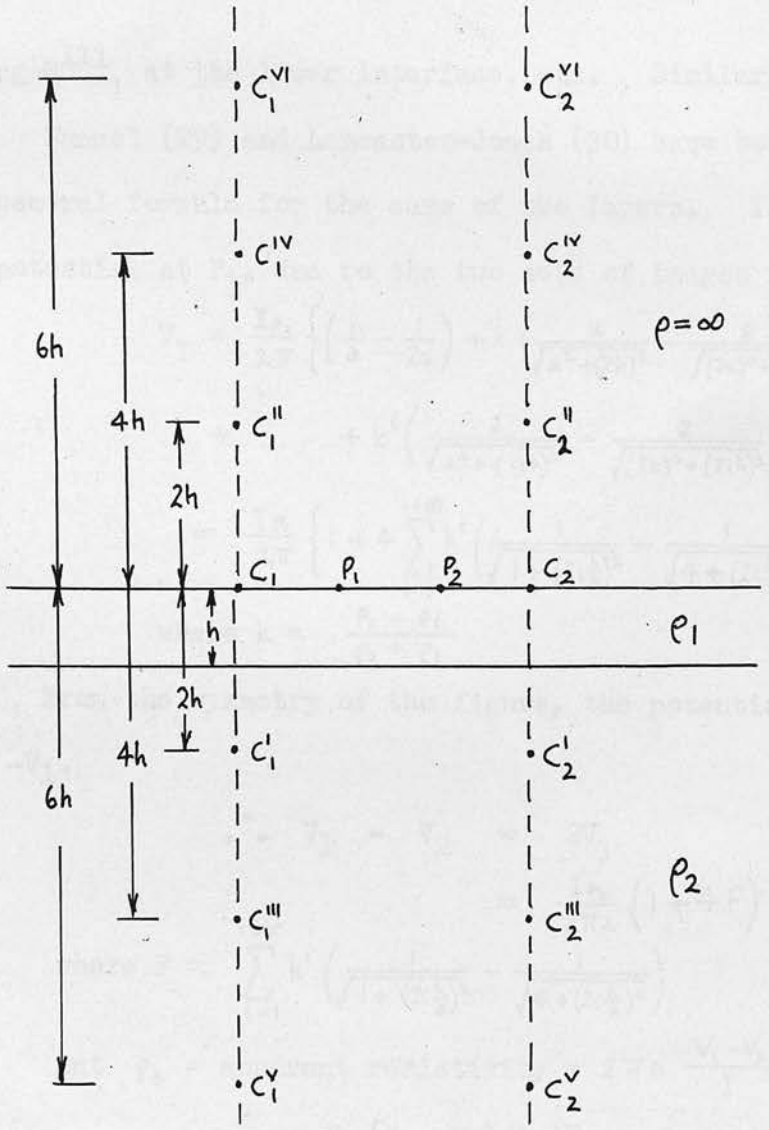

Fig. 57 Images in Two-Layer Problem

The problem is more correctly one of three layers, the third layer being air of infinite resistivity. Let the resistivity of the top layer of thickness, h, be ρ_1, and the resistivity of the bottom layer ρ_2. The current source C_1 forms an image C^1_1 at a distance h from the interface or 2h from the surface of the earth. C^1_1 forms an image C^{11}_1 in turn

giving C^{111}_1 at the lower interface, etc. Similarly with C_2.

Hummel (29) and Lancaster-Jones (30) have both deduced the general formula for the case of two layers. They show that the potential at P_1, due to the two sets of images is:-

$$V_1 = \frac{I\rho_1}{2\pi}\left\{\left(\frac{1}{a}-\frac{1}{2a}\right)+k\left(\frac{2}{\sqrt{a^2+(2h)^2}}-\frac{2}{\sqrt{(2a)^2+(2h)^2}}\right)\right.$$

$$\left.+\ldots\ldots+k^i\left(\frac{2}{\sqrt{a^2+(2ih)^2}}-\frac{2}{\sqrt{(2a)^2+(2ih)^2}}\right)\right\}$$

$$= \frac{I\rho_1}{2\pi}\left\{1+4\sum_{i=1}^{i=\infty}k^i\left(\frac{1}{\sqrt{1+(2i\frac{h}{a})^2}}-\frac{1}{\sqrt{4+(2i\frac{h}{a})^2}}\right)\right\}$$

where $k = \dfrac{\rho_2-\rho_1}{\rho_2+\rho_1}$

From the symmetry of the figure, the potential at P_2 is $V_2 = -V_1$.

$$\therefore\ V_1 - V_2 = 2V_1$$

$$= \frac{I\rho_1}{2\pi a}(1+4F)$$

where $F = \sum_{i=1}^{i=\infty}k^i\left(\frac{1}{\sqrt{1+(2i\frac{h}{a})^2}}-\frac{1}{\sqrt{4+(2i\frac{h}{a})^2}}\right)$

But ρ_a = apparent resistivity $= 2\pi a\,\dfrac{V_1-V_2}{I}$

$$\therefore\ \rho_a/\rho_1 = 1 + 4F, \qquad 63$$

the term F depending on the ratio of the resistivities of the two layers and on the ratio of depth of the first layer to the electrode separation.

The first criterion used to forecast the depth of the first stratum was that put forward by Gish and Rooney (10). This was that, if resistivity was plotted against electrode separation, and the curve exhibited an abrupt change in resistivity, then the corresponding electrode separation was equal to the depth to the interface. A study of two-layer curves shows that no such sudden change occurs in the slope of the curve. Samples of such

curves together with three-layer examples are to be found in the Water Supply Manual issued by the War Office (31). A method of interpretation has been based on such theoretical curves, the field curve being compared with the theoretical ones, and the best fit accepted. This can be satisfactory if the field curves approximate to the two-layer form, and there are no lateral anomalies present, but the method is somewhat crude. Three-layer theoretical curves are valuable in indicating the types of curves to be obtained under given conditions, but so many would be required for adequate comparison that they are of little further use in field interpretation.

Tagg (32) evolved an interesting and valuable graphical method of interpretation of the two-layer equation:-

$$\rho_a/\rho_1 = 1 + 4\sum_{i=1}^{i=\infty} k^i\left(\frac{1}{\sqrt{1+(2i\frac{h}{a})^2}} - \frac{1}{\sqrt{4+(2i\frac{h}{a})^2}}\right) \qquad 63$$

A series of curves, Fig. 58, can be drawn showing the relationship between ρ_a/ρ_1 and h/a for various values of h. When k is positive it is more convenient to use the conductivity ratio σ_a/σ_1 instead of ρ_a/ρ_1, σ_a being the apparent conductivity as measured = $1/\rho_a$, and σ_1 the conductivity of the top stratum.

Resistivity measurements are made using the expanding Wenner configuration of electrodes, the electrodes being symmetrically disposed about the point where the depth of the first layer is required. The first few readings provide an average value of ρ_1, the resistivity of the top layer. Further

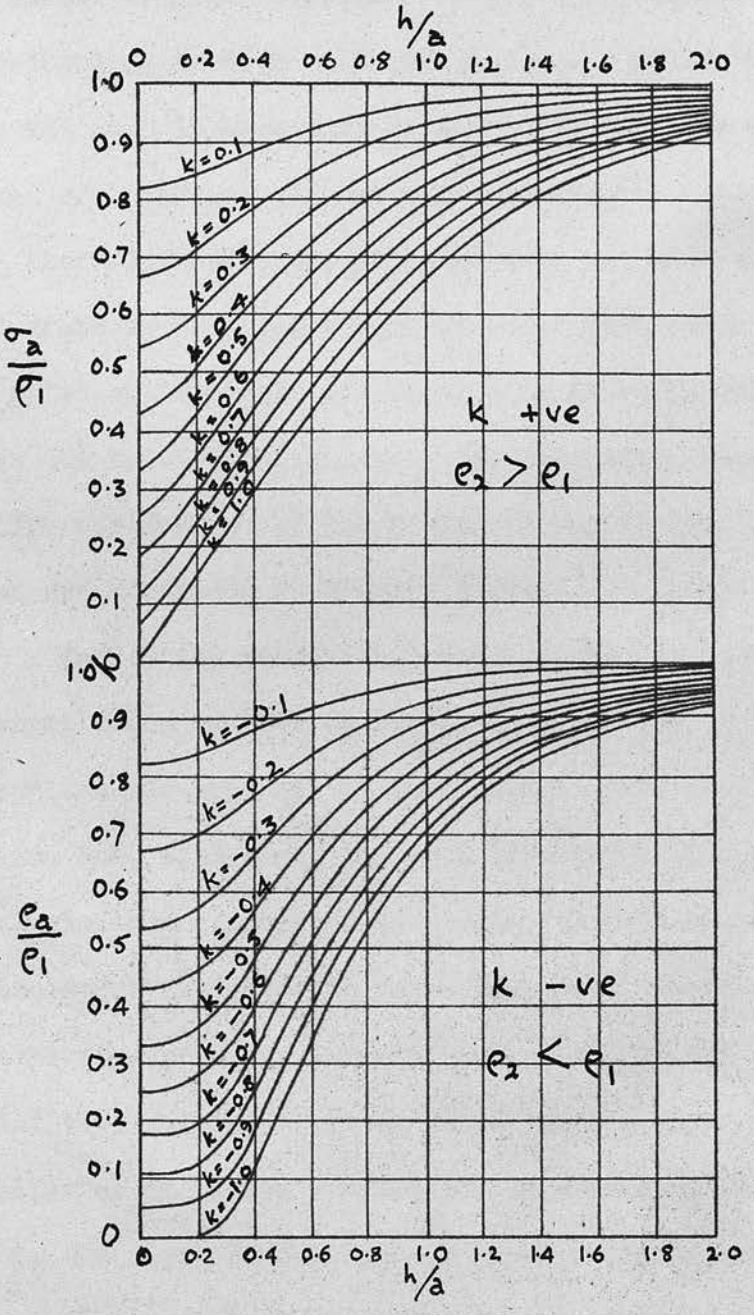

Fig. 58, Relationship between σ_a/σ_1 and e_a/e_1 for values of k

values of the apparent resistivity for, say, 150, 200, 250 feet and so on are read off. If these ratios are less than unity, the curves of Fig. 58 provide a series of values of h/a and k corresponding to each value of ρ_2/ρ_1. Since the electrode interval a is known, these are converted into a series of values of h and k. If the curve accurately follows equation 63 there will be a unique value of h and k to satisfy it, and so a graph is drawn of h against k for each value of a. The point or centre of the small area in which they intersect gives the values of h and k. This has often been found useful, and the application of the method to certain field curves are shown and discussed in Chapter VIII.

One of the most recent suggestions for resistivity interpretation is that by Moore, (33) and (34). In his paper he applies his analysis to many curves previously published, dealing both with field and with laboratory examples. The usual electrode spacing-resistivity curve is drawn, and the data on the curve is replotted as a cumulative electrode spacing-resistivity curve by successive summation of the individual resistivity values. The slope of this cumulative curve appears to alter as it passes a value of the electrode spacing corresponding to the depth of the surface layer. Lines are drawn through those points on the curve approximately in a straight line, and the electrode interval corresponding to the intersection of these lines gives the depth of the first layer. He shows examples where more than one layer can be differentiated. The

method is novel, and he makes no claim for any theoretical basis. Indeed, Muskat (35) has considered it from the theoretical point of view, and has shown it to be without physical foundation. There is little doubt, though, that his paper is convincing and it is worthwhile applying his ideas to field curves. Again, this is done in Chapter VIII.

If the resistivity of the lower layer is very much higher than that of the top one, it can be shown that when the apparent resistivity is 50% greater than the resistivity of the first layer, the depth, h, of the high resistance layer will be approximately equal to the electrode separation, a (36). This is often helpful in providing a good first approximation.

Theoretical values of functions useful in earth-resistivity methods have been calculated by Roman (23). Roman's tables are a function of $W = \sum_{i=1}^{i=\infty} k^i \left(\frac{1}{i} - \frac{1}{\sqrt{i^2+\alpha^2}}\right)$ for the arguments k and α, k varying from -1 to +1 ($\rho_2/\rho_1 = 0$ to ∞) at intervals of 0.1 and α from 0 to 5 at intervals of 0.01. W can be referred to the two-layer formula as follows:-

$$W = \sum_{i=1}^{\infty} \frac{k^i}{i} - \sum_{i=1}^{\infty} \frac{k^i}{\sqrt{i^2+\alpha^2}}$$

$$= -\log(1-k) - \frac{1}{\alpha} \sum_{i=1}^{\infty} \frac{k^i}{\sqrt{1+(\frac{i}{\alpha})^2}}$$

$$\therefore \quad \sum_{i=1}^{\infty} \frac{k^i}{\sqrt{1+(\frac{i}{\alpha})^2}} = -\alpha \log_e (1-k) - \alpha W$$

$$= \alpha \log_e \frac{1}{1-k} - \alpha W$$

Now, the two-layer equation is

$$\rho_a/\rho_1 = 1 + 4 \sum_{i=1}^{\infty} \left[\frac{k^i}{\sqrt{1+(2i\frac{h}{a})^2}} - \frac{k^i}{\sqrt{4+(2i\frac{h}{a})^2}} \right]$$

$$= 1 + 4 \sum_{i=1}^{\infty} \left[\frac{k^i}{\sqrt{1+(\frac{1}{\frac{1}{2}\frac{a}{h}})^2}} - \frac{\frac{1}{2}k^i}{\sqrt{1+(\frac{1}{\frac{a}{h}})^2}} \right]$$

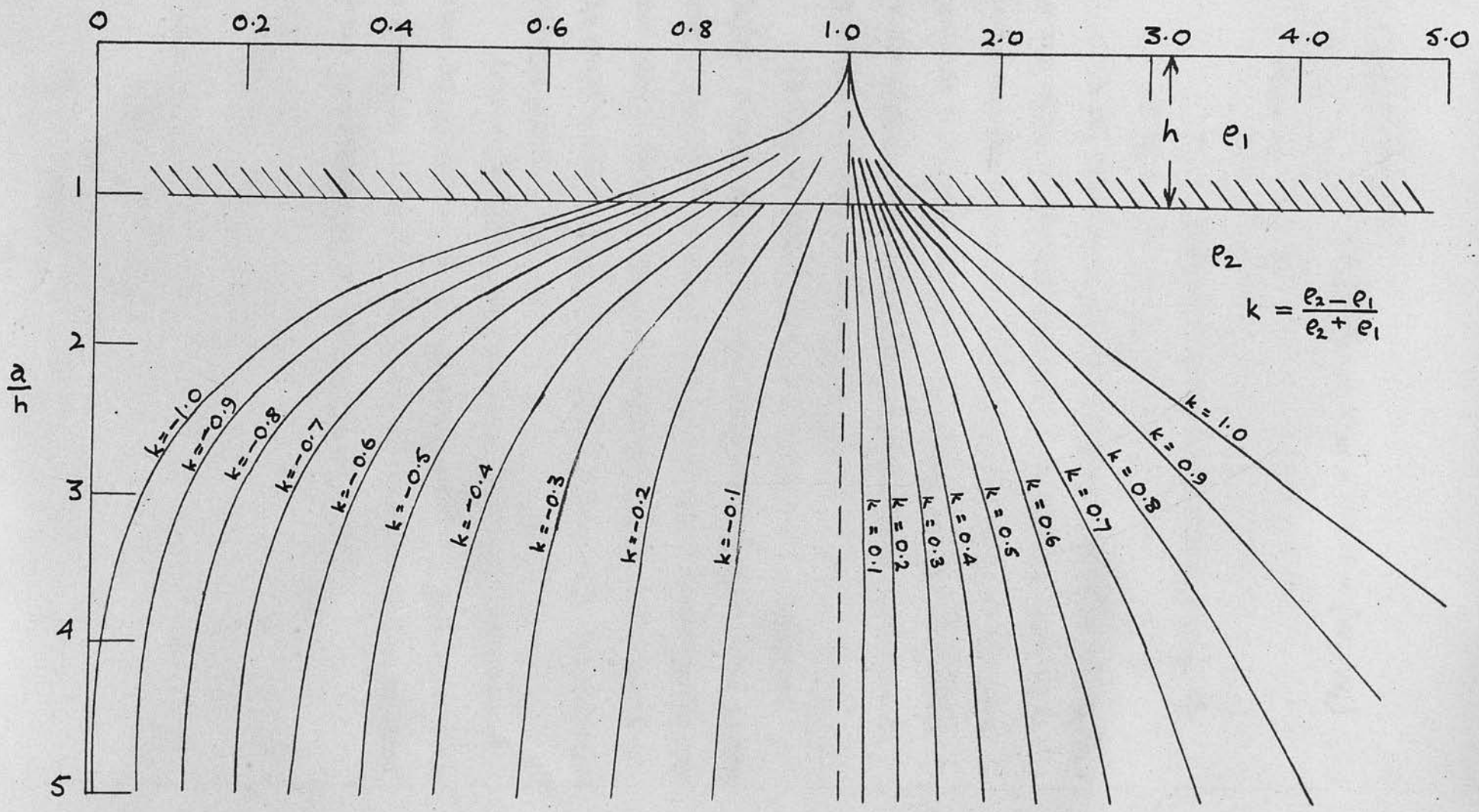

Fig. 59, Two-Layer Resistivity Curves

$$= 1 + 4\left[\alpha W_1 - \alpha W_2\right] = 1 + 4\alpha (W_1 - W_2)$$

where $\alpha = \frac{1}{2} \cdot \frac{a}{h}$.

W_1 = Value of W from Roman's Tables for $\frac{1}{2} \cdot \frac{a}{h}$

and W_2 = " " " " " " " $\frac{a}{h}$

It is, therefore, easy to calculate the value of ρ_a/ρ_1, for any value of a/h corresponding to an assumed value of k. The resistivity curves for values of k from 1 to -1 (perfect insulator to perfect conductor) are shown in Fig. 59. They are perfectly smooth curves, and no inflections correspond to any single function of a/h.

It will be seen from the curve for k = 1, that when ρ_a/ρ_1 = 1.5, a/h = 1, or electrode separation is equal to the depth of the first stratum. If we make this assumption for any curve with a positive slope, the errors will be less than 5% if k is greater than 0.9, but for smaller values of k, the method is of little worth.

Another method is that by Roman (37) using superimposed master curves plotted on a logarithmic scale for both resistivity and electrode interval. His paper includes the tables required for the compilation of the master graphs.

CHAPTER VIII.

DEPTH MEASUREMENTS IN THE FIELD

DEPTH MEASUREMENTS IN THE FIELD

Depth Measurements at Oxenfoord.

Seven expanding electrode probes were surveyed at Oxenfoord, 3 miles South-East of Dalkeith, Midlothian, where the land undulates slightly, and the surface boulder clay overlies the rockhead to a depth of 40 to 140 feet. The area is agricultural land with more woodland than usual, the trees and undergrowth often making the survey very difficult, and their positions often dictating the points where probes had to be made. One of these probes was located at the site of a borehole while a second was 100 feet from another. The seven profiles are shown in Fig. 60, in which it is obvious that they are each of the same form i.e. a high resistivity decreasing to a minimum and finally increasing more or less uniformly. Readings were taken at electrode spacings from 5 to 300 feet at intervals of 5 or 10 feet. The results show slight variations either side of the smooth curve drawn but at spacings beyond 100 feet these were never more than 10% and usually much less than 5%. It was impossible, as it should be from theory, to attempt to correlate any changes in the curve to coals or sandstones lying beneath the rockhead. The curves are those of three layers, and, indeed, are similar to that treated by Tagg (32) as two-layer. The negative slope for small electrode separations indicates a thin highly resistive surface layer as might be expected from the well aerated surface soil. Considering these curves as being two-layer, the resistivity of the top layer cannot be greater

than the minimum shown and is most probably less. First of all, Tagg's method is used, the minimum resistivity being taken as the resistivity of the first layer.

In five out of the seven cases dealt with, Tagg's method gave satisfactory intersections. No.4 was centred on the site of a borehole put down to prove coal seams in the area, and gave a depth of 90 feet, but no satisfactory result by the Tagg method; No.5 was also unsatisfactory. However it will be seen that the slope of curves 4, 5, 6 and 7 are very close to one another. Curves 6 and 7 gave depths of 82 and 86 feet respect-:ively, so that it is not unreasonable to suggest similar depths for Nos. 4 and 5. The depth for No.4 would then be quite near to that given by the borehole. No.7 resistivity depth probe was about 100 feet from another borehole showing a depth of 55 feet to the rockhead. This does not compare well with the 86 feet of the resistivity survey, but the fluctuations in the bedrock known in the area are enough to take up at least part of the difference. From the resistivity traverses shown in Fig. 46, it will be seen that there are significant lateral anomalies in resistivity to account for the poor answers given to the curves 4 and 5 also, perhaps, the probable error in No.7.

The depths found are not altogether proved, but they are very unlikely to be greatly in error. Fig. 60 shows the five successful curves together with the theoretical curves calcul-ated from the data proved by the graphical method.

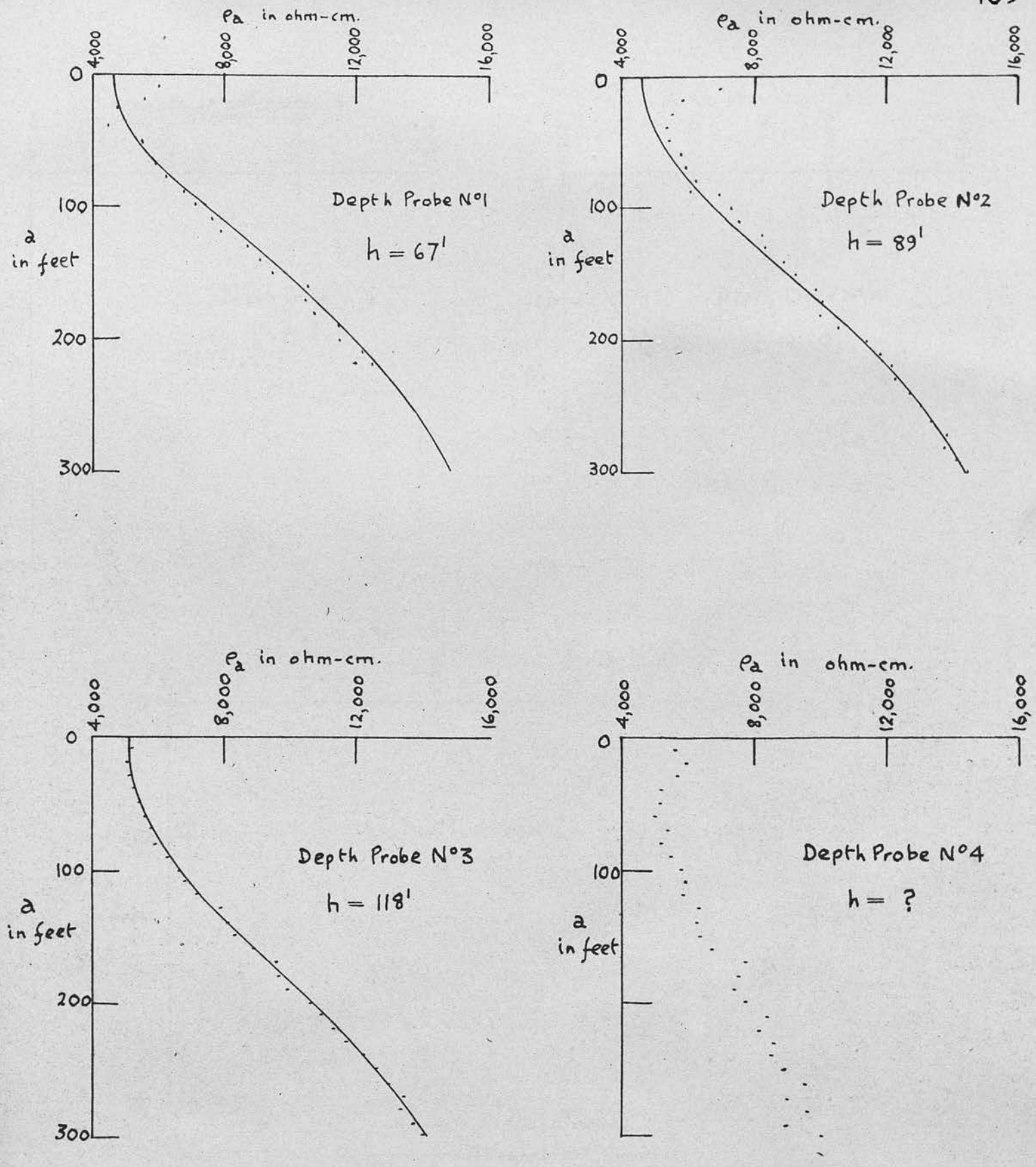

Fig. 60, Depth Probes at Oxenfoord

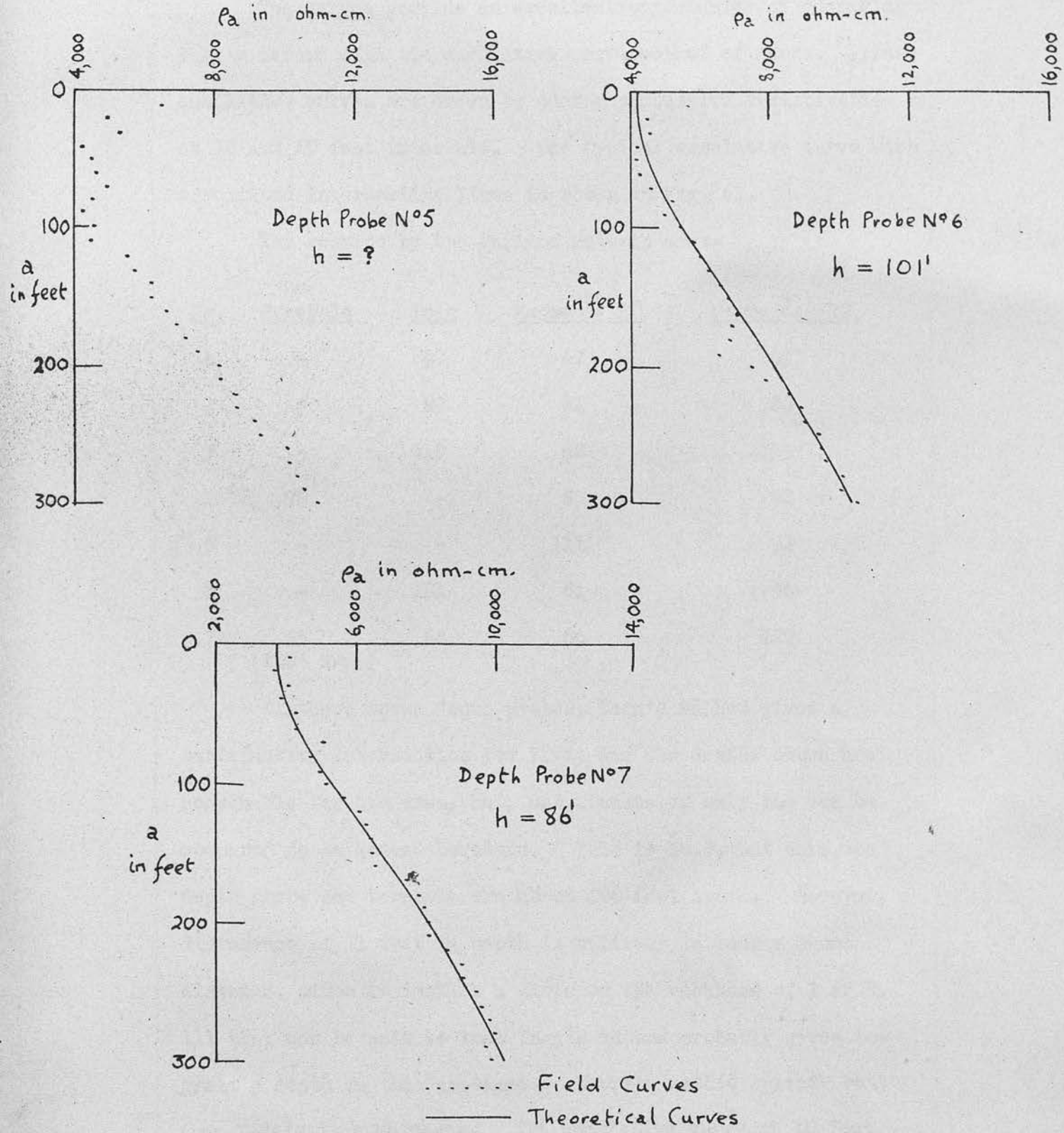

Fig. 60, Depth Probes at Oxenfoord

The curves provide an excellent opportunity of comparing Tagg's method with the cumulative curve method of Moore. These cumulative curves are drawn by adding successive resistivities at 10 and 20 feet intervals. One typical cumulative curve with associated intersecting lines is shown in Fig. 61.

The results by the various methods are:-

No.	By Borehole	Tagg	Moore Σ 10	Moore Σ 20
1	-	67	67	69
2	-	89	84	88
3	-	118	60	111
4	90	-	85	92
5	-	-	111	92
6	-	101	81	96
7	55 (100' away)	86	66	127

Of these seven depth probes, Tagg's method gives a satisfactory intersection for five, and the depths shown are reasonable for the area, but, unfortunately, only one can be compared to an actual borehole. This is No.7, but here the depth probe and borehole are about 100 feet apart. However, a difference of 31 feet in depth is unlikely in such a short distance, since it implies a slope on the rockhead of 1 in 3. All that can be said is that Tagg's method probably gives too great a depth in this instance. Moore's method appears better than Tagg's in some cases. The cumulative curve at 10 feet

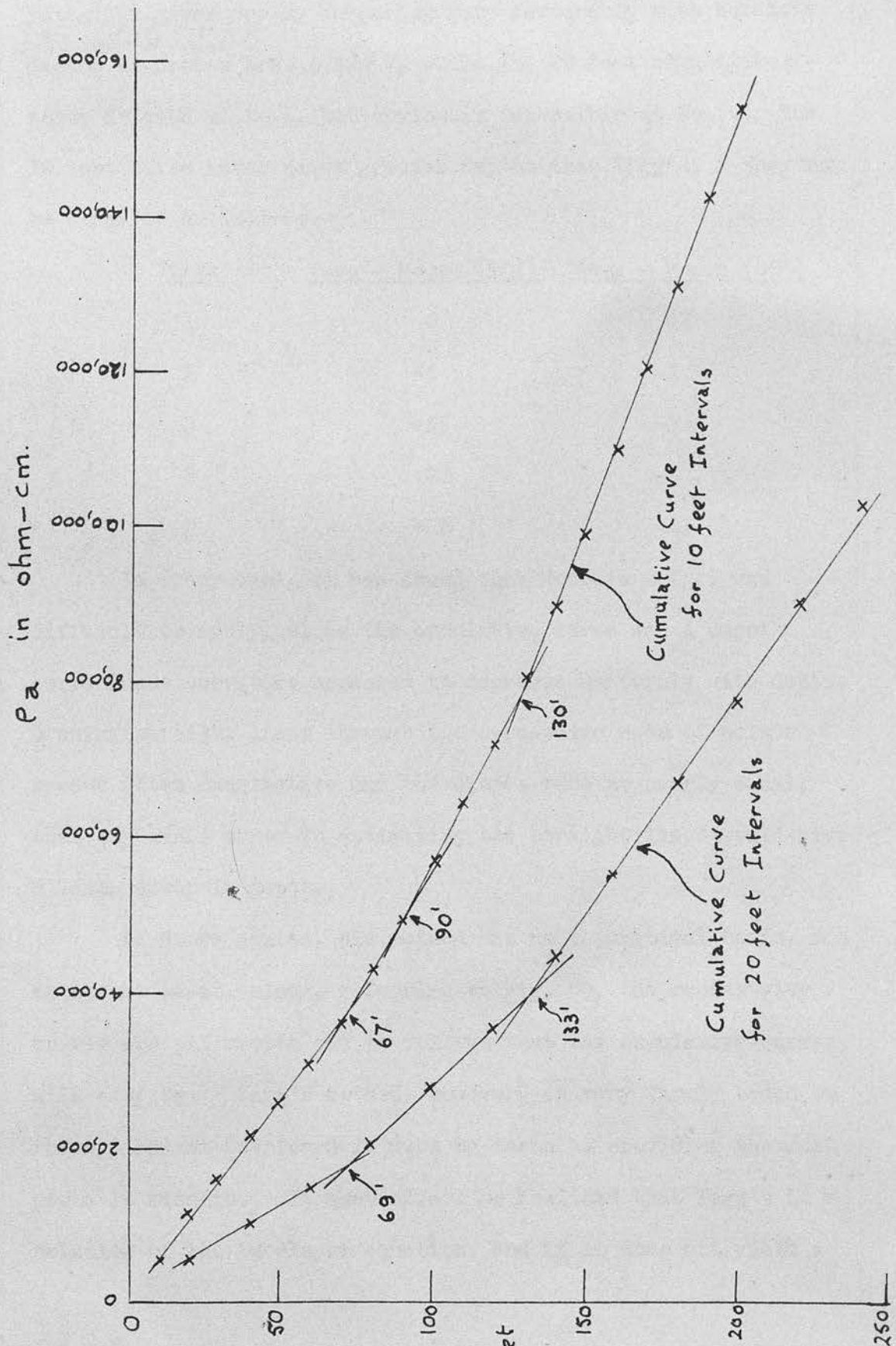

Fig. 61, Cumulative Curves for Depth Probe N°1 at Oxenfoord

intervals gives depths comparing very favourably with borehole depths at probes Nos. 4 and 7, while the 20 feet cumulative curve is good at No.4, but obviously impossible at No.7. The 10 feet curve never gives greater depths than Tagg's. They may be compared as follows:-

Probe	Tagg - Moore (10')	Tagg - Moore (20')
1	0	-2
2	+5	-1
3	+58	-7
8	+20	-5
9	+20	+41

In every case, it was found that Moore's method was difficult to apply, since the cumulative curve was a smooth curve whose curvature appeared to decrease uniformly with depth. Drawing straight lines through two successive sets of points seemed often imaginative and the slopes were so nearly equal, that any small error in estimating the straight lines would give a large error in depth.

As Moore admits, his method has no theoretical basis, and this must be so, since, referring to Fig. 59, the resistivity curves are all smooth and it follows that the cumulative curves will also be. Tagg's method, however, is very firmly based on theory, and at Oxenfoord it must be taken as providing the most probable results. It must always be realised that Tagg's is a solution of the two-layer equation, and if it does not yield a

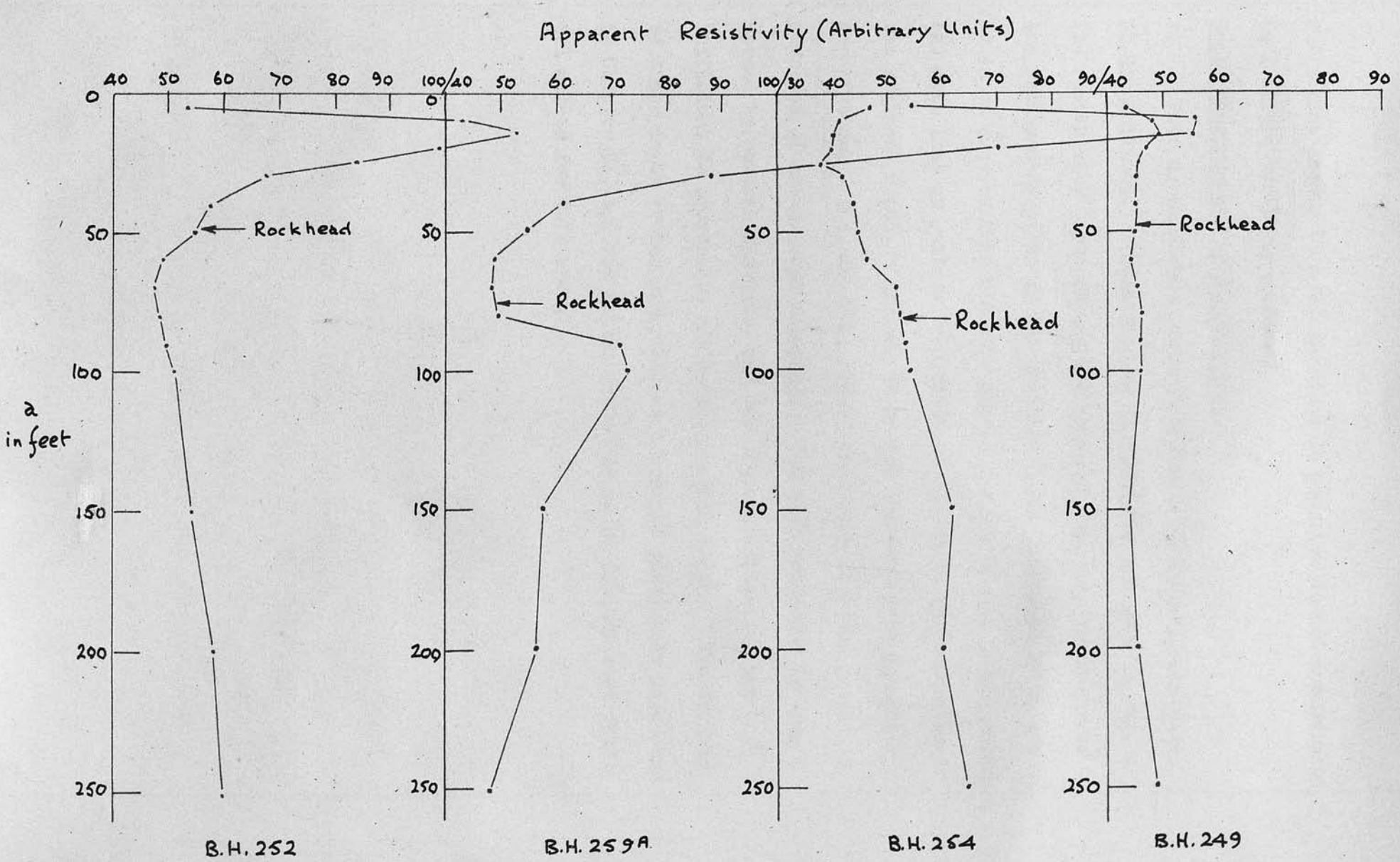

Fig. 62, Depth Probes at Rig Colliery

sufficient answer then the readings in question do not approximate to a simple two-layer problem.

Depth Measurements at Rig Colliery.

Four depth probes, centred on known boreholes, were made at Rig Colliery. These are Nos 252, 259A, 254 and 249 in Fig. 47, The resistivity depth curves are drawn in Fig. 62, the depth to the rockhead as given by the drillers being indicated by an arrow. It is at once evident that the curves are not simple layer problems, and also that no maximum or minimum on the curve is comparable to the rockhead depth. Indeed, it proved impossible to elucidate any of them. One, No. 249, almost indicates that the ground is composed of homogeneous material. The area concerned is traversed by several channels, and the lateral variations are sufficient to overshadow any variation with depth. The failure of these depth probes prompted the traverses previously discussed in Chapter VI, and the latter proved to be by far the most fruitful method for this area.

CHAPTER IX.

EFFECT OF LATERAL VARIATIONS IN RESISTIVITY ON DEPTH PROBES

EFFECT OF LATERAL VARIATIONS IN RESISTIVITY ON DEPTH PROBES

The foregoing analyses of Chapter V relating to the problem of longitudinal and transverse traverses over sheets of varying thicknesses and resistivities afford an opportunity of calculating the influence of such lateral variations on the resistivity-depth curves obtained by different configurations of electrodes for depth probing. For the sake of simplicity it is assumed that the ground is normally of uniform resistivity, ρ_1, so that the normal resistivity-depth curve will be a straight line parallel to the depth or electrode interval axis.

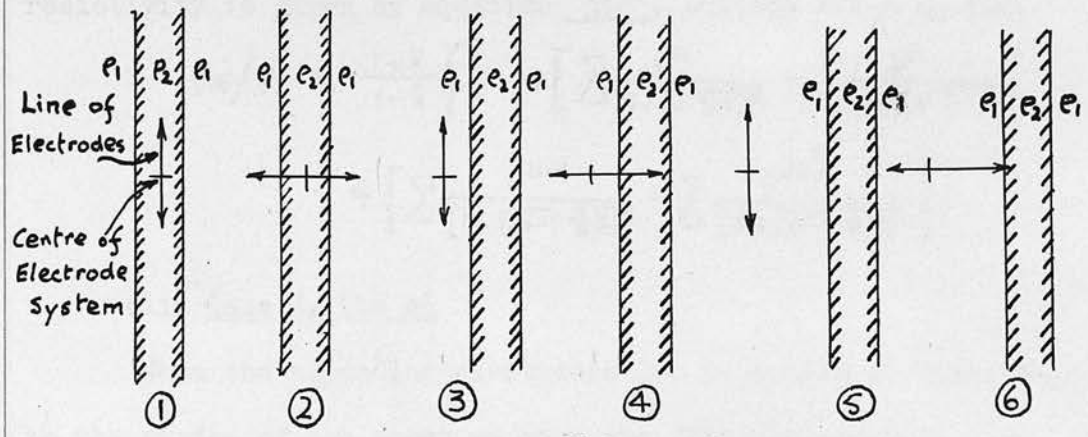

Fig. 63

To illustrate the effect of interposing a vertical sheet of different resistivity and reaching right to the surface, it is proposed to examine the cases illustrated in Fig. 63, i.e. Wenner type depth probes expanded

(a) at the centre of the vertical sheet,

(i) with the line of electrodes parallel to the sheet

(ii) with the line of electrodes at right angles to the sheet

(b) at a distance from the centre of the sheet equal to the width of the sheet, both parallel and at right angles to the strike of the sheet

(c) at a distance from the centre of the sheet equal to twice the width of the sheet, with the line of electrodes again parallel and at right angles to the strike of the sheet.

(a) At Centre of Vertical Sheet

(i) Case 1, Fig. 63

The formula expressing the ratio of apparent to normal resistivity is given by equation 55, putting x/a = 0, i.e.

$$\rho_a/\rho_1 = \frac{1+k}{1-k}\left\{1 + 4\left[\sum \frac{k^{2i}}{\left[1+(2i\frac{d}{a})^2\right]^{1/2}} - \sum \frac{k^{2i}}{\left[4+(2i\frac{d}{a})^2\right]^{1/2}}\right]\right.$$

$$\left. - 4\left[\sum \frac{k^{2i-1}}{\left[1+(2i-1\ \frac{d}{a})^2\right]^{1/2}} - \sum \frac{k^{2i-1}}{\left[4+(2i-1\ \frac{d}{a})^2\right]^{1/2}}\right]\right\}$$

(ii) Case 2, Fig 63

When the expanding electrodes lie in a line at right angles to the strike of the sheet we have the following conditions:-

(1) All electrodes within the sheet.

Equation 53 with x/a = 0 becomes:-

$$\rho_a/\rho_1 = \frac{1+k}{1-k}\left\{2\left[\sum_{i=0}^{\infty} \frac{k^{2i}}{2i\frac{d}{a}+1} - \sum_{i=0}^{\infty} \frac{k^{2i}}{2i\frac{d}{a}+2} + \sum \frac{k^{2i}}{2i\frac{d}{a}-1}\right.\right.$$

$$\left.\left. - \sum \frac{k^{2i}}{2i\frac{d}{a}-2} - \sum_{i=0}^{\infty} \frac{k^{2i+1}}{2i+1\ \frac{d}{a}+2} + \sum_{i=0}^{\infty} \frac{k^{2i+1}}{2i+1\ \frac{d}{a}+1}\right]\right\}$$

(2) Current electrodes outside the sheet, but potential electrodes within the sheet,

From equation 52,

$$\rho_a/\rho_1 = 2(1+k)\left\{\frac{1}{2} + \sum \frac{k^{2i}}{2i\frac{d}{a}+1} - \sum \frac{k^{2i}}{2i\frac{d}{a}+2} + \sum \frac{k^{2i-1}}{2i-1\ \frac{d}{a}+1} - \sum \frac{k^{2i-1}}{2i-1\ \frac{d}{a}+2}\right\}$$

(3) All electrodes outside the sheet.

When x/a = 0, equation 49 becomes

$$\rho_a/\rho_1 = 2\left\{1 + \frac{k}{2-\frac{d}{a}} - (1-k^2)\left(\sum_{i=0}^{\infty} \frac{k^{2i}}{2i\frac{d}{a}+2} + \sum \frac{k^{2i-1}}{2i-1\ \frac{d}{a}+2}\right)\right\}$$

Similar considerations give formula for the other cases portrayed in Fig. 63.

To illustrate these equations each case has been evaluated for k = $\pm$ 0.6, i.e. for vertical sheets whose resistivities are four times (Fig. 64) and one-quarter the normal country resistivity (Fig. 65), i.e. relatively an insulator and a conductor respectively.

Those curves dealing with expanding electrode lines parallel to the strike are, of course, continuous, smooth curves exhibiting no irregularities. Those relating to expansion of electrodes about the centre of the sheet have the characteristics of simple two-layer curves. Those expanded outside the sheet yield curves which might readily be interpreted as three-layer. The curves illustrating expanding lines at right angles to the strike may be compared to longitudinal traverses, and display similar discontinuities. The farther the centre of the electrodes is from the centre of the sheet, then the greater is the elec-

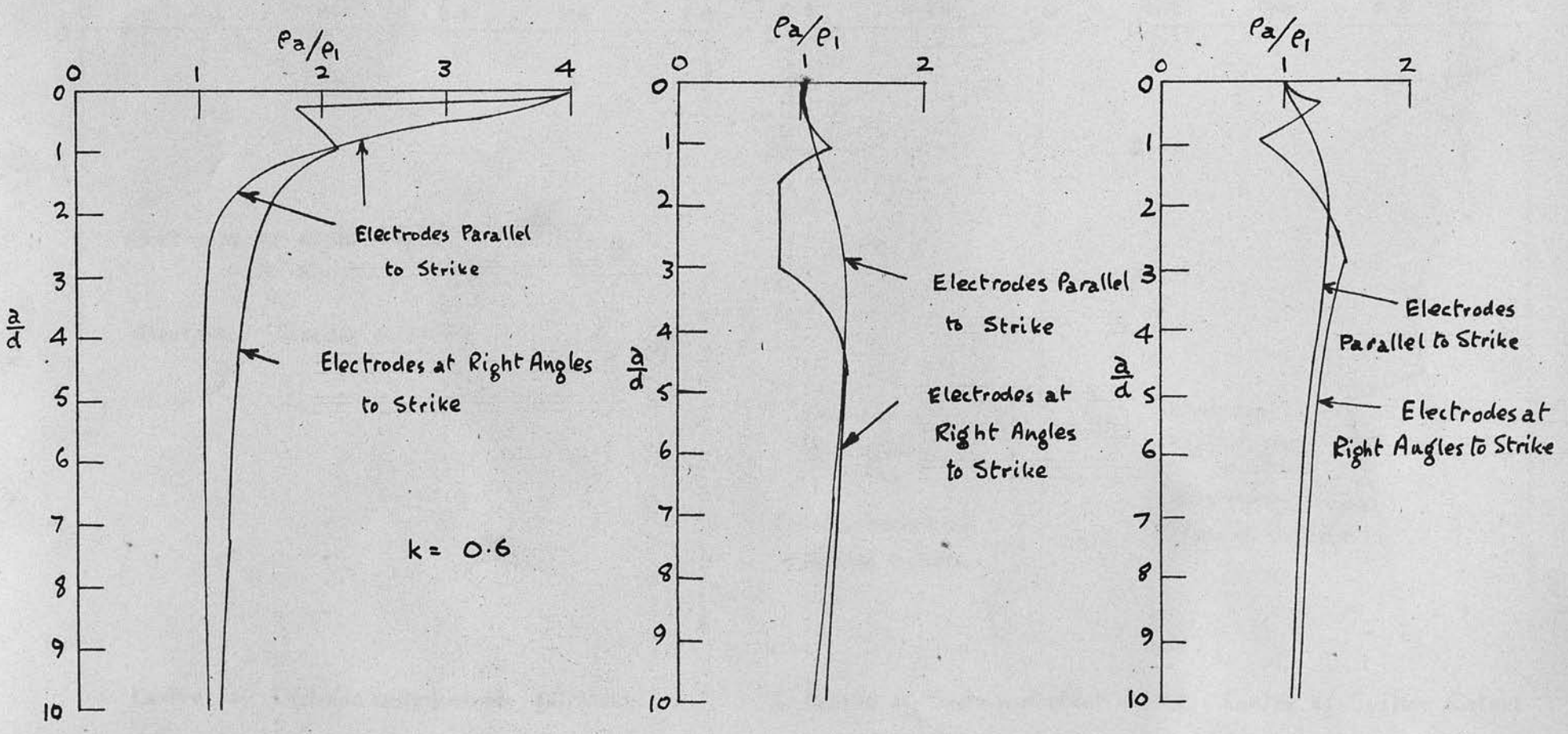

1. Centre of Electrode System at Centre of Sheet

3. Centre of System distant 2d from Centre of Sheet

2. Centre of System distant d from Centre of Sheet

Fig. 64, Effect of Lateral Variations on Depth Probes

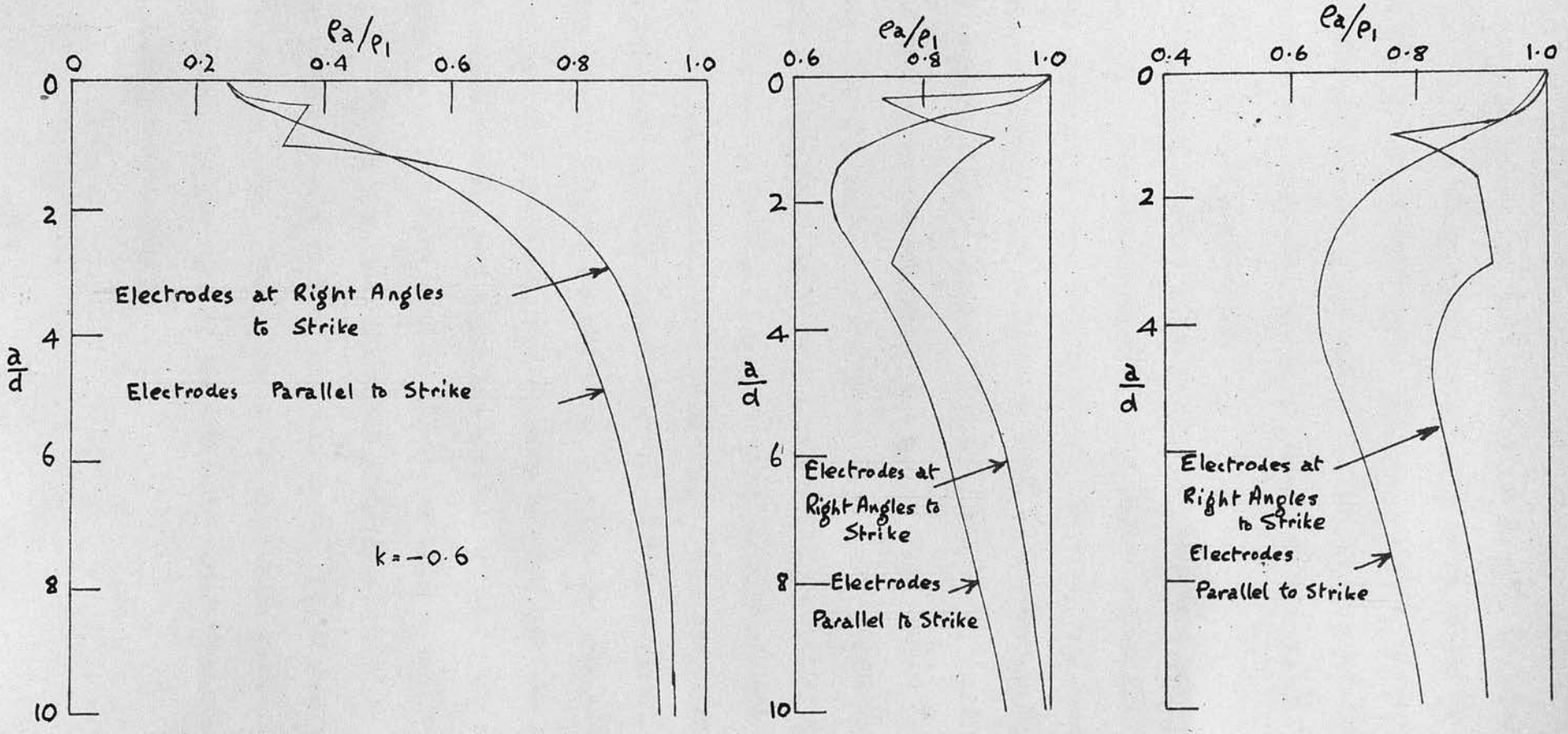

1. Centre of Electrode System at Centre of Sheet

2. Centre of System distant d from Centre of Sheet

3. Centre of System distant 2d from Centre of Sheet

Fig. 65, Effect of Lateral Variations on Depth Probes

trode interval before the first discontinuity. It is important to notice that the slope often changes sign as an electrode passes into or out of the sheet. Once again, such curves will affect many depth probes, and sudden changes of slope of field curves must be interpreted as due to lateral variation.

Examples of Lateral Variations.

The first example, shown in Fig. 66, is from a paper by Enslin (37). The two curves were taken over a narrow diabase dyke at Groenfontein near the Zaaiplaats Tin Mine, and possess the same characteristics as shown in Figs. 64 and 65 for depth probes over disturbing sheets. The one parallel to the strike of the dyke is continuous, while the one at right angles exhibits the same discontinuities as discussed above. The field curves closely resemble these taken over a relatively insulating dyke.

The second example is from a survey carried out over Burdiehouse Limestone Mine near Edinburgh. Here the Burdiehouse Limestone has been worked from the outcrop to the dip, the working of this 27 feet deposit being by stoop and room methods. The pillars left are small, and at about 20 feet over the limestone occurs a shale seam which has been extracted. The surface is therefore very broken, and in places the falls extend to the surface. In the area near the depth probe illustrated in Fig. 67 the ground is very broken, and open cracks can be observed in the surface soil. The centre of the electrode system was on solid ground, but one side of the expanding electrodes passed over visibly broken ground.

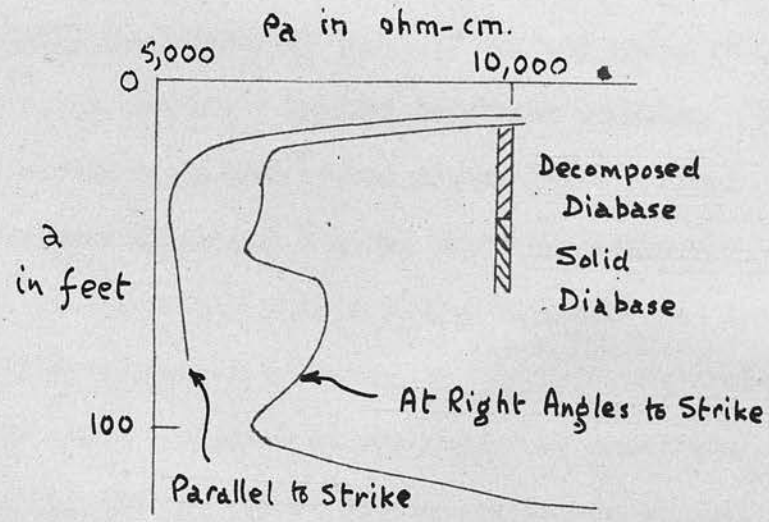

Fig. 66, Depth Probes over Dyke at Groenfontein

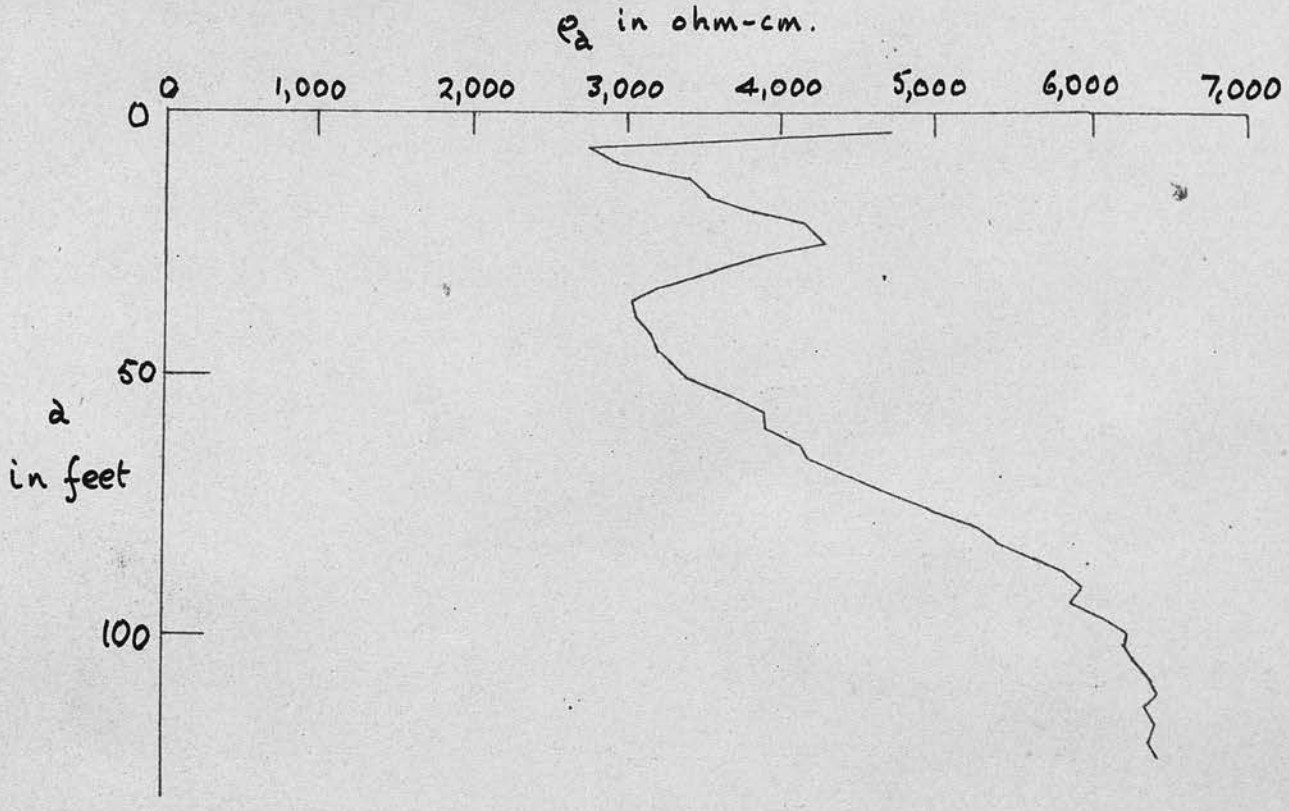

Fig. 67 Depth Probe at Burdiehouse

The curve is essentially that of a three-layer type with a very thin highly resistive top layer of surface soil, but, neglecting this, it becomes a typical two-layer problem. The effect of the highly resistive broken ground gives a local increase in resistivity as the leading current electrode approaches it, followed by a corresponding decrease when the broken ground lies between a potential and current electrode. The resistivity again increases as the potential electrode finally clears it, and the effect due to the breaks gradually merges with the normal increase in resistivity with depth as the electrode interval expands.

CHAPTER X.

CONCLUSIONS

CONCLUSIONS

The main conclusions and findings of this investigation may be summarised as follows:-

(1) The Geophysical Megger Earth Tester is an admirable machine for resistivity work. The only trouble experienced was the entry of water into the generator during very wet weather.

(2) With very thin vertical sheets the longitudinal traverse gives a more positive and more easily recognised anomalous resistivity curve.

(3) With thin vertical sheets the transverse traverse gives a better idea of the likely direction of the sheet.

(4) W-shaped resistivity curve is obtained from longitudinal traverse over both conductors and insulators, but with the former, the centre of the anomaly never rises above the country resistivity.

(5) The problem of traversing over vertical sheets may be solved by the theory of images. The resulting equations, although complicated looking, may be solved by various short cut methods.

(6) The types of curves obtained from longitudinal traverses vary greatly according to the thickness of the sheet, there

being a typical curve for widths of sheet between integral multiples of the electrode interval until the sheet becomes wider than the whole electrode spread. These curves should be valuable in the interpretation of vertical bodies with wide extension along the strike such as dykes, fault planes or zones and highly dipping strata.

(7) Transverse traverses over thin insulating sheets yield a double peaked apparent resistivity curve. This soon gives way to a single peak as the sheet width increases. The converse, i.e. double and single troughs, is found over conductors.

(8) The problem of traverses over inclined sheets cannot be solved by the theory of images, but type curves can be obtained from laboratory experiments.

(9) Buried sheets yield similar but more rounded and less evident curves as the depth of cover increases.

(10) The method of traversing can often prove valuable in the field in the location and exploration of faults, dykes and buried channels. Shallow underground fires may also be within its scope.

(11) Two-layer problems are best solved by Tagg's method. Moore's method of cumulative resistivity curves cannot be held as satisfactory.

(12) The effect of lateral variations in resistivity on depth

probes can be investigated by the theory of images, and can often be recognised in the field curves. Expanding probes crossing an interposed sheet of different resistivity will yield resistivity-depth curves with recognisable discontinuities. Depth probes parallel to the strike of such a sheet yield curves similar to those of two or three horizontal layers, and great care will be required in their interpretation and recognition.

BIBLIOGRAPHY

(1) G.C. Wood, "Determination of the Specific Electrical Resistance of Coal, Ores, etc.", Trans. Inst. Min. Eng., 1905, Vol. XXX, pp. 99 - 109.

(2) M. Ewing, A.P. Crary, J.W. Peoples and J.A. Peoples, "Prospecting for Anthracite by the Earth-resistivity Method", A.I.M.E. Tech. Pub. 683, Feb. 1936.

(3) A.H. Cox and S.W. Price, "Report on Certain Trials of Geoelectric Methods in S. Wales, with Special Reference to the Possibility of their Use in Detecting Underground Water in Mining Areas," D.S.I.R. Report, H.M.S.O., 1935.

(4) J.G. Koenigsberger, "Field Observations of Electrical Resistivity and their Practical Application," Trans. A.I.M.E., 1929, Vol. 81, pp. 221 - 237.

(5) R.H. Hawkins, "Application of Resistivity Methods to Northern Ontario Lignite Deposits," A.I.M.E., Geophysical Prospecting, 1934, p. 76.

(6) Granville Poole, J.T. Whetton and A. Taylor, "Earth-Resistivity Surveys on Various Geological Structures Related to Mining," Trans. Inst. Min. Eng., 1933, Vol. LXXXVI, p. 312.

(7) J.M. Bruckshaw, "Electrical Methods of Geophysical Surveying," Jour. Inst. Elect. Eng., Vol. 73, 1933, pp. 521-533.

(8) F. Wenner, "A Method of Measuring Earth Resistivity," Bulletin of the Bureau of Standards, 1915-16, Vol. 12, p. 469.

(9) J.J. Jakosky, "Exploration Geophysics," Times Mirror Press, Los Angeles, 1950, p. 517.

(10) W.J. Rooney and O.H. Gish, "Measurements of Resistivity of Large Masses of Undisturbed Earth," Terrestrial Magnetism and Atmospheric Electricity, 1925, Vol. 30, p. 161.

(11) W.J. Rooney and O.H. Gish, "Results of Earth Resistivity Surveys near Watheroo, Western Australia and at Ebro, Spain," Terr. Magn. and Atmos. Electr., 1927, Vol. 32, p. 49.

(12) O.H. Gish, "Apparatus for the Study of the Earth's Crust," U.S. Patent No. 1,813,845, July 7, 1931.

(13) E. Lancaster-Jones, "The Earth-Resistivity Method of Geophysical Prospecting," Mining Magazine, 1930, Vol. XLIII, p. 24.

(14) W.F. Lee, "Measuring Variation of Ground Resistivity with a Megger," U.S. Bureau of Mines, Tech. Paper 440, 1928.

(15) S.J. Pirson, "Effect of Anisotropy on Apparent Resistivity Curves," Bull. A.A.P.G., Jan. 1935, Vol. 19, pp. 37 - 57.

(16) L.B. Slichter, "The Interpretation of the Resistivity Prospecting Method for Horizontal Structures," Physics, Sept. 1933, Vol. 4, pp. 307 - 322.

(17) J.H. Jeans, "Mathematical Theory of Electricity and Magnetism," Cambridge University Press, 1923, pp. 200 - 207.

(18) C.A. Heiland, "Geophysical Exploration," Prentice-Hall, New York, 1940, p. 711.

(19) M.K. Hubbert, "Results of Earth-Resistivity Surveys on Various Geological Structures in Illinois," A.I.M.E., Tech. Pub. 463, 1932.

(20) J.J. Jakosky, "Exploration Geophysics," Times Mirror Press, Los Angeles, 1950, p.477.

(21) D.O. Ehrenburg and R.J. Watson, "Mathematical Theory of Electrical Flow in Stratified Media with Horizontal Homogeneous and Isotropic Layers," A.I.M.E., Tech. Pub. 400, 1931.

(22) E.T. Whittaker and G. Robinson, "Calculus of Observations," Blackie, 4th Edition, 1944, p.369.

(23) I. Roman, "How to Compute Tables for Determining Electrical Resistivity of Underlying Beds and their Applications to Geophysical Problems," U.S. Dept. of Commerce, Tech. Paper 502, 1930.

(24) R.F. Aldredge, "The Effect of Dipping Strata on Earth Resistivity Determinations," Colorado School of Mines Quarterly, Vol. 32(1), Jan. 1937, pp. 171 - 186.

(25) W. Fisch, "Geoelektrische Untersuchungsmethoden in Dienste der Wassersorgung," Monatsbulletin des Schweizerischen Vereins von Gas-und Wassfachmannern, No.5 Jahrgang, 1946.

(26) C.F. Tolman, "Ground Water," McGraw-Hill, New York, 1937.

(27) R. McAdam, "Geophysical Surveying with an Oscillating Magnetic Needle," Trans. Inst, Min. Eng., 1935, Vol. XC, pp. 259 - 266.

(28) Granville Poole, J.T. Whetton and A. Taylor, "Magnetic Observation on Concealed Dykes and Other Intrusions in the Northumberland Coalfield," Trans. Inst. Min. Eng., Vol. LXXXIX, 1934, pp. 34 - 35.

(29) J.N. Hummel, "A Theoretical Study of the Apparent Resistivity in Surface Potential Methods," A.I.M.E., Geophysical Prospecting, 1932, pp. 392 - 422.

(30) E. Lancaster-Jones,"The Earth-Resistivity Method of Electrical Prospecting," Mining Magazine, 1930, Vol. 42, pp. 355 - 362, and Vol. 43, pp. 19 - 28.

(31) 42nd Geological Section, S.A.E.C., "The Location of Under-Ground Water by Geological and Geophysical Methods," Military Engineering, Vol. VI - Water Supply, Supplement No.1, 1945, War Office.

(32) G.F. Tagg, "Interpretation of Resistivity Methods," A.I.M.E., Tech. Pub. 477, 1932.

(33) R.W. Moore, "An Empirical Method of Interpretation of Earth-Resistivity Measurements," A.I.M.E., Tech. Pub. 1743, 1944.

(34) J.T. Whetton and J.O. Myers, "Geophysical Surveying," Mine and Quarry Engineering, Vol. 16, Oct. 1950, p. 307.

(35) M. Muskat, "The Interpretation of Earth-Resistivity Measurements", A.I.M.E., Tech. Pub. 1761, 1945.

(36) Manufacturer's Booklet, "A Pocket-Book on Resistivity Prospecting", Evershed and Vignoles, Ltd., Acton Lane Works, Chiswick, London, W.4, Publication No.245.

(37) I. Roman, "Superposition Method," Peele's Mining Engineers' Handbook, 3rd Edition, Vol. I, Section 10-A, pp. 14 - 16.

(38) J.F. Enslin, "Lateral Effects on Electrical Resistivity Depth Probe Curves," Trans. Geol. Soc. of South Africa, Vol. 51, 1948, pp. 249 - 263.